A novel and integrated process for the valorization of kraft lignin

by

Ajinkya Rajkumar More

A dissertation submitted to the Graduate Faculty of
Auburn University
in partial fulfillment of the
requirements for the Degree of
Doctor of Philosophy

Auburn, Alabama
August 6, 2022

Keywords: Lignin, Oxidation, Retro-aldol reaction, Vanillin, Vanillic Acid, Vitrimers

Approved by

Zhihua Jiang, Chair, Associate Professor, Chemical Engineering
Thomas Elder, Co-Chair, Professor Emeritus, School of Forestry
Maria Soledad Peresin, Associate Professor, College of Forestry, Wildlife and Environment
Xinyu Zhang, Professor, Chemical Engineering
Andrew Adamczyk, Assistant Professor, Chemical Engineering
Yucheng Peng, Assistant Professor, College of Forestry, Wildlife and Environment

Abstract

In this work, the main objective was to produce high value products from kraft lignin with an integrated approach in the pulp and paper industry. Production of vanillin, vanillic acid and bio-based vitrimers represent the value-added products that are mainly focused in this study. Vanillin is commonly used as a flavoring agent in food, pharmaceutical and chemical industries. Recently, vanillic acid is gaining notable interest due to its anti-microbial, anti-bacterial, and chemo-preventive properties. Vanillin and vanillic acid have both been obtained as the main products from oxidation of kraft lignin. Vitrimers represent a new class of plastics that are derived from thermosetting polymers which possess self-healing and easy processibility in a wide temperature range. The recent development of bio-based vitrimers from oxidation kraft lignin has received considerable interest.

The oxidative conversion of lignin in an alkaline medium using oxygen results in the formation of vanillin and vanillic acid. The yield of these products depends on the reaction chemistry, time, temperature, oxygen partial pressure, lignin concentration and feedstock. In this work, a novel approach using the retro-aldol reaction chemistry was utilized to enhance the yields of vanillin and vanillic acid. The amount of oxygen charged during the retro-aldol reaction plays a key role in determining the product yield. The conventional oxidation of softwood kraft lignin using oxygen at 140°C for 40 min results in a total of 5.17% by wt. of vanillin and vanillic acid. In contrast, using the new approach in which oxygen is charged for only 20 min during the 40 min reaction improved this yield significantly to 6.95% by wt. The precipitated lignin after the reaction has a maximum carboxyl content of 1.41 mmol/g at 130°C. The improvement in the amount carboxylic acid groups allows for further utilization of the precipitated kraft lignin.

One of the main issues encountered in the valorization of kraft lignin is its incompatibility with other components due its branched aromatic structure, high molecular weight, and brittle nature. Therefore, it is crucial to understand the structural changes in lignin during oxidation especially in the operating conditions of current kraft pulping processes. The softwood kraft lignin before and after oxygen and ozone oxidations treated in the LignoForce operating conditions were thoroughly characterized using a variety of conductometric titration and ^{31}P NMR techniques. The progressive reduction in aliphatic and condensed OH units accompanied by the marked improvement in carboxylic OH units are the major structural changes occurring in the softwood kraft lignin. Among the oxidizing agents, the amount of carboxylic OH units formed from ozone oxidation was higher compared to oxygen oxidation under similar conditions. Furthermore, the softwood kraft lignin that is obtained after sequential oxidation treatment from oxygen at 130°C and from ozone at 80°C (OxL-COOH) contained 4.06 mmol/g of carboxylic OH units. The higher amount of carboxylation obtained after sequential oxidation treatment allows for improved compatibility of lignin with other components.

To further expand the scope of carboxylated softwood kraft lignin, bio-based vitrimers were synthesized using polyethylene glycol diglycidyl ether (PEG-epoxy), zinc acetylacetonate $Zn(acac)_2$, and sequentially oxidized kraft lignin (OxL-COOH). All OxL-COOH/PEG-epoxy showed high mechanical strength, thermal stability and self-healing. For the first time, the problems in film formation which are bubble formation and porosity are briefly discussed and strategies to troubleshoot these problems are discussed. In aqueous NaOH solutions, the bio-based vitrimer exhibited swelling which is one of the prime indicators of the dynamic transesterification in the cured network. In 0.1 M NaOH solution, the OxL-COOH/PEG-epoxy system showed a swelling ratio of 26.6% in the initial 10 min which further increased to 52.6% in 20 min at a

stoichiometric ratio ‘R’ of 1:1 on mole basis. The vitrimers were formed at three different stoichiometric ratios 1.0, 1.3 and 1.5 with maximum lignin content of 49.5% by wt. In summary, a high lignin content utilization was demonstrated for formation of high value products with lower consumption of oxidizing agents and solvents. Overall, this research established a novel and integrated approach to valorize kraft lignin into diverse products.

Acknowledgments

I would like to express my sincere gratitude to my research advisor, Dr. Zhihua Jiang for his mentorship and motivation throughout my graduate studies at Auburn University. He supported and believed in me throughout my Ph.D. project and without his guidance this dissertation would not have been possible. I would also like to express my deepest gratitude towards Dr. Thomas Elder for his support and constant encouragement towards achieving research goals. His valuable guidance and feedback has helped me become an independent researcher. There were times when I faced challenges during my journey, but Dr. Zhihua Jiang and Dr. Thomas Elder have always motivated me to look forward and learn from my previous mistakes.

I would also like to thank my committee members, Dr. Xinyu Zhang, Dr. Maria Soledad Peresin and Dr. Andrew Adamczyk for providing their beneficial insights towards completion of this dissertation. I would also like to thank Dr. Yucheng Peng for agreeing to serve as the University reader on my dissertation committee. Acknowledgement and thanks are also extended to Dr. Ilari Filpponen, Dr. Ramsis Farag and Dr. Burak Aksoy for their help in the research activities. I am also grateful to the support and guidance of Dr. Dimitris Argyropoulos, Nicolo Pajer, Dr. Melissa Boersma, Dr. Suan Shi, Dr. Jing Li, Archana Bansode, Yuyang Wang and Navid Etebari for developing and assisting with characterizations in different analytical techniques. I also thank the members of the Alabama Centre for Paper and Bioresource Engineering (AC-PABE) for their help and support in the laboratory. Finally, I would like to thank my parents, Jayshree and Rajkumar More and my brother, Vikrant for their love and support.

Table of Contents

Abstract 2

Acknowledgments 5

List of Tables 11

List of Figures 12

List of Abbreviations 16

Chapter 1 Introduction and dissertation outline 22

1.1 Introduction 22

1.2 Dissertation outline 25

1.3 References 28

Chapter 2 A review of lignin hydrogen peroxide oxidation chemistry with emphasis on aromatic aldehydes and acids 33

2.1 Introduction 33

2.2 Lignin structure 36

2.3 Sources of Lignin 40

2.3.1 Kraft lignin 40

2.3.2 Lignosulfonates 41

2.3.3 Biorefinery lignin 42

2.4 Mechanism of lignin oxidation by oxygen and peroxide 44

2.4.1 Oxygen oxidation 45

2.4.2 Hydrogen peroxide oxidation 49

2.4.2.1 Effect of pH 54

2.4.2.2 Effect of temperature 58

2.4.2.3 Effect of metal ions 61
2.4.2.4 Effect of lignin feedstock 65
2.5 The continuous process of kraft lignin oxidation 66
2.6 Thermodynamic and kinetic studies of kraft lignin and vanillin oxidation 71
2.6.1 Kinetic laws for kraft lignin and vanillin oxidation 71
2.6.2 Energy balance for kraft lignin and vanillin oxidation in a batch reactor 72
2.6.2.1. Estimation of heat of reaction of kraft lignin oxidation $\Delta H_{r,1}$ 73
2.6.2.2. Estimation of heat of reaction of vanillin oxidation $\Delta H_{r,2}$ 74
2.6.3 Energy balance for kraft lignin and vanillin oxidation in the column sections in SBCRs and BCRs 76
2.7 Conclusion 77
2.8 Scope for future work 78
2.9 References 80
Chapter 3 Towards bio-based vitrimers from lignocellulosic feedstock 89
3.1 Introduction 89
3.2 Chemistry of vitrimers 91
3.2.1 Concerted type network rearrangement 91
3.2.2 Dissociative type network rearrangement 92
3.2.3 Associative type network rearrangement 92
3.3 Bio-based vitrimers 93
3.3.1 Lignin-based vitrimers 93
3.3.2 Cellulose-based vitrimers 97
3.3.3 Hemicellulose-based vitrimers 99

3.4 Conclusions 101
3.5 References 102
Chapter 4 Towards a new understanding of the retro-aldol reaction for oxidative conversion of lignin to aromatic aldehydes and acids 111
4.1 Introduction 111
4.2 Materials and methods 119
4.2.1 Chemicals 119
4.2.2 Raw materials 120
4.2.3 Oxidation of lignin 120
4.2.4 Quantification of yield using high-performance liquid chromatography 122
4.2.5 Carboxyl content determination using conductometric titration 123
4.2.6 Comparing results for statistical significance using Tukey test 123
4.3 Results and discussion 124
4.3.1 Effect of temperature on vanillin and vanillic acid yield 124
4.3.2 Effect of temperature on carboxyl content of lignin 126
4.3.3 Effect of time 127
4.3.4 Effect of controlling the amount of oxygen charged 129
4.3.5 Effect of controlling the amount of oxygen charged during the reaction on different lignin feedstocks 131
4.4 Conclusion 135
4.5 References 136
Chapter 5 Effect of oxygen and ozone oxidation on functional group content in softwood kraft lignin 143

5.1 Introduction 143
5.2 Materials and methods 146
5.2.1 Oxygen oxidation of SKL 146
5.2.2 Ozonation of SKL and sequential oxidation of OKL 147
5.2.3 ^{31}P NMR characterization 147
5.2.4 Carboxyl content determination using conductometric titration 148
5.3 Results and discussion 148
5.3.1 ^{31}P NMR characterization 148
5.3.2 Carboxyl content in ozonated and sequentially oxidized kraft lignin 152
5.4 Conclusions 156
5.5 References 156
Chapter 6 A novel and integrated process for the valorization of kraft lignin to produce lignin-based vitrimers 162
6.1 Introduction 162
6.2 Materials and methods 166
6.2.1 Chemicals 166
6.2.2 Carboxyl content determination using conductometric titration 167
6.2.3 Ozonation of SKL and sequential oxidation of OKL 167
6.2.4 Preparation of OxL-COOH/PEG-epoxy vitrimers 168
6.2.5 Characterization of lignin-based vitrimers 169
6.3 Results and discussion 170
6.3.1 Sequential oxidation of softwood kraft lignin 170
6.3.2 Film formation 171

6.3.3 Structural characterization 173
6.3.3.1 FTIR analysis 173
6.3.3.2 Dynamic mechanical properties 176
6.3.3.3 Thermal stress relaxation and repairability 177
6.3.3.4 Swelling study 181
6.3.3.5 Self-healing 184
6.4 Conclusions 184
6.5 References 185
Chapter 7 Conclusions and future work 192
7.1 Summary 192
7.1.1 Towards a new understanding of the retro-aldol reaction for oxidative conversion of lignin to aromatic aldehydes and acids 193
7.1.2 Effect of oxygen and ozone oxidation on functional group content in softwood kraft lignin 194
7.1.3 A novel and integrated process for the valorization of kraft lignin to produce lignin-based vitrimers 194
7.2 Potential directions for future work 195
7.2.1 Towards a new understanding of the retro-aldol reaction for oxidative conversion of lignin to aromatic aldehydes and acids 195
7.2.2 Effect of oxygen and ozone oxidation on functional group content in softwood kraft lignin 196
7.2.3 A novel and integrated process for the valorization of kraft lignin to produce lignin-based vitrimers 197

List of Tables

Table 2.1 Different interunit linkages, their structure, abundance and bond dissociation energies found in softwood, hardwoods and grasses 39

Table 2.2 Main features of Biorefinery lignin 43

Table 2.3 First order reaction rate constants $k_1(obs)$ for the decomposition of hydrogen 55

Table 2.4 Effect of lignin feedstock on aromatic aldehyde yield 66

Table 2.5 Advantages and disadvantages of Bubble Column Reactor (BCR) 68

Table 2.6 Advantages and disadvantages of Structured Packed Bubble Column Reactor (SPBCR) 68

Table 2.7 Experimental conditions and results of continuous oxidation of kraft lignin 70

Table 2.8 Predicted heat capacities of kraft lignin, vanillin and vanillic acid 75

Table 2.9 Estimated heat of reaction of vanillin oxidation at different temperatures from 120°C to 160°C 76

Table 3.1 Effect of oxidation treatments on carboxyl content of kraft lignins 95

Table 4.1 Structural characterization of different lignins 120

Table 4.2 Ash and carbohydrate content of different lignin feedstocks 132

Table 4.3 Statistical significance of yield improvements using Tukey honest significance test 135

Table 5.1 Acquisition parameters for ^{31}P NMR 148

Table 5.2 Functional groups content in SKL before and after oxygen oxidation (mmol/g) 150

Table 5.3 The changes in carboxylic OH groups present in softwood kraft lignin after ozone oxidation 153

Table 6.1 Different stoichiometric formulations of OxL-COOH/PEG-epoxy systems 175

List of Figures

Figure 2.1 Monolignols present in the lignin 36

Figure 2.2 Nomenclature followed in lignin model compounds 37

Figure 2.3 Major interunit linkages found in lignin 38

Figure 2.4 Structure of kraft lignin 41

Figure 2.5 Structure of lignosulfonate 42

Figure 2.6 Course of oxygen and hydrogen peroxide oxidation cycle 44

Figure 2.7 Hydrogen peroxide oxidation of phenolic-lignin mechanisms 51

Figure 2.8 Hydrogen peroxide oxidation of non-phenolic lignin with aryl-α-carbonyl conjugated structures 52

Figure 2.9 Hydrogen peroxide oxidation of non-phenolic lignin with cinnamaldehyde conjugated structures 53

Figure 2.10 Hydrogen peroxide oxidation of non-phenolic lignin with α-carbinol structures and dimer formation in the reaction of α-carbinols 53

Figure 2.11 The effect of pH on the reaction mechanism of apocynol 56

Figure 2.12 The effect of pH on the reactivity of apocynol at 90°C 56

Figure 2.13 Stabilization of quinone methide from apocynol through hyperconjugation 58

Figure 2.14 Effect of DTMPA and Temperature on Hydrogen Peroxide Stability pH 11.5 59

Figure 2.15 Low molecular weight products obtained from the oxidation of kraft lignin by hydrogen peroxide 60

Figure 2.16 Transition metal induced decomposition of hydrogen peroxide 62

Figure 2.17 Proposed mechanisms for lignin depolymerization and aromatic nuclei oxidation, aromatic ring cleavage, and formation of final products 65

Figure 2.18 Arrhenius plots, k_{NC} and k_{CI}, versus $\frac{1}{T}$, for the calculation of the activation energy of lignin oxidation (eq 9; runs 1, 2, 4-7, and 9) and vanillin oxidation (eq.4; runs 1, 2 and 4-7) respectively 72
Figure 3.1 Concerted type molecular network rearrangement 91
Figure 3.2 Dissociative type molecular network rearrangement 92
Figure 3.3 Associative type molecular network rearrangement 93
Figure 3.4 Transesterification reaction for lignin-based vitrimers 94
Figure 3.5 Transesterification reaction for CNF based vitrimers 97
Figure 3.6 Transcarbonation exchange reaction for vitrimer based papers 99
Figure 3.7 Imine-amine exchange chemistry; equilibrium of imine formation, transamination between imines and amines and imine metathesis 100
Figure 4.1 Structure of kraft lignin 112
Figure 4.2 Mechanism of alkaline oxidation of lignin using oxygen 117
Figure 4.3 Aldol condensation of vanillin and acetone resulting in vanillidenacetone* according to the literature 118
Figure 4.4 Effect of temperature on the yield of vanillin and vanillic acid 126
Figure 4.5 Effect of temperature on carboxyl content of SKL 127
Figure 4.6 Effect of time on the yield of vanillin and vanillic acid 128
Figure 4.7 Effect of controlling the amount of oxygen charged during the reaction on the yield of vanillin and vanillic acid 130
Figure 4.8 Proposed pathway of formation of vanillin, vanillic acid and guaiacol 131
Figure 4.9 Effect of controlling the amount of oxygen charged during the reaction on the yield of vanillin and vanillic acid from different lignin feedstocks 132

Figure 5.1 Main depolymerization pathways during kraft pulping and protonation followed by an internal nucleophilic substitution of non-phenolic lignin subunits 144
Figure 5.2 ^{31}P NMR spectra of derivatized lignin samples 149
Figure 5.3 The changes in various hydroxyl units present in softwood kraft lignin before and after oxygen oxidation 150
Figure 5.4 A mechanism for the degradation reactions of phenolic units during oxygen de-lignification of kraft pulps 152
Figure 5.5 The changes in the amount of ozone charged w.r.t to the duration of the reaction..... 154
Figure 5.6 The changes in carboxylic OH groups present in SKL after ozone oxidation 155
Figure 5.7 Conductometric titration of sequentially oxidized kraft lignin obtained from OKL 155
Figure 6.1 LignoForce process and modified LignoForce process for the development of high-value products 165
Figure 6.2 Proposed reaction pathway for vitrimer formation; Curing reaction of OxL-COOH and PEG-epoxy and transesterification exchange reaction within the cross-linked network..... 166
Figure 6.3 Bubble formation in vitrimers before troubleshooting 172
Figure 6.4 Front and back view of vitrimers after post troubleshooting 173
Figure 6.5 Comparative FTIR spectra of untreated SKL, oxygen oxidized SKL (L-COOH), and ozone & oxygen treated SKL (OxL-COOH) 174
Figure 6.6 FTIR spectral changes of the cured OxL-COOH/PEG-epoxy system at different stoichiometric ‘R’ values 175

Figure 6.7 The storage modulus of OxL-COOH/PEG-epoxy films with different R values ... 176
Figure 6.8 tan δ of OxL-COOH/PEG-epoxy films with different R values 177
Figure 6.9 Thermogravimetric analysis (TGA) and derivative thermogravimetric analysis (DTG) study of PEG-epoxy 178
Figure 6.10 Thermogravimetric analysis (TGA) of OxL-COOH/PEG-epoxy films with different R values 179
Figure 6.11 Derivative thermogravimetric analysis (DTG) of OxL-COOH/PEG-epoxy films with different R values 179
Figure 6.12 The stress relaxation behavior of epoxy thermoset prepared from DGEBA, glutaric anhydride and $Zn(acac)_2$ at different temperatures ranging from 80°C to 200°C 180
Figure 6.13 Stress relaxation curves of OxL-COOH/PEG-epoxy films with different R values 181
Figure 6.14 Swelling of OxL-COOH/PEG-epoxy with R: 1 in NaOH solution with different concentrations (0.01 M, 0.05 M, 0.1 M, and 0.2 M) 183
Figure 6.15 Swelling of OxL-COOH/PEG-epoxy with R: 1 in 0.1 M NaOH solution at different time intervals (0, 5, 10, 15, 20, 30, and 60 min) 183
Figure 6.16 Self-healing for R:1 sample after crack, after 15 min curing and after 30 min curing 184

List of Abbreviations

SKL	Softwood kraft lignin
OKL	Oxidized kraft liquor
P_{O_2}	Oxygen partial pressure in Parr reactor, bar
P_{NaOH}	Water partial pressure above the NaOH solution, bar
p^0	Equilibrium partial pressure of water vapor over pure water, bar
T	Temperature of the reaction, Kelvin
T_i	Initial temperature of the reaction, Kelvin
T_F^{set}	Set point of thermostatic bath, Kelvin
I	Ionic strength of the liquid medium
$[O_2^{liq}]$	Concentration of dissolved oxygen, mol per liter
t	Reaction time duration, min
t_{max}^*	Duration of time in which oxygen is charged in the reactor, min
LInAT	Indulin AT
H-lignin	Enzymatic hydrolysis lignin
LMarAG	Marasperse AG
COOH	carboxylic OH units
HPLC	High-performance liquid chromatography
SKL80	Precipitated lignin after oxygen oxidation treatment at 80°C
SKL88	Precipitated lignin after oxygen oxidation treatment at 88°C
SKL96	Precipitated lignin after oxygen oxidation treatment at 96°C
LPM	Liter per minute

ppm	Parts per million
FTIR	Fourier transform infrared
ATR	Attenuated Total Reflection
DMA	Dynamic mechanical analysis
$\tan\delta$	Ratio of the loss modulus to storage modulus in a viscoelastic material
FWHM	Full width at half minimum
TGA	Thermogravimetric analysis
DTG	Derivative thermogravimetric analysis
NMR	Nuclear magnetic resonance
UV/vis	Ultraviolet visible
PEG	Poly (ethylene glycol) diglycidyl ether
PTFE	Polytetrafluoroethylene
LCOOH	Carboxylated kraft lignin after oxygen treatment
TER	Transesterification exchange reaction
EEW	Epoxy equivalent weight, grams per equivalence
COOH	Carboxyl content, millimoles per gram
N.D.	Not detected
L	Liter
R	Ratio of the epoxy to the carboxyl group content in vitrimers
A_0	parameter of the Antoine equation relating vapor pressure to temperature
B_0	parameter of the Antoine equation relating vapor pressure to temperature
C_0	parameter of the Antoine equation relating vapor pressure to temperature
$\Delta H_{r,1}$	heat of reaction of lignin oxidation kJ mol^{-1}

$\Delta H_{r,2}$ heat of reaction of vanillin oxidation kJ mol^{-1}

ΔV_l volume of liquid taken from the system in each sample collection, m^3

Δt time interval between collection of two consecutive liquid samples, s

ΔV_l volume of liquid taken from the system in each sample collection, m^3

$\lambda_{H_2O}^{vap}$ heat of vaporization of water, kJ/mol

n_i number of moles of species i, mol

F_i molar flow rate of species i, mol/s

H_i enthalpy of formation of species i, mol/s

E_i total energy of species i, mol/s

W_s shaft work, W

C_L concentration of lignin, mol/l

C_v concentration of vanillin, mol/l

C_{O_2} concentration of oxygen, mol/l

P partial pressure of species i, bar

P_i partial pressure of species i, bar

Q heat received by the system from the surroundings, W

Cp_i heat capacity of species or substance i, J mol^{-1} K^{-1} or J kg^{-1} K^{-1}

r_1 rate of formation of vanillin, mol l^{-1} min^{-1}

r_2 rate of oxidation of vanillin, mol l^{-1} min^{-1}

k_1 kinetic constant for formation of vanillin, $(l/mol)^{1.75}$ min^{-1}

k_2 kinetic constant of oxidation of vanillin, l mol^{-1} min^{-1}

R universal gas constant, l atm mol^{-1} K^{-1}

A velocity reaction constant for vanillin oxidation, l mol^{-1} min^{-1}

A_{ext1} area of the external wall of the cylindrical glass of the reaction, m^2

r_{ext1} radius of the external wall of the glass that limits the reaction zone, m

r_{int} radius of the internal wall of the internal cylindrical glass, m

A_1 internal area of the cylindrical glass limiting the reaction zone, m^2

A_2 surface area of the steel plates, m^2

E_a activation energy of lignin oxidation, J/mol

$f(pH)$ function of concentration of H^+ ions

h_{als} heat transfer coefficient from the external wall of the lower steel plate to the ambient, W m^{-2} K^{-1}

h_{aus} heat transfer coefficient from the external wall of the upper steel plate to the ambient, W m^{-2} K^{-1}

h_{fgl} heat transfer coefficient from the thermo fluid to the external glass walls of the reactor, W m^{-2} K^{-1}

h_{gll} heat transfer coefficient from the internal glass walls to the liquid inside the reactor, W m^{-2} K^{-1}

h_{sg} heat transfer coefficient from the gas inside the reactor to the internal wall of the upper steel plate, W m^{-2} K^{-1}

h_{sl} heat transfer coefficient from the liquid inside the reactor to the internal wall of the upper steel plate, W m^{-2} K^{-1}

R_1 radius of the internal wall of the reactor column, m

R_2 radius of the external wall of the reactor column, m

R_3 radius of the internal wall of the outer jacket tube, m

A_R internal cross-section area of the column, m^2

A_w difference between the external and the internal cross-section area of the column, m^2

L height of the cylindrical glass, m

D_s width of stainless steel plates, m

U_1 overall heat transfer coefficient from the thermo fluid in the jacket to the liquid inside the reactor, W m^{-2} K^{-1}

U_2 overall heat transfer coefficient from inside of the reactor to the ambient through the top and bottom stainless steel plates, W m^{-2} K^{-1}

k_s thermal conductivity of stainless steel, W m^{-1} K^{-1}

k_{gl} thermal conductivity of glass, W m^{-1} K^{-1}

V_l volume of the liquid phase inside the reactor, m^3

V_g volume of the gas phase inside the reactor, m^3

ε_G gas hold up

ε_L liquid hold up

ε_S volume fraction of the structured packing

u_{GS} superficial gas velocity, m/s

u_{LS} superficial liquid velocity, m/s

U overall heat transfer coefficient from the thermo fluid in the jacket to the liquid insider the reactor, W m^{-2} K^{-1}

T_F thermo fluid temperature inside the jacket, K

$C_{p,i}$ heat capacity of substance *i*, J kg^{-1} K^{-1}

λ_{ef} effective thermal dispersion coefficient, W m^{-1} K^{-1}

$k_L a$ liquid side mass transfer coefficient, s^{-1}

Subscripts

D	vanillic acid
g	gas phase
H_2O	water
l	liquid phase
L	lignin
NaOH	sodium hydroxide
others	intermediates that can be formed during lignin degradation
O_2	oxygen
V	vanillin

Superscripts

l	liquid phase
g	gas phase

Chapter 1 | Introduction

1.1 Introduction

The current challenges of the 21st century involves the large-scale use of non-renewable and non-recyclable resources. This calls for development of technologies which are focused on producing reusable waste and utilizing renewable bio-based resources [1]. Biomass derived materials are promising alternatives to conventional petroleum based products due to their bio-degradability and sustainability. Lignin and cellulose which comprise the major structural components in trees and plants are abundantly available bio-based materials [2]. In the process of wood pulping, delignification occurs by chemical degradation of lignin to liberate cellulose. The lignin obtained as a by-product from the conventional kraft and sulfite pulping routes are often termed 'technical lignins' [3]. The structural characteristics of lignin obtained from technical processes depend on the wood species, delignification type and recovery process from pulping liquors [4, 5].

Oxidation is one of the most extensively studied lignin valorization processes [6-12]. It produces low molecular weight phenolic compounds which are high value chemicals. Vanillin (4-hydroxy-3-methoxybenzaldehyde) is one of the most prominent value-added chemicals produced from this process. It is predominantly used as a flavoring agent and has wide range of applications in food, cosmetic, chemical and pharmaceuticals industries. Recently, the interest in vanillin is growing due to its antioxidant and anti-cancer properties and its role in bacterial cell to cell signaling [13, 14]. It is a key constituent of vanilla flavor, and sold as a crystalline solid in two grades, technical and Food Chemicals Codex (FCC) grade. Vanillic acid (4-hydroxy-3-methoxybenzoic acid), the oxidized form of vanillin, is a dihydroxybenzoic acid derivative that is also used as a flavoring agent. Recently, it is gaining significant interest due to its role in preventing

human diseases. It also has antimicrobial, antibacterial, and chemo-preventive properties which are significant [15].

Vanillin production using guaiacol first began in the late 18th century by Haarmann and Reimer. About 40 years later, it was then discovered that vanillin could be produced from the lignin present in the sulfite liquor of pulp and paper industry [16]. The first lignin based production of vanillin from sulfite liquor started in the United States in the year 1936 as a joint venture between Marathon Paper Mills Co. of Wisconsin and Salvo Chemical Corp. using the technology developed by Howard [17]. However, by the end of 1990's, majority of lignin to vanillin plants were shut down due to growing environmental concerns, reduced lignin availability due to the dominance of the kraft process and also due to the increasing availability of cheap chemical intermediates from petroleum [18]. Today, only about 20% of vanillin in the market is produced from lignin and the remaining 80% is produced from crude oil. Vanillin produced from lignin has a higher demand in specific market sectors including perfume industry, European chocolate manufacturers and in the Japanese market. The difference in price of lignin and guaiacol based vanillin is approx. $1 to $2 per kg and their market value according to Smolarski is about 12,000 USD/MT [19, 20].

Among technical lignins, kraft lignin accounts for 85% of all the lignin produced in the world, which accounts to approximately 45 millions tons/year produced worldwide [21]. The highly modified structure of kraft lignin is a result of sulfidolytic cleavage of phenolic propane units and alkaline cleavage of non-phenolic propane units [22]. In this aspect, the addition of an oxygen stage in lignin recovery cycle is recently gaining interest in the LignoForce process [23]. The structural changes before and after oxidation in the operating conditions of Lignoforce process are crucial to develop an integrated process for valorization of softwood kraft lignin. Modern NMR

techniques represent the most powerful approach to elucidate structural details of lignin [24-28]. It allows for quantitative analysis of various phenolic OH, aliphatic OH and carboxylic OH units present in the softwood kraft lignin in detail.

The development of bio-based vitrimers from the oxidation of kraft lignin is a relatively new field of research [29-31]. Vitrimers represent a new category of polymers in addition to thermoplastics and thermosetting polymers. Thermoplastic polymers exhibit melting when sufficient thermal energy is provided. When heated beyond a specific temperature level, thermoplastics behave like viscoelastic liquid and flow. They also dissolve when exposed to good solvents. In contrast, thermosetting polymers become soft, but do not flow when heated above a certain temperature range. Thermosetting polymers do not dissolve in good solvents and only exhibit swelling when immersed into a good solvent. Vitrimers are unique polymers which behave like a viscoelastic liquid when heated but exhibit swelling when exposed to good solvents [32]. In these types of cross-linked networks, the introduction of exchangeable chemical bonds leads to dynamic cross-linking mechanism allowing vitrimers to possess plasticity in the network. Polymer networks which are comprised of exchangeable bonds are termed as 'Covalent Adaptable Networks (CAN)'.

CANs are classified into three main categories depending upon the exchange mechanism: concerted, dissociative and associative. In the concerted cross-link exchange mechanism, the original cross-link is only broken when a new covalent bond to another position has been formed without any kind of intermediate step. In practical scenarios, the chemical bond exchange takes place via an intermediate step, therefore, the concerted cross-link exchange mechanism is considered as an 'ideal' scenario for vitrimer formation. In contrast, in a dissociative exchange, bonds are broken and formed again at another place via a less cross-linked intermediate state. One

of the key criteria for formation of vitrimeric polymer materials is that the overall cross links should not decrease upon heating. Therefore, dissociative CANs do not meet the ideal requirements about topology and network fluctuations for vitrimer formation. In the third group of CANs, the original cross-link is only broken when a cross-link to another position has been formed via a more cross-linked intermediate state. As a result, network de-crosslinking is not possible and this scenario is expected to meet or at least approach ideal vitrimer formation requirements. This type of network re-arrangement allows vitrimers to possess notable self-healing, swelling and stress relaxation properties.

1.2 Dissertation outline

Chapter 2 provides a review of lignin hydrogen peroxide oxidation chemistry with emphasis on aromatic aldehydes and acids. It highlights the basic patterns, mechanisms and optimal conditions for utilizing hydrogen peroxide for oxidation of lignin. It also provides commonalities between the oxidative chemistries of lignin by oxygen and peroxide and the current challenges of valorizing lignin using nitrobenzene, oxygen and hydrogen peroxide. In this review, the effect of pH, temperature, metal ions and lignin feedstock on the hydrogen peroxide oxidation of lignin are briefly discussed. The results and mechanisms discussed provide details on developing processes for production of the aromatic aldehydes and acids from hydrogen peroxide oxidation of lignin.

Chapter 3 provides a background information on the development of bio-based vitrimer polymers from lignocellulosic feedstock. Vitrimers are novel materials that exhibit permanent molecular networks which can change their molecular configuration through segmental diffusion simultaneously preserving network integrity. This allows vitrimers to have interesting properties such as self-healing, solvent swelling and shape memory. The development of bio-based

technologies is interesting since it allows to address the major limitations in valorization of lignocellulosic feedstock. This background review addresses the current technologies for producing bio-based vitrimers in an integrated biorefinery.

Chapter 4 is focused on oxidation of softwood kraft lignin using oxygen in alkaline medium to produce vanillin and vanillic acid. Currently, the industrial production of vanillin is mainly focused from the oxidation of lignosulfonates despite the fact that they represent less than 10% of the total lignins extracted [33]. Typically, higher yields of vanillin ranging from 5 to 7% are obtained from lignosulfonates in the presence of transition metal catalysts [34]. Kraft lignin which represents the main source of lignin is currently used as a source of low-grade fuel in the pulping operation and only about 100,000 tons of kraft lignin available are valorized every year [35]. Oxygen is preferentially used as an oxidizing agent due to its high atom economy, environmental friendliness, and low price. However, due to the lower yields attained in this process, catalysts in combination with oxygen are required to improve the yield by a factor of 1.5-2 [36]. In an integrated approach, it is critical to avoid the use of catalysts for downstream processing of kraft liquor in evaporators and recovery boilers. Other problems with the conventional processes include high consumption of oxygen and solvents, lower yields of products and large amounts of unutilized lignin after the oxidation reaction [37]. This part of work was focused on addressing these problems encountered in the oxidation of kraft lignin to vanillin and vanillic acid. Through analyzing the reaction mechanism and kinetics thoroughly, we identified a novel approach to enhance the yield of vanillin and vanillic acid. Specifically, instead of applying oxygen throughout the entire reaction processes, we discovered that oxygen should be applied only in the initial reaction phase.

Chapter 5 of this research is focused on understanding the effect of oxygen and ozone oxidation on functional group content in softwood kraft lignin under the operating conditions of LignoForce process. Lignin is one of the most abundant natural polymers, however, it shows incompatibility with other components due to its branched aromatic structure, high molecular weight, and brittle nature. For this reason, understanding the structural changes in lignin during oxidation is crucial for its applications. The softwood kraft lignins before after oxygen and ozone oxidations were thoroughly characterized using a variety of conductometric titration and ^{31}P NMR techniques. Among the oxidizing agents, the amount of carboxylic OH units formed from ozone oxidation was higher compared to the oxygen oxidation under similar conditions. These results indicate the importance of an ozonation stage at lower temperatures to induce carboxylic OH units in softwood kraft lignin. The higher amount of carboxylation obtained after ozone treatment allows for improved compatibility of lignin with other components. Further, the optimized conditions were there used for sequential oxidation with oxygen and ozone.

Chapter 6 of this research is focused on developing bio-based vitrimer polymer films with novel self-healing and swelling properties. Currently, finding a long term solution to the disposal thermoset waste remains one of the main challenges to be addressed. Most of the thermoset waste is disposed of by incineration and landfill due to the lack of suitable methods. To address this issue, researchers have considered the modification of thermosetting polymers using vitrimer chemistry. The associative bond exchange mechanism in vitrimers allows for dynamic covalent linkages which imparts repairability and recyclability to the thermosetting polymers. In this part of work, we utilized oxidized kraft liquor available after oxidation from oxygen to further utilize the lignin. Further, the kraft liquor was subject to ozone treatment to improve the carboxyl content in lignin. The sequentially oxidized kraft lignin was cured with polyethylene glycol diglycidyl ether (PEG-

epoxy) to vitrimer films with a high thermal stability, self-healing and fast relaxation due to the presence of bond exchangeable cross-linked networks. The vitrimer films also exhibited notable swelling properties in aqueous alkaline solutions which is a key indicator of the dynamic transesterification in the cured network.

The organization of this dissertation is as follows: **Chapter 2** provides a review of lignin hydrogen peroxide oxidation chemistry with emphasis on aromatic aldehydes and acids. **Chapter 3** provides a background information on the development of bio-based vitrimer polymers from lignocellulosic feedstock. **Chapter 4** describes a new insight of the retro-aldol reaction for oxidative conversion of lignin to vanillin and vanillic acid. **Chapter 5** highlights the effect of oxygen and ozone oxidation on functional group content in softwood kraft lignin. **Chapter 6** highlights a novel and integrated approach for the valorization of kraft lignin to produce lignin based vitrimers. **Chapter 7** outlines the conclusions and discusses the future work of this research.

1.3 References

[1] W. Post, A. Susa, R. Blaauw, K. Molenveld, and R. J. Knoop, "A review on the potential and limitations of recyclable thermosets for structural applications," *Polym. Rev*., vol. 60, no. 2, pp. 359-388, 2020.

[2] L. Shen, J. Haufe, and M.K. Patel, "Product overview and market projection of emerging bio-based plastics," PRO-BIP; Final Report, Report No: NWS-E-2009-32, pp. 243, 2009. Utrecht, The Netherlands: Utrecht University [accessed 31 May 2022].

[3] S. Guadix-Montero, and M. Sankar, "Review on catalytic cleavage of C-C inter-unit linkages in lignin model compounds: towards lignin depolymerization," *Top. Catal*., vol. 3, no. 4, pp. 183-198, 2018.

[4] P. C. R. Pinto, E. A. B. da Silva, and A. E. Rodrigues, “Lignin as source fine chemicals: vanillin and syringaldehyde,” Biomass Conversion, *Springer*, New York, pp. 381-420, 2012.

[5] D. Bajwa, G. Pourhashem, A. Ullah, and S. Bajwa, “A concise review of current lignin production, applications, products and their environmental impact,” *Ind. Crops. Prod*., vol. 139, pp. 111526, 2019.

[6] J. L. Cole, P. A. Clark, and E.I. Solomon, “Spectroscopic and chemical studies of the laccase trinuclear copper active site: geometric and electronic structure,” *J. Am. Chem. Soc*., vol. 112, no. 26, pp. 9534-9548, 1990.

[7] C. Crestini, R. Saladino, P. Tagliatesta, and T. Boschi, “Biomimetic degradation of lignin and lignin model compounds by synthetic anionic and cationic water soluble manganese and iron porphyrins,” *Bioorg. Med. Chem*., vol. 7, no. 9, pp. 1897-1905, 1999.

[8] B. Moodley, D. Mulholland, and H. Brookes, “The chemical oxidation of lignin found in Sappi Saiccor dissolving pulp mill effluent,” *Water S. A*., vol. 38, no. 1, pp. 1-8, 2012.

[9] X. P. Ouyang, Y. D. Tan, and X. Q. Qiu, “Oxidative degradation of lignin for producing monophenolic compounds,” *J. Fuel Chem. Technol*., vol. 42, pp. 677–682, 2014.

[10] H. S. Genin, K. A. Lawler, R. Hoffmann, W. A. Herrmann, R. W. Fischer, and W. Scherer, “Multiple bonds between main-group elements and transition metals. 138. Polymeric methyltrioxorhenium: some models for its electronic structure,” *J. Am. Chem. Soc*., vol. 117, no. 11, pp. 3244-3252, 1995.

[11] Y. Ni, A. Van Heiningen, and G. Kubes, “Mechanism of formation of chloro-organics during chlorine dioxide prebleaching of kraft pulp,” *Nord. Pulp Pap. Res. J*., vol. 8, no. 4, pp. 350-351, 1993.

[12] E.I. Solomon, and M.D. Lowery, “Electronic structure contributions to function in bioinorganic chemistry,” *Science*, vol. 259, no. 5101, pp. 1575-1581, 1993.

[13] D. P. Bezerra, A. K. N. Soares, and D.P. de Sousa, “Overview of the role of vanillin on redox status and cancer development,” *Oxid. Med. Cell. Longev*., vol. 2016, Article ID: 9734816, 2016.

[14] J. Choo, Y. Rukayadi, and J. K. Hwang, “Inhibition of bacterial quorum sensing by vanilla extract,” *Lett. Appl. Microbiol*., vol. 42, no. 6, pp. 637-641, 2006.

[15] C. S. Calixto-Campos, T. T. Carvalho, M.S. Hohmann, F. A. Pinho-Ribeiro, V. Fattori, M. F. Manchope, A. C. Zarpelon, M. M. Baracat, S. R. Georgetti, and R. Casagrande, “Vanillic acid inhibits inflammatory pain by inhibiting neutrophil recruitment, oxidative stress, cytokine production, and NFκB activation in mice,” *J. Nat. Prod*., vol. 78, no.8 pp. 1799-1808, 2015.

[16] J. D. P. Araújo, “Production of vanillin from lignin present in the Kraft black liquor of the pulp and paper industry,” Ph.D. thesis, University of Porto, Porto, Portugal, 2008 [accessed 31 May 2022].

[17] M. B. Hocking, “Vanillin: synthetic flavoring from spent sulfite liquor,” *J. Chem. Educ*., vol. 74, no. 9, pp. 1055, 1997.

[18] M. Fache, B. Boutevin, and S. Caillol, “Vanillin production from lignin and its use as a renewable chemical,” *ACS Sustain. Chem. Eng*., vol. 4, no. 1, pp. 35-46, 2016.

[19] H. L’udmila, J. Michal, S. Andrea, and H. Ales, “Lignin, potential products and their market value,” *Tech. Rep. CRDLR US Army Chem. Res. Dev. Lab*., vol. 60, pp. 973-986, 2015.

[20] N. Smolarski, “High-value opportunities for lignin: unlocking its potential,” Paris: Frost & Sullivan, pp. 1-15, 2012.

[21] H. Lange, S. Decina, and C. Crestini, “Oxidative upgrade of lignin–Recent routes reviewed,” *Eur. Polym. J*., vol. 49, pp. 1151-1173, 2013.

[22] C. Crestini, H. Lange, M. Sette, and D. S. Argyropoulos, "On the structure of softwood kraft lignin," *Green Chem.*, vol. 19, no. 17, pp. 4104-4121, 2017.

[23] L. Kouisni, A. Gagné, K. Maki, P. Holt-Hindle, and M. Paleologou, "LignoForce system for the recovery of lignin from black liquor: feedstock options, odor profile, and product characterization," *ACS Sus. Chem. Eng*., vol. 4, no. 10, pp. 5152-5159, 2016.

[24] G. Gellerstedt, and D. Robert, "Quantitative 13C NMR analysis of kraft lignins," *Acta Chem. Scand*., vol. B41, no. 7, pp. 541-546, 1987

[25] M. Y. Balakshin, and E.A. Capanema, "Comprehensive structural analysis of biorefinery lignins with a quantitative 13 C NMR approach," *RSC advances*, vol. 5, no. 106, pp. 87187-87199, 2015.

[26] L. Zhang, and G. Gellerstedt, "2D heteronuclear (^{1}H-^{13}C) single quantum correlation (HSQC) NMR analysis of Norway spruce bark components: Characterization of lignocellulosic materials" T. Q. Hu (ed.); Blackwell Publishing Ltd.: Oxford, pp. 3-16, 2008.

[27] H. Kim, and J. Ralph, "Solution-state 2D NMR of ball-milled plant cell wall gels in DMSO-d_6/pyridine-d_5," *Org. Biomol. Chem. Org*., vol. 8, no. 3, pp. 576-591, 2010.

[28] Y. Archipov, D. Argyropoulos, H. Bolker, and C. Heitner, "^{31}P NMR spectroscopy in wood chemistry. I. Model compounds," *J. Wood Chem. Technol*., vol. 11, no. 2, pp. 137-157, 1991

[29] D. Montarnal, M. Capelot, F. Tournilhac, and L. Leibler, "Silica-like malleable materials from permanent organic networks," *Science*, vol. 334, no. 6058, pp. 965-968, 2011.

[30] C. J. Kloxin, T.F. Scott, B.J. Adzima, and C.N. Bowman, "Covalent adaptable networks (CANs): a unique paradigm in cross-linked polymers," *Macromolecules*, vol. 43, no. 6, pp. 2643-2653, 2010.

[31] T. Liu, X. Guo, W. Liu, C. Hao, L. Wang, W.C. Hiscox, C. Liu, C. Jin, J. Xin, and J. Zhang, "Selective cleavage of ester linkages of anhydride-cured epoxy using a benign method and reuse of the decomposed polymer in new epoxy preparation," *Green Chem*., vol.19, no. 18, pp. 4364-4372, 2017.

[32] W. Denissen, J. M. Winne, and F.E. Du Prez, "Vitrimers: permanent organic networks with glass-like fluidity," *Chem. Sci*., vol. 7, no. 1, pp. 30-38, 2016.

[33] P.C.R. Pinto, E.A.B. da Silva, and A.E. Rodrigues, "Lignin as source of fine chemicals: vanillin and syringaldehyde," Biomass Conversion; C. Baskar, S. Baskar, R.D. Dhillon, Eds; Springer: London, pp. 381-420, 2012.

[34] A.W. Pacek, P. Ding, M. Garrett, G. Sheldrake, and A.W. Nienow, "Catalytic conversion of sodium lignosulfonate to vanillin: engineering aspects. Part 1. Effects of processing conditions on vanillin yield and selectivity," *Ind. Eng. Chem. Res*., vol. 52, pp. 8361-8372, 2013.

[35] T. Q. Hu, "Chemical modification, properties, and usage of lignin," Kluwer Academic/Plenum Publisher, New York, pp. 291, 2002.

[36] V.E. Tarabanko, and N. Tarabanko, "Catalytic oxidation of lignins into the aromatic aldehydes: general process trends and development prospects," *Int. J. Mol. Sci*., vol. 18, pp. 2421, 2017.

[37] M. Fache, B. Boutevin, and S. Caillol, "Vanillin production from lignin and its use as a renewable chemical," *ACS Sustain. Chem. Eng*., vol. 4, no. 1, pp. 35-46, 2016.

Chapter 2 | A review of lignin hydrogen peroxide oxidation chemistry with emphasis on aromatic aldehydes and acids

This review discusses the main factors that govern the oxidation processes of lignins into aromatic aldehydes and acids using hydrogen peroxide. Aromatic aldehydes and acids are produced in the oxidative degradation of lignin whereas mono and dicarboxylic acids are the main products. The stability of hydrogen peroxide under the reaction conditions is an important factor that needs to be addressed for selectively improving the yield of aromatic aldehydes. Hydrogen peroxide in the presence of heavy metal ions readily decomposes, leading to minor degradation of lignin. This degradation results in quinones which are highly reactive towards peroxide. Under these reaction conditions, the pH of the reaction medium defines the reaction mechanism and the product distribution. Under acidic conditions, hydrogen peroxide reacts electrophilically with electron rich aromatic and olefinic structures at comparatively higher temperatures. In contrast, under alkaline conditions it reacts nucleophilically with electron deficient carbonyl and conjugated carbonyl structures in lignin. The reaction pattern in the oxidation of lignin usually involves cleavage of the aromatic ring, the aliphatic side chain or other linkages which will be discussed in this review.

2.1. Introduction

Practically viable and economic conversion of lignocellulosic biomass to value added products is an important challenge that requires integrated processing and effective utilization of lignin [1]. Lignin is nature's second most abundant polymer after cellulose and it contributes as much as 30% of the organic carbon content in the biosphere [2, 3]. Lignin obtained from paper and biofuel production is currently being used as energy, however it can be further converted to value added chemicals [4, 5]. Several studies have reported on the conversion of lignin to value added chemicals including aromatic fine chemicals, carboxylic acids and monomers for polymer

production [6-9]. The controlled breaking of carbon-carbon and carbon-oxygen bonds in lignin represents a very selective de-polymerization that could produce a whole series of monomeric, aromatic species [10, 11].

Oxidation is one of the most widely studied lignin valorization processes. Over the years different routes have been followed to study lignin oxidation [12-19]. Oxidative degradation of lignin produces low molecular weight phenolic compounds which are value-added chemicals. Vanillin is one of the main value-added chemicals produced from this process. It is the major flavor constituent of vanilla and has a wide range of applications in the food and perfume industries. It is sold as a crystalline solid in two grades, technical and Food Chemicals Codex (FCC) grade. The FCC grade requires a minimum assay of 97.0% on dried basis. The technical grade is applied where there are no standards for quality and impurity levels and generally sells for about $2.00/kg less than FCC grade [20].

The commercial route for vanillin synthesis is being carried out by Solvay which is the world's leading producer of synthetic vanillin under the brand name Rhovanil® [21]. It is followed by Borregaard, the second largest producer of vanillin which also has ethyl vanillin production capacity and is the main supplier of vanillin to Europe [20]. The Borregaard process uses lignosulfonate as the starting lignin source which is catalytically oxidized at high pH with a transition metal catalyst at elevated temperature and pressure resulting in vanillin yields ranging from 5-7% with respect to lignosulfonate using oxygen as the oxidizing agent [22]. Over the recent years the demand for natural vanilla flavors from flavor manufacturers and from the food industry in general has been increasing. To answer the demand for natural vanillin, Solvay and Borregaard have developed Rhovanil® Natural and EuroVanillin respectively as an alternative to synthetic

vanillin [21, 23]. However, the raw material costs for natural vanillin are more expensive than the synthetic counterpart which makes synthetic vanillin more competitive and widely used [24].

From an industrial point of view, only sulfite lignin is currently used to prepare vanillin, despite the fact that it accounts for less than 10% of the total lignins extracted [24]. Kraft lignin which represents the majority of lignins separated, is mainly used as a low grade fuel in the pulping operation [25]. Therefore, there is a tremendous opportunity and economic incentive to use kraft lignin as a source to produce medium to high added value aromatic aldehydes. It is key to note that nitrobenzene is the oxidant that gives the highest yields of aromatic aldehydes and acids from kraft lignin. Nitrobenzene, however, is an expensive oxidant and its reduction products are harmful and difficult to separate, limiting its industrial application [26]. Oxygen is the preferred choice for producing value added products such as vanillin from kraft lignin, mainly because of its environmental friendliness, high atom economy and low price. However, catalysts in combination with oxygen are required to improve the yield of aromatic aldehydes by a factor of 1.5-2 [27]. In the kraft pulping process, it is imperative to avoid the use of catalysts so that downstream processing of kraft liquor is easily handled in evaporators and recovery boilers. Also, the oxidation of lignin with oxygen and nitrobenzene usually requires high temperatures and pressures and may result in many undesirable byproducts [28].

Hydrogen peroxide is an industrially attractive and environmentally benign chemical which is commonly used in pulp and paper industry [28]. It is easy to use and doesn't require any special equipment. Higher reactivity of hydrogen peroxide also enables it to cause significant degradation of non-phenolic lignin structures unlike oxygen [29]. The reduction potential of H_2O_2/H_2O pair is +1.763 V, compared to only +1.229 V for the O_2/H_2O pair in acidic medium whereas, in alkaline medium the reduction potential of H_2O_2/H_2O pair is +0.994 V, compared to

only +0.401 V for the O_2/H_2O [27, 30]. In contrast, nitrobenzene has a reduction potential (nitrobenzene to phenyl hydroxylamine) of -1.1 V in aqueous alkaline medium and -0.37 V in acidic medium [31]. A significant amount of experimental data in the field of lignin oxidation using oxygen and nitrobenzene has been accumulated and there are a number of modern reviews available based on these reagents. However, the recently published reviews only briefly discuss the use of hydrogen peroxide as an oxidizing agent for lignin [26, 27, 32]. The purpose of this review is to highlight the basic patterns, mechanisms and optimal conditions for utilizing hydrogen peroxide for oxidation of lignin.

2.2. Lignin Structure

Lignin is an amorphous high molecular mass biopolymer with a chemical structure distinct from the other constituents of wood. The chemical structure of the lignin is made up of phenyl-propane units that are not linked to each other in any systematic order. In general, lignins are categorized into three major groups: softwood, hardwood, and grass lignins. They arise from radical coupling of three main precursors: *p*-coumaryl, coniferyl and sinapyl alcohols (**Figure 2.1**) [33].

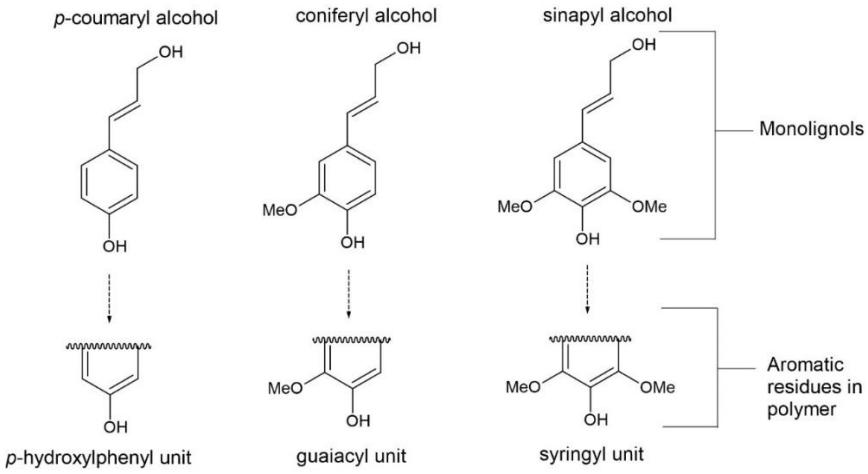

Figure 2.1. Monolignols present in the lignin [33] (reproduced with permission from John Wiley & Sons)

Peroxidase and laccase enzymes in the plant cell wall oxidize the phenolic OH groups of the monolignols, generating free radicals. Subsequently the complex lignin polymer is formed by homo-coupling or cross-coupling the monolignol radicals. Its composition is generally characterized by the relative abundance of *p*-hydroxyphenyl (H), guaiacyl (G) and syringyl (S) units (derived from each of the 3 major precursors) and by the distribution of interunit linkages in the polymer. The nomenclature followed in lignin model compounds is highlighted in **Figure 2.2**. Softwood, hardwood and grasses differ in major interunit linkages, abundance, methoxyl content and bond dissociation energies which are represented in (**Table 2.1** and **Figure 2.3**).

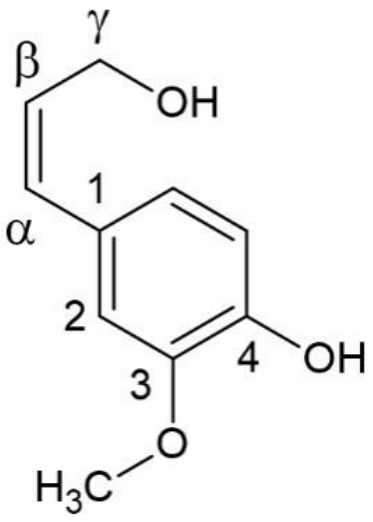

Figure 2.2. Nomenclature followed in lignin model compounds

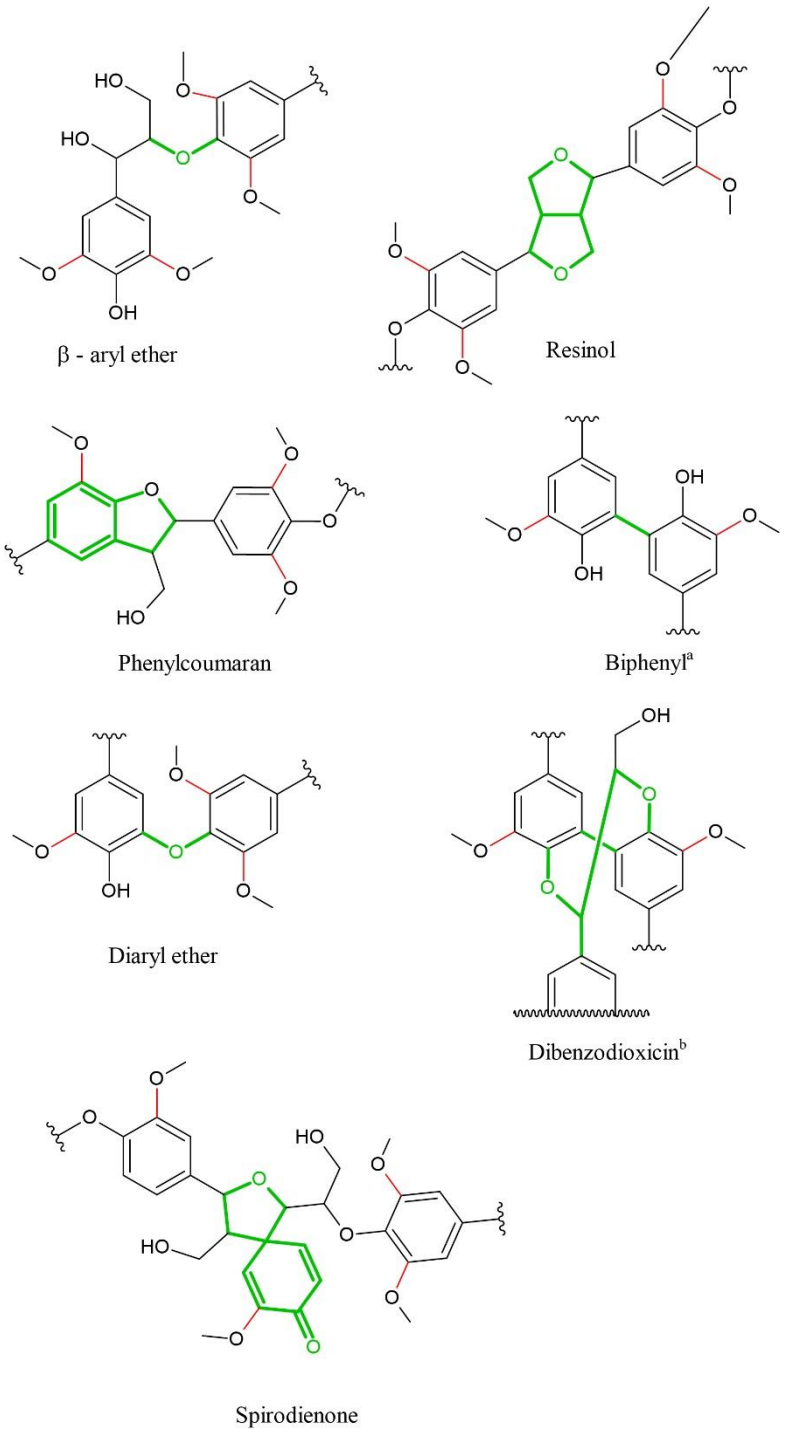

Figure 2.3. Major interunit linkages found in lignin [34] (reproduced with permission from John Wiley & Sons)

Major interunit linkages found in lignin	**β – aryl ether**	**Resinol**	**Phenyl-coumaran**	**Biphenyl[a] + Dibenzodioxicin[b]**	**Spirodienone**	**Diaryl ether**
Interunit linkage	β-O-4	(β-β) + (γ-O-α)	(β-5) + (α-O-4)	5-5[a] (5-5)+(α-O-4)+ (β-O-4)[b]	β-1 + (α-O-α)	4-O-5
Softwood (%)	45-50	2-6	9-12	5-7[b]	1-9	2
Hardwood (%)	60-62	3-16	3-11	<1[b]	1-7	2
Grasses (%)	74-84	1-7	5-11	n.d	n.d	n.d
Bond Dissociation Energy (kcal/mol)	C_β-O-C_4, 54-72 C_α-C_β 75-80	C_α-O 68 C_α-C_β 67 C_γ-O 79 C_β-C_β 81	C_α-O-C_4, 50-56 C_α-C_β 54-63	C_5- C_5, 115-118	C_β- C_1, 65-69 (for open structure)	C_4-O-C_5 78-83

Table 2.1. Different interunit linkages, their structure, abundance and bond dissociation energies found in softwood, hardwoods and grasses [34]

2.3. Sources of lignin

Lignins present in the raw plant biomass are termed native lignins. The extraction of native lignins from lignocellulosic biomass may be future targets. The byproduct lignin obtained from conventional pulping routes such as kraft and sulphite processes are often called as technical lignins [32]. The largest source of lignin comes wood pulping processes, most of which is derived from the kraft and sulphite processes [35]. In some mills, part of the liquor/lignin produced is diverted to increase the pulp production capacity. Since kraft technology is evolving, the utilization of kraft lignin to make value added products seems a viable approach.

2.3.1. Kraft lignin

Kraft lignin accounts for 85% of all the lignin produced in the world which is industrially produced from the kraft pulping process, and approximately 45 million metric tons/year of kraft lignin is produced worldwide. The aim of the kraft process is conversion of wood into pulp which is the main raw material for paper. Kraft lignin is commonly found in black liquor, the byproduct stream of pulp and paper mills. β-aryl ether bonds are broken via sulfidolytic cleavage in phenolic phenyl propane units and via alkaline cleavage in non-phenolic phenyl propane units to result in a highly modified structure of kraft lignin (**Figure 2.4**). It has low average molecular weight (M_n) of about 1000 – 3000 Da with a polydispersity between 2 and 4 and an estimated average monomer molecular weight of 180 Da. It is soluble in alkali and highly polar organic solvents [6].

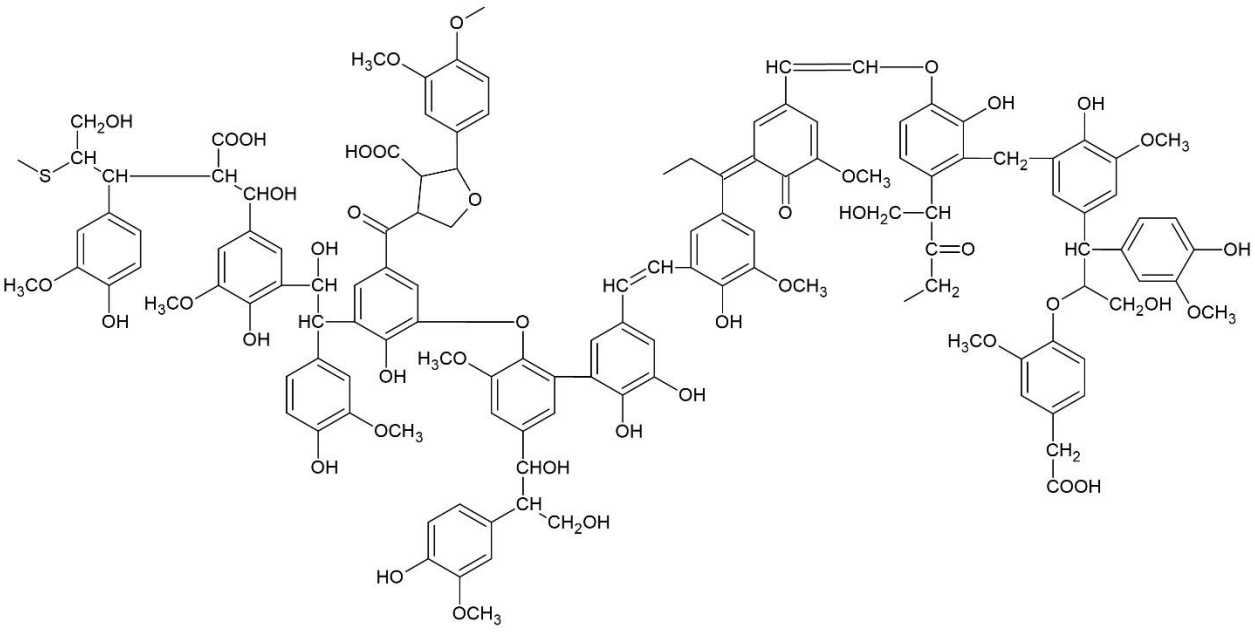

Figure 2.4. Structure of kraft lignin [36] (reproduced with permission from Elsevier)

2.3.2. Lignosulfonates

Sulfite lignins or lignosulfonates (**Figure 2.5**) are obtained from sulfite pulping of wood. The annual global production of lignosulfonates is 2 million metric tons/year [25]. In this process the wood is made soluble by sulfonation mainly at benzyl alcohol, benzyl aryl ether and benzyl alkyl ether linkages on the side chain of phenyl propane units [37]. Hardwood lignosulfonates and softwood lignosulfonates are obtained from waste pulping liquor concentrated by the Howard process after stripping and recovery of sulphur [38]. They have an average monomer molecular weights in the range of 188 Da, and 215-154 Da, for softwood and hardwood lignosulfonates respectively. They exhibit number-average molecular weight (M_n) from 1000 Da to 140,000 Da, with the majority lying between 5000 Da and 20,000 Da [6]. Lignosulfonate is soluble in acidic, basic and aqueous solutions, and in highly polar organic solvents but hydrolysis reactions, and eventually excessive sulfonations can occur.

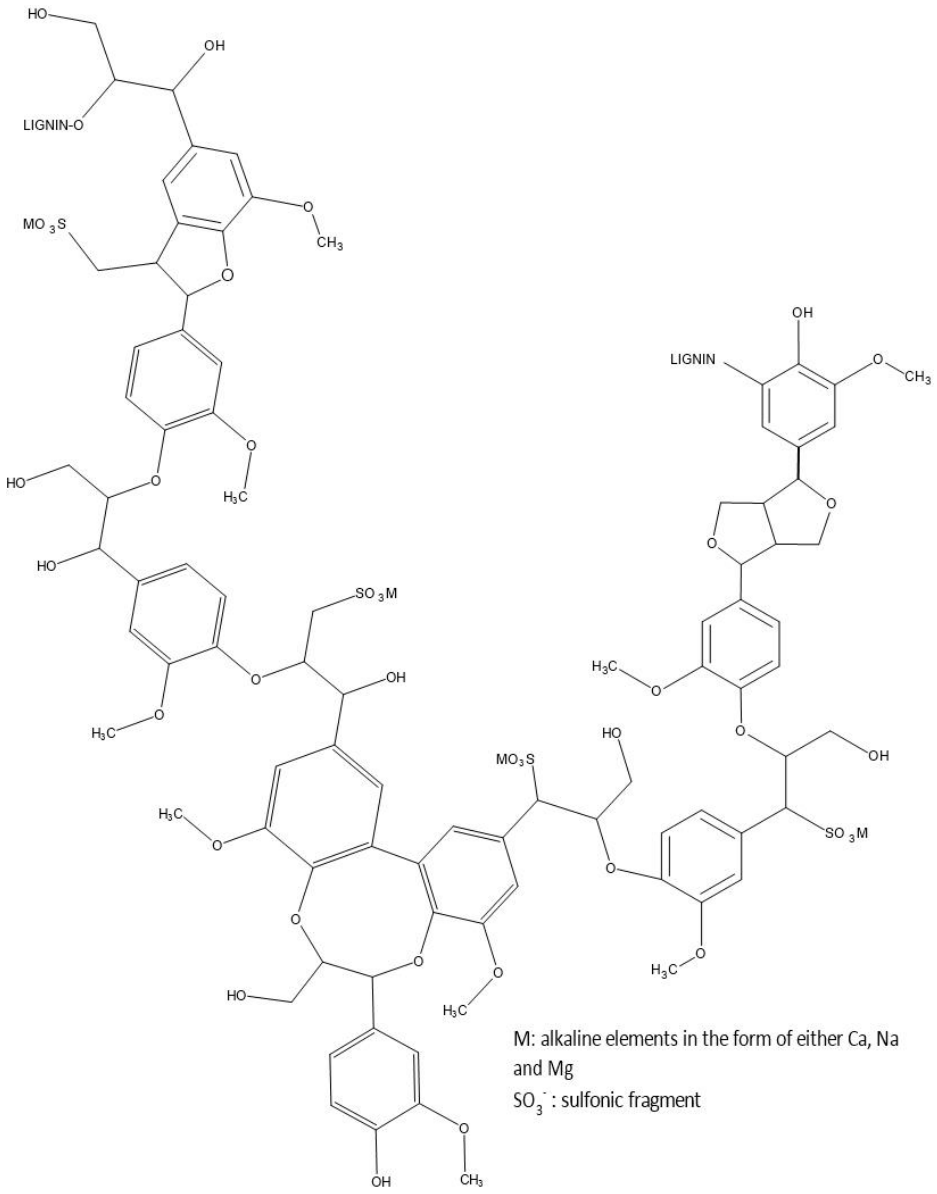

Figure 2.5. Structure of lignosulfonate [6] (reproduced with permission from Elsevier)

2.3.3. Biorefinery lignin

Biorefinery lignin refers to lignin that is isolated from both woody biomass and agricultural residues by different pretreatment methods. The structural characteristics of biorefinery lignin vary depending upon the pretreatment methods [39]. As the biomass refinery is emerging over the recent years, tremendous amounts of biorefinery lignin is becoming available in addition to kraft and sulfite lignin [10]. The main features of biorefinery lignin are represented in **Table 2.2**.

Spectral region	Number of moieties per aromatic ring				
	Milled Wood lignin (MWL)	**Deep Eutectic Solvent based lignin (DESL)**	**Dilute acid-pretreated corn-stover lignin (DACSL)**	**Steam-exploded spruce lignin (SESPL)**	**Soda-pretreated wheat-straw lignin (Soda-WSL)**
Methoxy content	0.97	0.90	1.19	0.97	1.25
C_{Ar}-H	2.75	3.09	2.45	2.46	2.67
C_{Ar}-C	1.66	1.69	1.93	2.12	1.80
C_{Ar}-O	1.59	1.22	1.62	1.42	1.53
phenolic hydroxyl	0.05	0.49	0.22	0.30	0.01
aliphatic hydroxyl	1.62	1.54	0.95	1.03	1.30
saturated CH_2 or CH_3 on aliphatic side chain	1.83	1.97	2.33	2.41	1.93
C_γ in β-5 and β-O-4 with C=O	0.65	ND[a]	0.26	0.29	0.36
C_α in β-O-4	0.57	ND[a]	0.21	0.28	0.51
C_β in β-O-4	0.42	0.16	0.36	0.20	0.21
[a] ND = not determined					

Table 2.2. Main features of Biorefinery lignin [39]

2.4. Mechanism of lignin oxidation by oxygen and peroxide

It is well documented that there are clear commonalities between the oxidative chemistries of lignin by oxygen and peroxide [27, 30, 40]. Both oxygen and peroxide are present and involved in the oxidation of lignin by oxygen and peroxide because hydrogen peroxide is formed during oxygen oxidation while oxygen is generated during peroxide oxidation [29, 30, 40, 41]. The chemistry of oxygen oxidation is also linked to hydrogen peroxide within the oxidation cycle via superoxide anion radicals as shown in **Figure 2.6** [40].

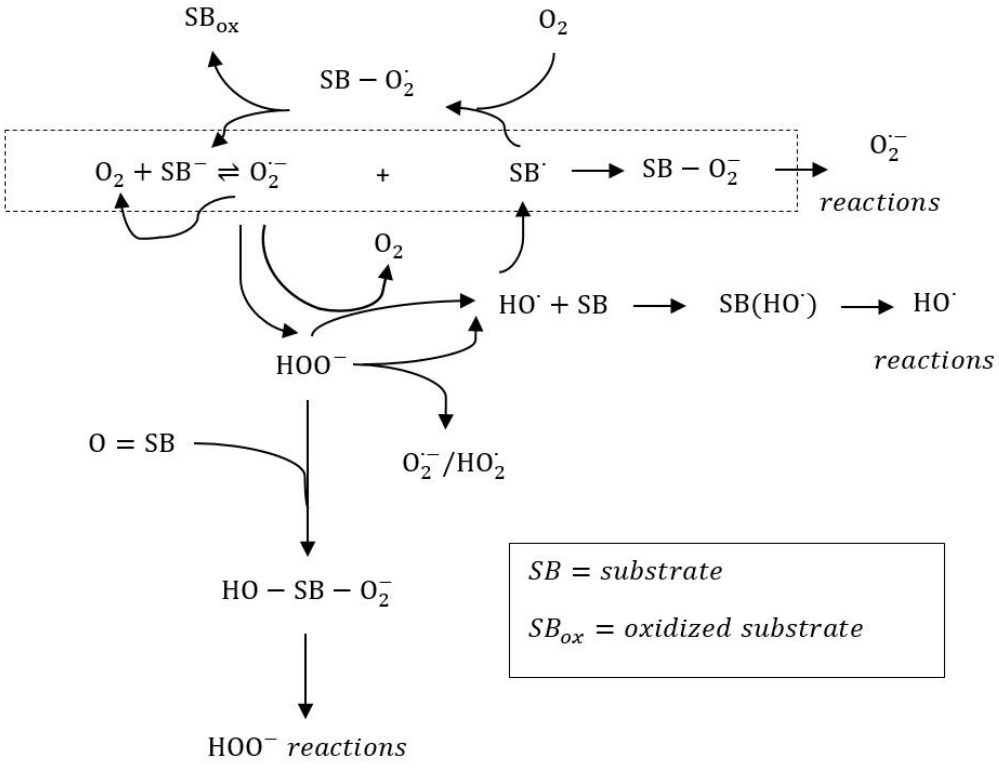

Figure 2.6. Course of oxygen and hydrogen peroxide oxidation cycle [40] (reproduced from Holzforschung)

2.4.1. Oxygen oxidation

The mechanism of lignin oxidation using oxygen has been proposed by various authors [20, 26, 27, 42]. The reaction mechanism of oxygen proceeds via formation of following species [30]:

$$\cdot O - O \cdot + e^- \rightleftharpoons O_2^{-\cdot}$$

$$O_2^{-\cdot} + HOO^{\cdot} \rightarrow \cdot O - O \cdot + HOO^-$$

$$HOOH + HOO^- \rightarrow O_2^{-\cdot} + H_2O + HO^{\cdot}$$

$$HO^{\cdot} + O_2^{-\cdot} \rightarrow \cdot O - O \cdot + HO^-$$

The mechanism of lignin oxidation using oxygen typically involves radicals. In the absence of catalysts, the oxidation proceeds via chain reactions involving alkoxyl, hydroxyl and peroxyl radicals that are too active to achieve process selectivity [27]. In alkaline conditions, the reaction begins with dehydration of C_α -C_β bond followed by electron abstraction from the phenoxyl anion (**Step 1**). The oxygen oxidation is initiated by single electron transfer from activated phenoxyl anion species with the formation of a superoxide anion radical $O_2^{-\cdot}$ and phenoxyl radical. This step happens at elevated temperatures or in the presence of traces of heavy metals which act as redox catalysts. This may further yield a substrate linked peroxide anion. The formation of a quinone methide intermediate can take place by the disproportionation of the phenoxyl radical [43] (**Step 2a**) or by the oxidation of this radical preceded by proton detachment (**Step 2b**). Under thermodynamic control, the addition of nucleophilic agents to quinone methides (**Step 3**) occurs mainly at the γ-position whereas under kinetic control the addition occurs at the α-position [42]. The formation of vanillin from retroaldol cleavage of an α – unsaturated aldehyde (**Step 5a**) requires strong alkalinity and if the conditions are not maintained, byproducts are formed by the oxidation of unsaturated aldehydes. The retro-aldol cleavage is a reversible reaction and the probability of the reaction favoring vanillin formation is dependent on the pH, thermodynamic and kinetic control of the reaction conditions. The final step proceeds through dissociation of C-H bond

of the phenoxyl anion [27]. Hence, from the mechanism proposed below, vanillin formation from lignin requires proper control of desired conditions. The following is the step by step explanation of the proposed mechanism.

Step 1: Initiation with electron detachment of phenoxyl anion to form phenoxyl radical

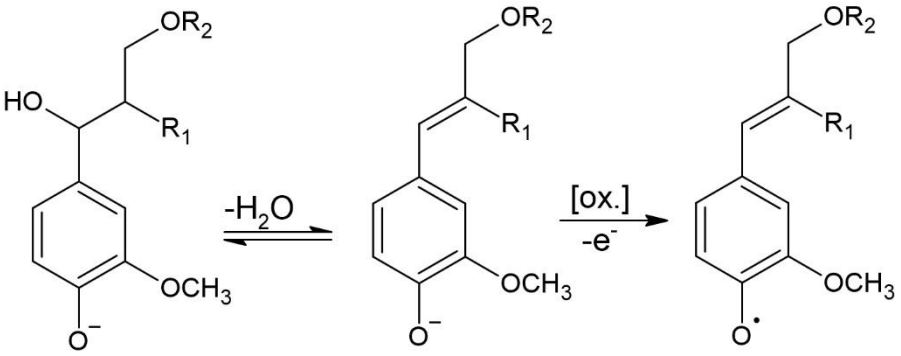

Step 2a: Disproportionation of phenoxyl radical to form quinone methide

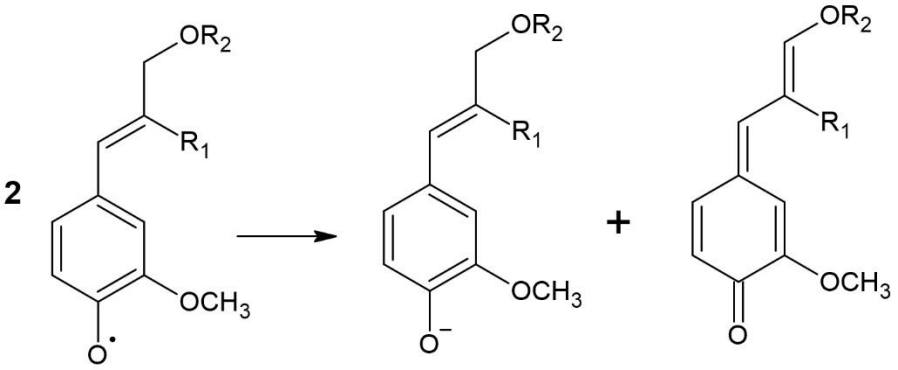

Step 2b: Oxidation of phenoxyl radical preceded by proton detachment

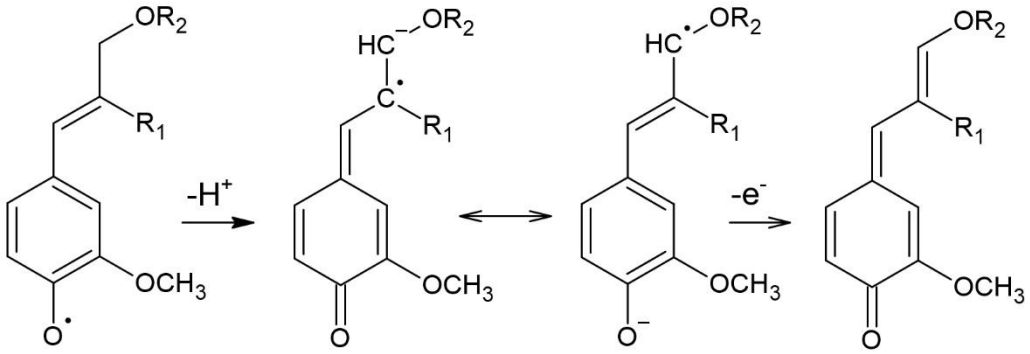

Step 3: Nucleophilic addition of hydroxide ion to form coniferyl alcohol structure from quinone methide

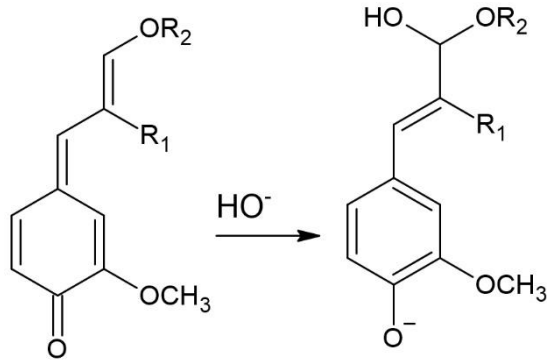

Step 4: Oxidation of coniferyl alcohol structure to γ-carbonyl group

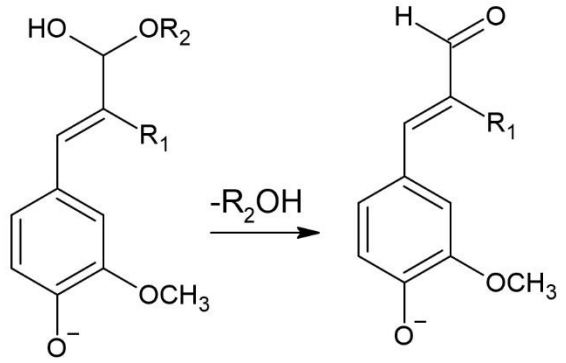

Step 5a: Retroaldol reaction of α- unsaturated aldehyde to form vanillin

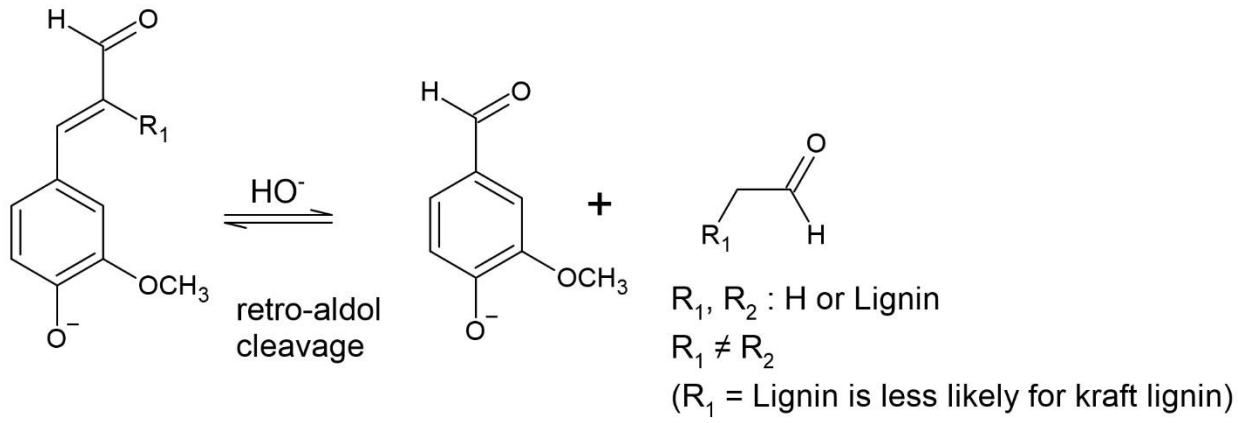

The formation of substrate linked peroxide anion from superoxide anion radicals may also further yield aromatic aldehydes such as vanillin (**Step 5b**) [30, 40]. This proceeds through cleavage of

conjugated double bonds. The drawback of this pathway is that it cannot be extrapolated towards selective oxidants such as nitrobenzene or copper oxide [27].

Step 5b: Formation of aromatic aldehydes via attack of superoxide anion radical $O_2^{-\cdot}$

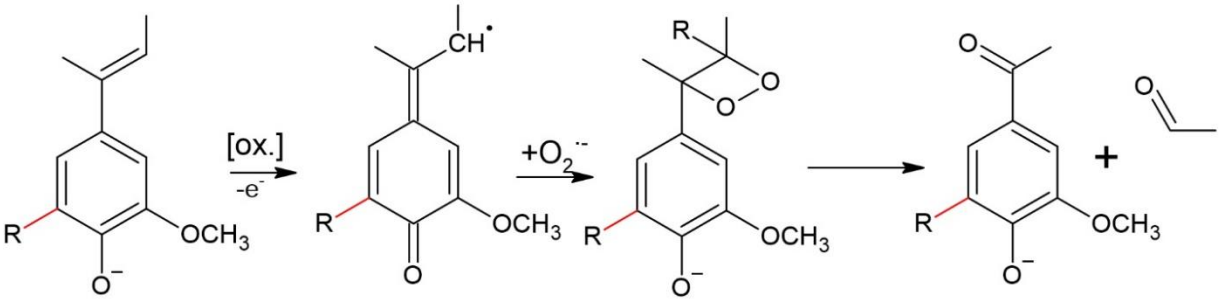

(Figures in **Step 1** to **5b** are reproduced from open access article published by MDPI)

Besides C-C cleavage, superoxide anion radicals may also undergo proton and heavy metal catalyzed dismutation under alkaline conditions (pH > 6) to form oxygen and hydrogen peroxide **Figure 2.6**. In presence of alkali promoted, heavy metal-catalyzed reactions, hydrogen peroxide may disproportionate to form hydroxyl and re-form superoxide anion radicals [40]. The hydroxyl radical is the most reactive among all the reactive oxygen species. The formation of the hydroxyl radical is accelerated in the presence of transition metal catalysts required in the oxygen oxidation of lignin [10, 27, 44]. In this oxidation cycle in the presence of metal catalysts, the Haber-Weiss reaction generates hydroxyl radicals from hydrogen peroxide and superoxide anion radical [45]. The following reactions occur:

a) Fe(III) reduction by $O_2^{\cdot-}$

$$Fe^{3+} + O_2^{\cdot-} \rightarrow Fe^{2+} + O_2 \qquad \text{(a)}$$

b) Fe(II) oxidation by hydrogen peroxide (Fenton reaction)

$$Fe^{2+} + H_2O_2 \rightarrow Fe^{3+} + OH^- + OH^{\cdot} \qquad \text{(b)}$$

$$O_2^{\cdot-} + H_2O_2 \rightarrow OH^{\cdot} + OH^- + O_2 \qquad \text{(net reaction)}$$

The presence of transition metal catalysts is crucial for the Haber-Weiss reaction since the rate of reaction in the absence of catalysts is negligible. The effect of the hydroxyl radical in the oxidation processes can be explained through the redox potential. In alkaline media, the redox potential of hydroxyl radical is +1.89 V, whereas the superoxide anion radical is close to the redox potential of molecular oxygen +0.40 V [27, 40]. The hydroxyl radical is too active for vanillin preservation. Therefore, it is evident that to enhance the yield of vanillin, it is important to decrease the impact of oxygen and its reactive radical forms such as hydroxyl radicals. This may be addressed by using hydrogen peroxide which is relatively stable compared to other reactive oxygen species. Also, non-phenolic lignin structures are not attacked by oxygen to any noticeable extent since the initial step of electron transfer (**Figure 2.6**) from the non-phenolic substrate to oxygen does not take place [40]. Hydrogen peroxide is moderately active and does not have unpaired electrons unlike oxygen radicals. Another major advantage of using hydrogen peroxide is that non-phenolic lignin structures are also reactive during oxidation reaction unlike oxygen [29]. An effort to address the developments in oxidation of lignin using hydrogen peroxide is made in following sections to further develop the understanding.

2.4.2. Hydrogen peroxide oxidation

Phenolic cinnamaldehyde structures of the coniferaldehyde type are readily cleaved by alkaline hydrogen peroxide giving rise to corresponding aromatic aldehyde such as vanillin which can be further converted to aromatic acids such as vanillic acid [30, 46]. The reaction proceeds with nucleophilic attack of hydrogen peroxide at C_α position forming an intermediate epoxide. The α-carbonyl structures in phenolic units are quantitatively cleaved to form the corresponding methoxy-hydroquinone derivatives [29, 30]. In the presence of phenolic units, the reaction proceeds via a Dakin-reaction and the intermediate formation of an epoxide which under alkaline

conditions is rapidly hydrolyzed accompanied by cleavage of the C_α – C_1 forming the corresponding methoxy hydroquinone derivatives. The mechanism representing this cleavage reactions is shown in **Figure 2.7, scheme A**.

Scheme A

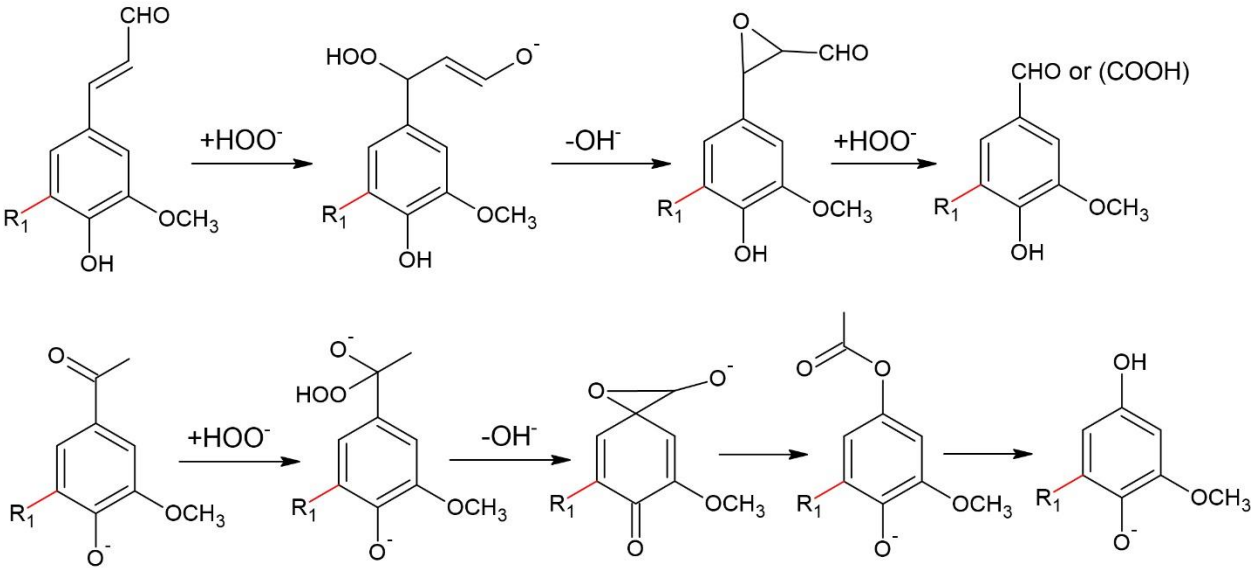

Scheme B

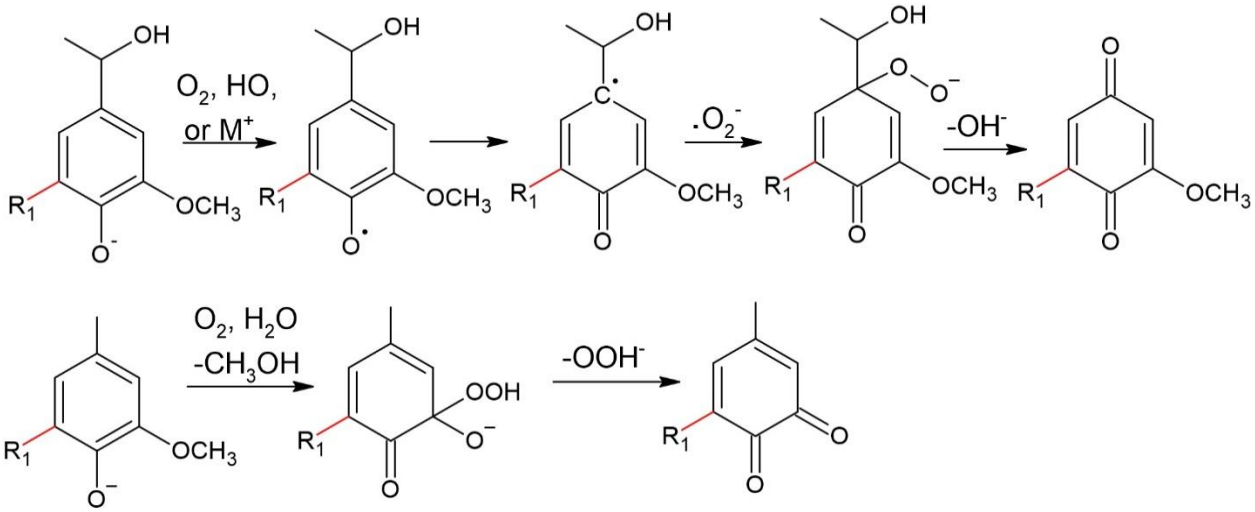

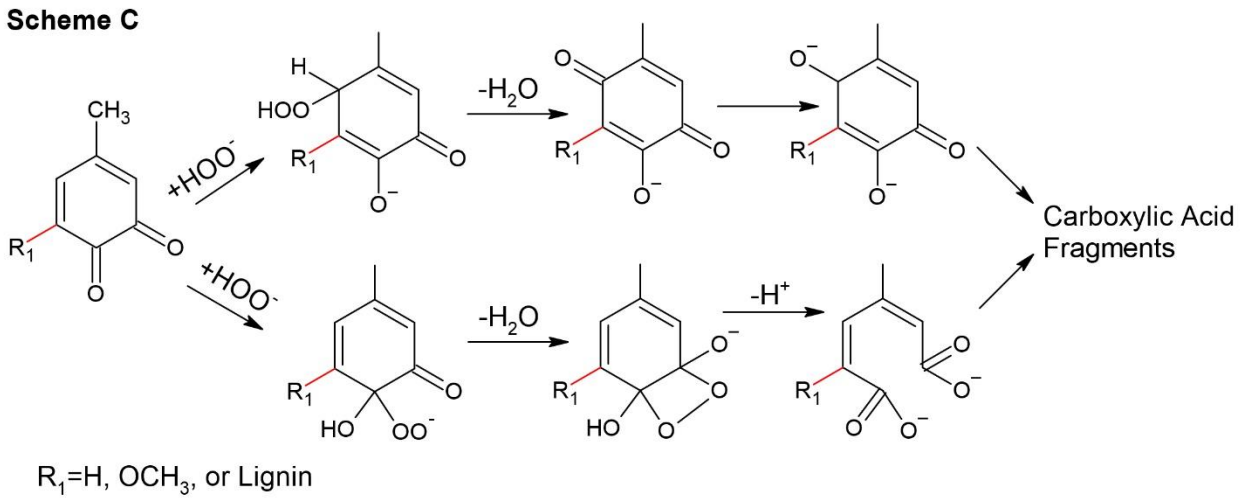

Figure 2.7. Hydrogen peroxide oxidation of phenolic-lignin mechanisms: A) conjugated side-chain oxidation, B) aromatic ring oxidation to benzoquinone structures, C) aromatic ring cleavage [30] (reproduced with permission from John Wiley & Sons)

For α-carbinol structures, the reaction proceeds via formation of a quinone methide intermediate followed by the Daikin-like reaction as represented in **Figure 2.7, scheme B**. The corresponding hydroperoxide is formed when the quinone methide rapidly reacts with superoxide ions [41]. The hydroperoxide derivative then forms *p*-quinone type structures. In the case where reactive moieties are absent in the α- position, nucleophilic attack by the hydroperoxide takes place at ortho- position, where the methyl group is eliminated. Subsequently, *o*-quinone type structures are then formed. Multiple reaction sites present in the *o*- and *p*- quinone rings are feasible for attack by hydroperoxide anions leading to ring opening products as shown in **Figure 2.7, scheme C**.

Unlike oxygen oxidation of lignin, hydrogen peroxide can react with non-phenolic lignin structures. In the case of non-phenolic units with aryl-α-carbonyl conjugated structures, intramolecular nucleophilic attack leads to formation of a new phenolic hydroxyl group and a dioxetane intermediate which decomposes to the corresponding benzaldehyde which can further

oxidize [29]. The Dakin reaction is precluded in this case due to absence of a free-phenolic hydroxyl group as shown in **Figure 2.8.**

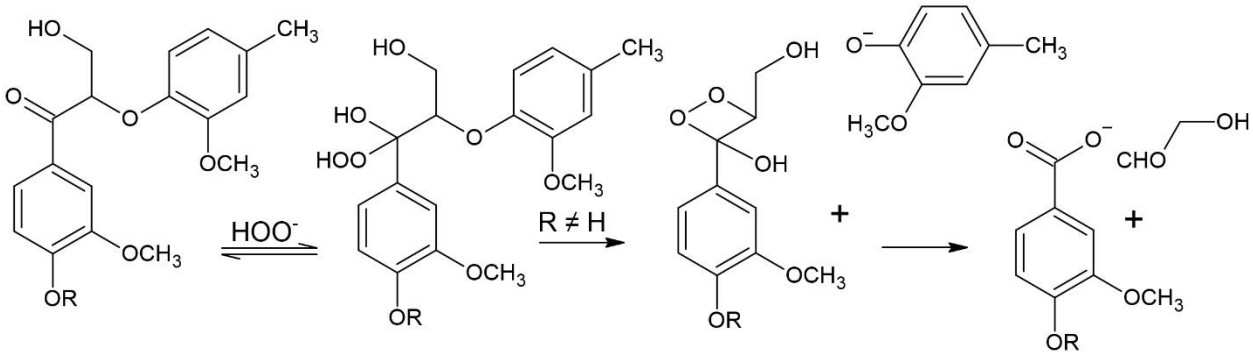

Figure 2.8. Hydrogen peroxide oxidation of non-phenolic lignin with aryl- α-carbonyl conjugated structures [29] (reproduced with permission from American Chemical Society)

In non-phenolic cinnamaldehyde type structures, the hydroperoxide anion nucleophilically attacks α-carbon. An intermediate epoxide is formed after elimination of a hydroxide ion, which subsequently forms veratraldehyde type structures as shown in **Figure 2.9**. The side chain of these compounds is simultaneously oxidized to form an intermediate glyoxal which further results into the formation of formic acid [46]. In the case of α-carbinol structures like veratryl alcohols, the reaction proceeds via formation of veratric acid as shown in **Figure 2.10. Scheme A**. The reaction proceeds by way of an S_N2 mechanism due to the presence of an etherified phenolic hydroxyl group. An intermediate formation of veratraldehyde takes place due to deprotonation-oxidation of hydroperoxide formed from veratryl alcohol. Veratraldehyde is further nucleophilically attacked by the hydrogen peroxide anion to form hydroperoxyacetal which is a highly unstable tetrahedral intermediate. This intermediate finally results in veratric acid via deprotonation followed by oxidation [47]. Due to the low pK_a of the perhydroxy anion, competition between oxidation and

dimerization takes place between veratryl alcohol and its corresponding hydroperoxide intermediate as shown in **Figure 2.10. Scheme B.**

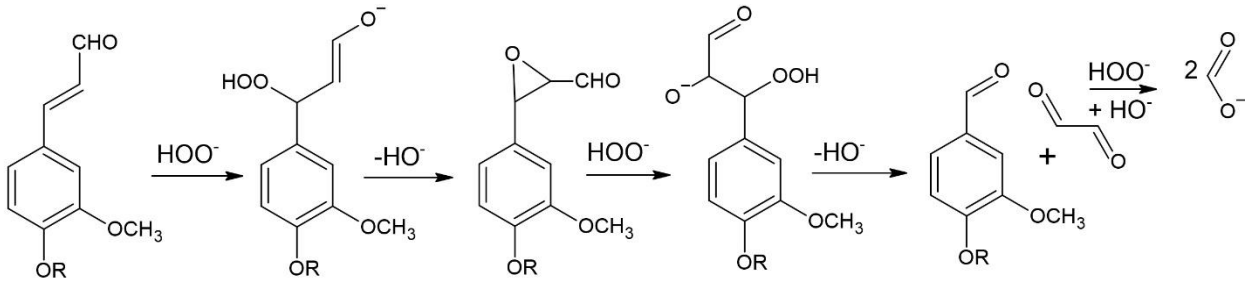

Figure 2.9. Hydrogen peroxide oxidation of non-phenolic lignin with cinnamaldehyde conjugated structures [46] (reproduced with permission from John Wiley & Sons)

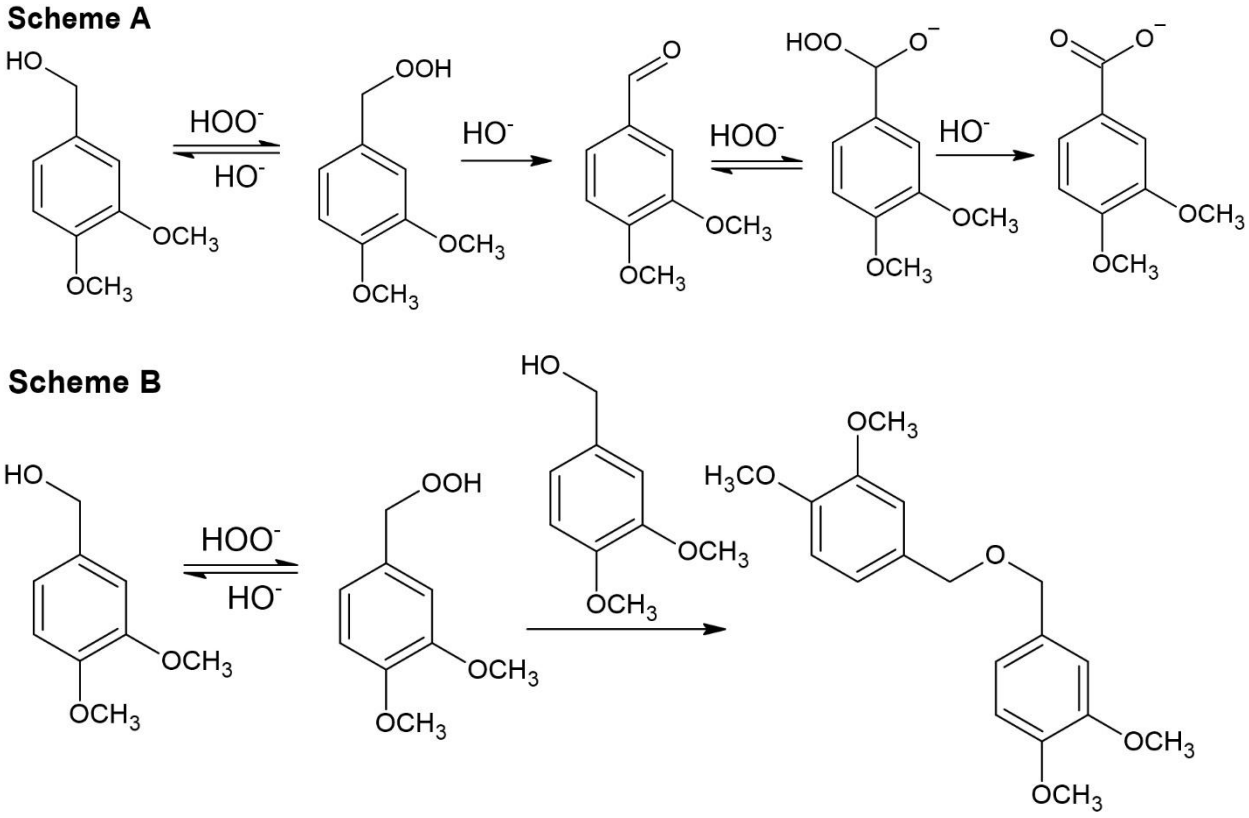

Figure 2.10. Scheme A. Hydrogen peroxide oxidation of non-phenolic lignin with α-carbinol structures. **Scheme B**. Dimer formation in the reaction of α-carbinols [47] (reproduced from Holzforschung)

2.4.2.1. Effect of pH

Hydrogen peroxide is a powerful oxidizing agent reacting both as an electrophile and nucleophile depending upon the pH of the medium. Under acidic conditions, it acts as an electrophile by forming OH^+species [48]. The reaction is summarized as follows:

$$H_2O_2 + H^+ \leftrightarrow H_2^+OOH \leftrightarrow H_2O + OH^+$$

Whereas, under alkaline conditions it mainly works by forming the perhydroxyl ion OOH^- as shown in the following reactions [49, 50]

1) $H_2O_2 + OH^- \leftrightarrow OOH^- + H_2O$
2) $OOH^- + \text{chromophore} \rightarrow \text{bleaching (chromophore destroyed)}$

In nucleophilic reactions, it is commonly accepted that the conjugate base perhydroxyl anion HOO^- is the active species. This improved nucleophilicity is due to unshared pair of electrons on the atom adjacent or the alpha to the nucleophilic atom and is termed as 'the alpha effect' [29]. At 30°C, the rate of decomposition of hydrogen peroxide is maximized at pH 11.5. In a study of reaction of hydrogen peroxide with α-methyl syringyl alcohol, it was found that the rate of decomposition of peroxide was directly related to the rate of degradation of phenol. Hence, the maximum degradation of phenol was obtained at pH of 11.5 [41]. The rate constants for the decomposition of hydrogen peroxide as a function of pH are shown in **Table 2.3**. Another study showed that reactivity of *p*-hydroxybenzyl alcohols is yet another factor dependent on the pH of the system [47]. It also affects the formation of quinone methide and the reactivity of hydroperoxyl intermediate **Figure 2.11.** As the pH is increased, the amount of quinone methide is decreased resulting in a decrease in reaction rate as shown in **Figure 2.12**. Also, the pK_a of the hydroperoxyl intermediate is likely to be 12-12.5, thereby contributing to the decrease in reactivity of apocynol at higher alkalinity [47]. Hence, pH control is an important parameter and should be maintained at

pH 11.5 to prevent ionization of the hydroperoxyl intermediates that are formed and maximize lignin oxidation.

pH	**Temperature °C**	$\boldsymbol{k_1(obs)}$ $\boldsymbol{/10^{-3}\ min^{-1}}$
10.0	30	3.09
10.5	25	3.24
10.5	30	5.50
10.5	40	12.08
11.0	30	10.38
11.5	30	11.72
12	30	3.36
12.5	30	0.68

Table 2.3. First order reaction rate constants $k_1(obs)$ for the decomposition of hydrogen peroxide [41].

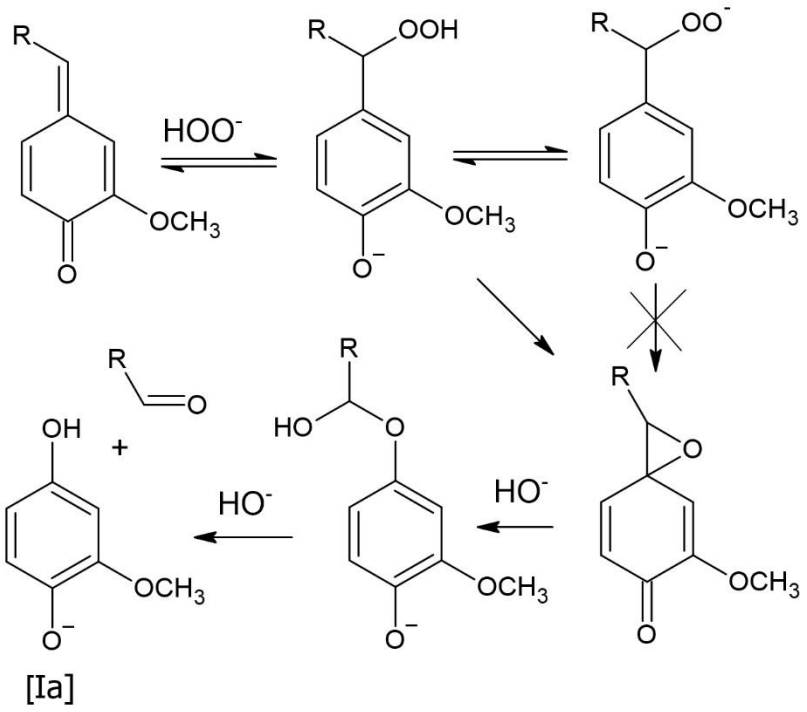

Figure 2.11. The effect of pH on the reaction mechanism of apocynol [47] (reproduced from Holzforschung)

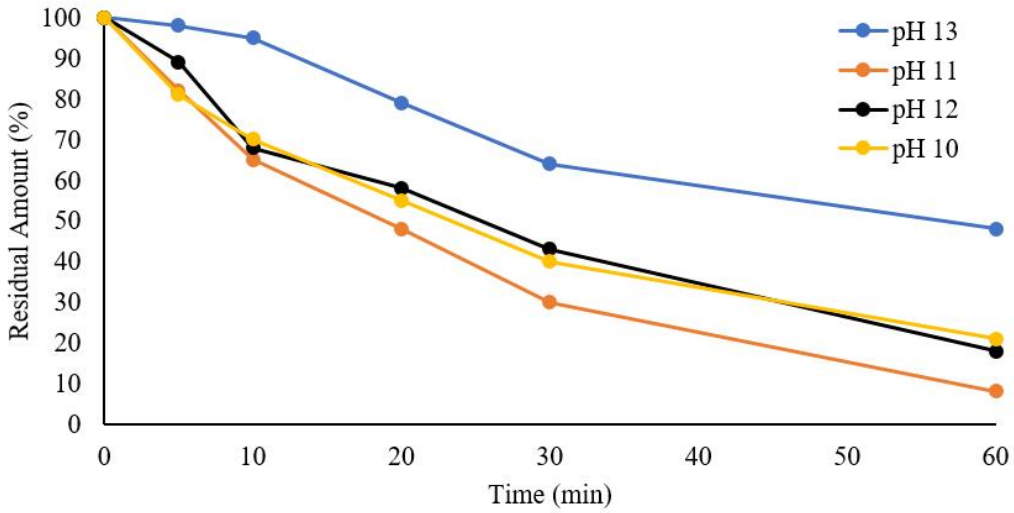

Figure 2.12. The effect of pH on the reactivity of apocynol at 90°C [47] (reproduced from Holzforschung)

In the mechanism of *p*-hydroxyacetophenone oxidation, the reaction rate was profoundly dependent on the base type and concentration [51]. The reaction rate proceeds at a maximum when the base concentration is about 0.3 M. It was also found that hydroquinone monoacetate – **HMA** (reaction intermediate) can be hydrolyzed to hydroquinone and acetate if hydroxide ions are present in excess of the amount required to produce hydroperoxide anion. Hence, hydroxide ions can compete with the hydroperoxide anion for the available HMA causing a lower steady state concentration of both HMA and peracetate, and a slower reaction. Therefore, aqueous sodium carbonate can provide enough alkalinity in this case with a lower concentration of hydroxide ions compared to sodium hydroxide solution. At higher pH, *o*-hydroxyacetophenone reacted by the same mechanism whereas *m*-hydroxyacetophenone does not react with hydrogen peroxide under these conditions due to electronic reasons [51].

The degradation of precipitated hardwood lignin (PHL) using hydrogen peroxide was investigated at moderate to high temperatures [48]. It was found that under alkaline conditions, the reaction proceeds even at low temperatures (80-90°C) compared to higher temperatures of (130-160°C) required under acidic conditions. Mono- and dicarboxylic acids were obtained as the major products. Under alkaline conditions, the main mono- and dicarboxylic acids detected were oxalic acid and formic acid with maximum yields of 17.4% (w/w) and 15.8% (w/w) respectively at 90°C for short reaction time of 10 min. Aldehydes and aromatic acids which are the intermediate products were detected only in trace amounts [48]. The yield of vanillin and vanillic acid was 0.12% (w/w) and 0.15% (w/w) under alkaline hydrogen peroxide oxidation of PHL. On the other hand, these compounds were not detected by GC-MS in acidic condition of oxidation. This was due to the acid insoluble nature of PHL and aromatic structure instability of phenolic aldehydes in acidic conditions. The yield of mono- and dicarboxylic acids were lower compared to similar

operating conditions in basic conditions. The maximum yields of formic and acetic acid were 26.6% (w/w) and 10.1% (w/w) respectively obtained at 140°C for the reaction period of 30 min.

2.4.2.2. Effect of Temperature

The dissociation constants for various phenols depends on the temperature of the system. As the temperature is increased, the dissociation constants for various phenols decrease. This in turn increases the amount of quinone methide intermediate because it depends on the ionization of the phenol and the tendency of α-hydroxide elimination [47]. Also at higher temperatures, the stabilization effects due to hyperconjugation **(Figure 2.13)** can be eliminated due to the thermal energy of the system.

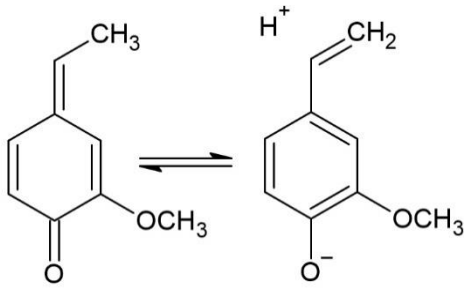

Figure 2.13. Stabilization of quinone methide from apocynol through hyperconjugation [47] (reproduced from Holzforschung)

Higher temperatures also enable ionization of hydrogen peroxide. The effect of stabilization on hydrogen peroxide at higher temperatures by using DTMPA (diethylenetriaminepentamethylene phosphonic acid) is shown in **Figure 2.14**. In this study of the oxidation of lignin model compounds using hydrogen peroxide at 90°C, phenolic compounds such as apocynol and *p*-hydroxybenzyl alcohol reacted completely in the presence of DTMPA at a pH of 11.2 [47]. At lower temperatures of around 50°C, the formation of the quinone methide is the rate determining step and is under thermodynamic control. Whereas at higher temperatures of

around 90°C, oxidation of the hydroperoxy intermediate determines the rate and extent of reaction. Hydrogen peroxide decomposition at 90°C and 110°C is bimolecular with 2nd order rate constants of 1.67×10^{-4} and $3.98 \times 10^{-4} lmol^{-1}s^{-1} (R^2 = 0.99)$ respectively [52].

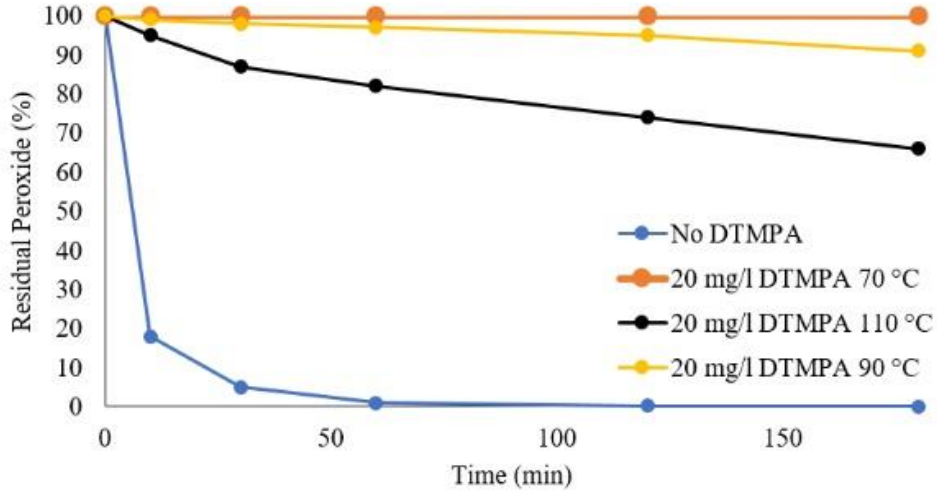

Figure 2.14. Effect of DTMPA and Temperature on Hydrogen Peroxide Stability pH 11.5 [52] (reproduced from Holzforschung)

In a study of oxidation of pine kraft lignin (Indulin AT), the highest percentage reduction of phenolic hydroxyl group/methoxyl group as a function of hydrogen peroxide consumed (g/l) was observed at 90°C in the presence of DTMPA [52]. The compounds that were identified as the products of hydrogen peroxide oxidation of kraft lignin are shown in **Figure 2.15**.

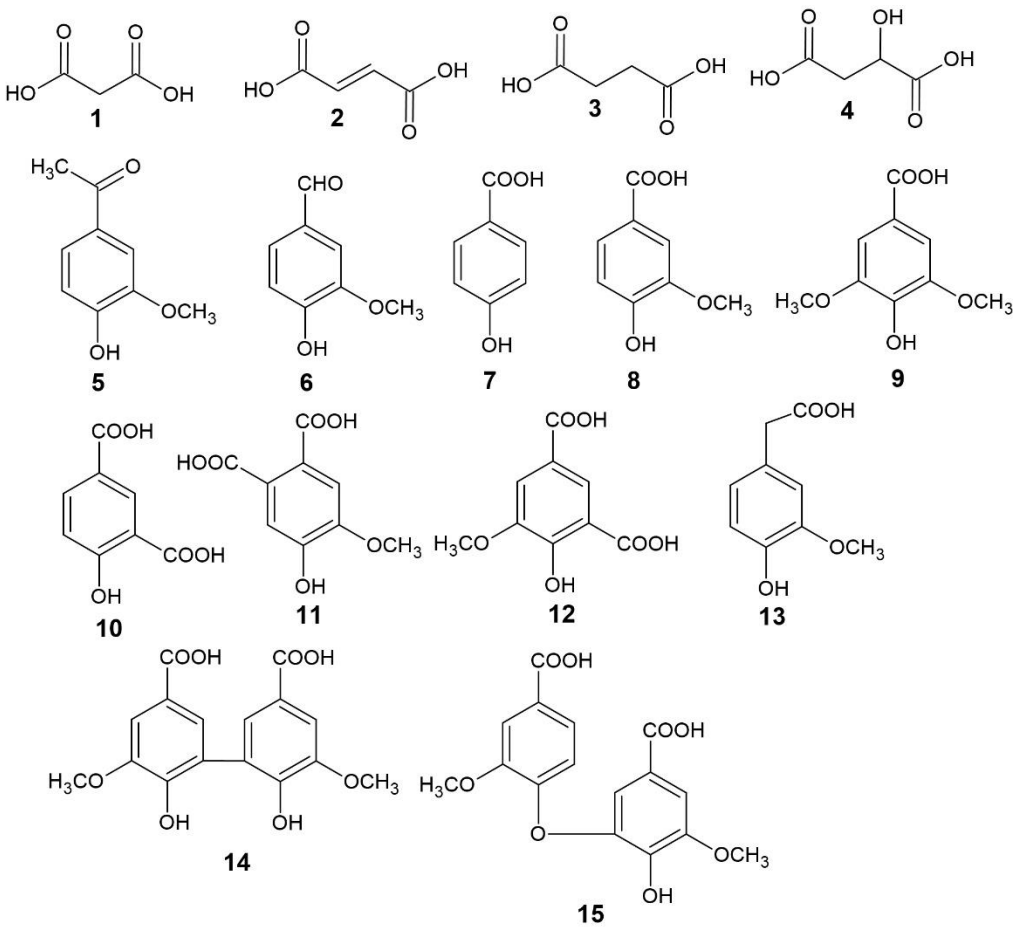

Figure 2.15. Low molecular weight products obtained from the oxidation of kraft lignin by hydrogen peroxide [52] (reproduced from Holzforschung)

A significant amount of the lignin (around 80%) was degraded at 110°C which was the highest degradation based on yield and it accounted for 90% hydrogen peroxide consumption under stabilized conditions. Since the presence of radical species limits the extent of lignin degradation by consuming oxidizing agents, the extensive degradation of the lignin along with low residual hydrogen peroxide implies radicals may not be involved under these operating conditions. Significant amounts of isophthalic acid and aliphatic dicarboxylic acids were generated at these conditions. Isophthalic derivatives such as compound **10** and **12** are a result of oxidation of phenolic phenylcoumaran structures. Compound **12** comprised over 60% of the isolated

compounds at 110°C. In non-stabilized systems the amount of compound **12** was extremely low at 90°C. The reduced yield at 90°C in the absence of DTMPA is due to the consumption of available oxidant by radical species limiting lignin degradation. On the contrary, the higher yield obtained at 110°C under stabilized conditions suggests that the use of extreme conditions facilitate the degradation of condensed lignin structures and enhance the formation of new phenolic hydroxyl groups [52]. Therefore, the percentage reduction of phenolic group/methoxy group at 90°C was higher compared to 110°C under stabilized conditions. The effect of temperature was also observed in case of aliphatic dicarboxylic acids. Trace levels of aliphatic acids were obtained at 70°C with and 90°C without DTMPA. Substantial amounts of malonic acid **1**, maleic/fumaric acid **2**, and succinic acid **3** from ring opening reactions of transient quinone intermediates were formed from lignins at 90°C and 110°C with DTMPA. Vanillin (compound **6**) and acetoguaiacone (compound **5**) were only detected in the non-stabilized system at 90°C. It is suggested that rapid decomposition of H_2O_2 avoids the further degradation of these compounds. The amount of vanillin formed in this study is unclear [52], but it can be concluded that the amount of vanillin formed in non-stabilized conditions will be significantly lower compared to stabilized conditions due to enhanced degradation of condensed lignin structures and formation of new phenolic hydroxyl groups.

2.4.2.3. Effect of metal ions

Transition metal catalysts in their highest oxidation state enhance the process of electron abstraction as shown in **Figure 2.16** [10, 44]. The phenoxyl radical is formed by abstraction of an electron from phenolate anion (PhO^-). It is evident that presence of catalytic amounts of copper (II), iron (III) or manganese (IV) increases the rate of reaction of phenolic lignin model compounds [10, 41, 46].

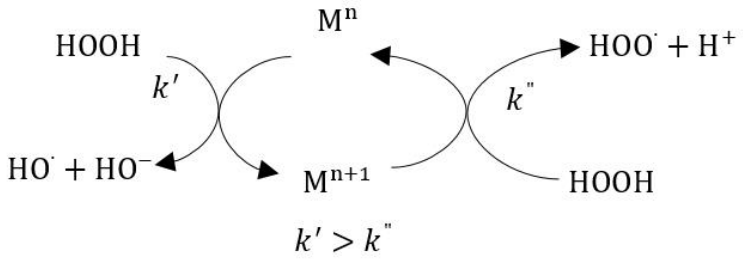

Figure 2.16. Transition metal induced decomposition of hydrogen peroxide [47] (reproduced from Holzforschung)

Hydrogen peroxide is also susceptible to thermal and transition metal induced homolytic fragmentation reactions in which hydroxyl ($HO\cdot$) and superoxide anion ($O_2^{\cdot -}$) radicals are generated [29]. Peroxides in alkaline conditions decompose via a disproportionation reaction with a maximum rate at the pH of its pK_a of 11.6 at 25°C [48]

$$HOOH + HOO^- \rightarrow HO^{\cdot} + HOO^{\cdot} + HO^- \quad (1)$$

$$HOOH + HOO^- \rightarrow HO^- + O_2 + H_2O \quad (2)$$

Disproportionation leads to autocatalytic decomposition of hydrogen peroxide. The following reactions occur in aqueous media which provide the base induced decomposition of hydrogen peroxide into oxygen and water [29].

$$HOO^- + HO^{\cdot} \rightarrow O_2^{\cdot -} + H_2O \quad (3)$$

$$HOOH + HO^{\cdot} \rightarrow HOO^{\cdot} + H_2O \quad (4)$$

$$HOO^{\cdot} \leftrightarrow O_2^{\cdot -} + H^+ \quad (5)$$

$$HO^{\cdot} + O_2^{\cdot -} \rightarrow HO^- + O_2 \quad (6)$$

$$HOOH + O_2^{\cdot -} \rightarrow HO^{\cdot} + HO^- + O_2 \quad (7)$$

As discussed in earlier sections, hydrogen peroxide decomposes in aqueous media to form hydroxyl and superoxide radicals. The $HO^{\cdot}$ radical is one of the strongest thermodynamically stable one-electron oxidants in aqueous media. The reduction potential in acidic solution E_0 ($HO^{\cdot}$, H^+/ H_2O) = +2.72 V and in neutral and alkaline solution E_0 ($HO^{\cdot}/ HO^-$) = 1.89 V [53, 54]. It exhibits strongly electrophilic properties and selectively attacks electron-rich aromatic and olefinic moieties in lignins. It can also react with the aliphatic side chains at a comparatively lower rate. In strongly alkaline conditions (pH > 12), the hydroxyl radical $HO^{\cdot}$ is converted into its conjugate base $O^{\cdot -}$, the oxyl anion radical. The oxyl anion can only react with aliphatic side chains in lignins. In contrast to $HO^{\cdot}$, the superoxide anion radical ($O_2^{\cdot -}$, H^+/ HO_2^-) =+0.2 V; ($O_2^{\cdot -}$, $2H^+/ H_2O_2$) = +0.87 V, does not oxidize lignin to a substantial extent [40]. Kraft lignin and phenolic model compounds were not degraded when reacted with potassium superoxide at room temperature [55]. The decomposition products of hydrogen peroxide such as hydroxyl radicals, superoxide ions and oxygen can attack phenols present in lignin [41]. The phenoxyl radicals also have the tendency to react with superoxide ions that are formed due to decomposition giving rise to hydroperoxide which is subsequently degraded to low molecular weight compounds.

The formation of aliphatic acids such as malonic, succinic, malic acid from aromatic ring opening of lignin and its model compounds have been reported in the literature [10, 48, 52]. It has been hypothesized that initial ring hydroxylation is responsible for the formation of dicarboxylic acids. This reaction takes place due to the reactive species such as $HO^{\cdot}$ and HO^+. $HO^{\cdot}$ radicals react with aromatic and aliphatic structures initially generating radical sites but are unable to result in direct degradation by opening aromatic rings or fission of conjugated structures [40]. The depolymerization of lignin by side chain substitution and/or oxidative side chain cleavage using HO^+ is the initial step to form low molecular weight aromatic compounds. They are further

oxidized to *p*- and *o*- quinone derivatives. Quinones further convert to maleic/fumaric acid and muconic acid derivatives by aromatic ring cleavage. It is probable that quick conversion of muconic acid takes place to form maleic/fumaric acid. This acid then forms malonic/succinic acid by hydrolysis. The reaction scheme is shown in **Figure 2.17**. Radical formation can be inhibited by addition radical scavenging agents. Hence, the ring opening reactions can be minimized, and aromatic ring stability can be improved [10].

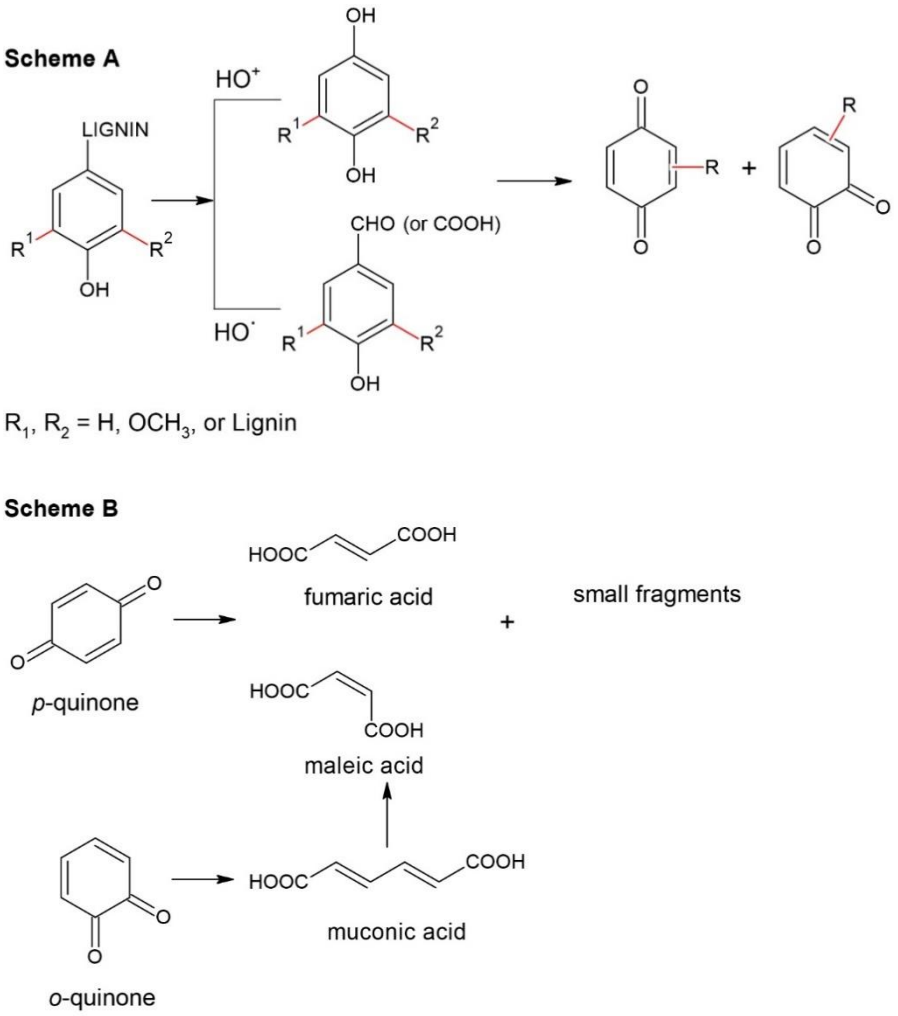

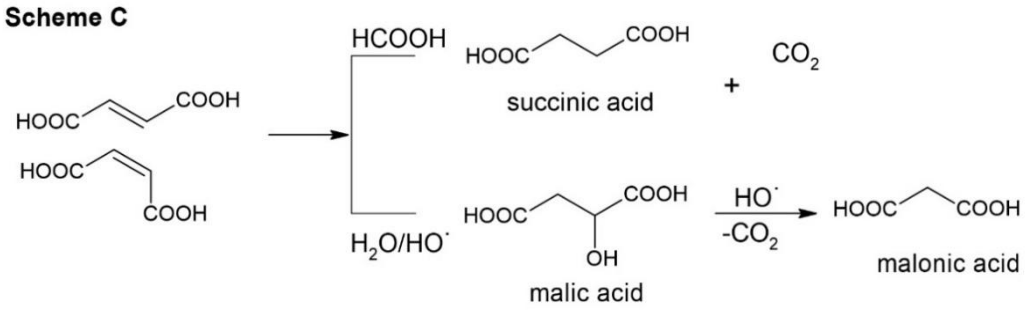

Figure 2.17. Proposed mechanisms for A) lignin depolymerization and aromatic nuclei oxidation, B) aromatic ring cleavage, and C) formation of final products [10] (reproduced with permission from John Wiley & Sons)

2.4.2.4. Effect of lignin feedstock

The origin of lignin is yet another important parameter affecting the aldehyde yields [27]. The use of low molecular weight lignin provides better yields whereas the presence of impurities such as sugars can negatively impact the yield. The isolation processes also modifies lignin structure. Hence, chemically treated lignins such as technical lignins show reduced yields compared to native lignins. This is due to the condensation reactions happening at C-5 position as a result of acid preparation of lignin [26]. The low yields obtained from various lignin sources are shown below in **Table 2.4**. The effect of lignin feedstock on yield of aromatic aldehydes using hydrogen peroxide as an oxidizing agent is still a matter of study [41, 46, 47]. Hence, this section highlights the available literature to show the effects lignin feedstock on yield of aromatic aldehydes.

Sr No	Lignin source	Literature source	Oxidizing agent	Yield %
1	*Pinus spp*. kraft	[56]	Nitrobenzene	V: 13
2	Calcium salt in alcohol precipitated kraft	[57]	Nitrobenzene	V+S: 14

3	Indulin AT kraft	[20]	Oxygen	V: 3.7
4	Lignoboost softwood kraft	[58]	Oxygen	V: 3.1
5	Hardwood kraft	[59]	Oxygen, CuO	V: 1.1, S: 3.5 SA: 1.5
6	Lignosulfonates	[60]	Oxygen, $Cu(OH)_2$	V: 12[a]
7	Lignosulfonates	[22],[61]	Oxygen, $CuSO_4$	V: 5 – 7[b]
8	Precipitated hardwood kraft	[48]	Hydrogen Peroxide	V: 0.12 VA: 0.15 OA: 17.4 FA: 15.8

Table 2.4. Effect of lignin feedstock on aromatic aldehyde yield

Note: [a] – 65 wt.% of lignosulfonates assumed, [b] – ash content of lignosulfonate is unclear (V-vanillin, S-syringaldehyde, VA-vanillic acid, SA-syringic acid, OA-oxalic acid, FA-Formic acid)

2.5. The continuous process of kraft lignin oxidation

In an integrated process for lignin valorization, a continuous mode of lignin oxidation is more attractive than the batch mode due to the high volumes of kraft liquor that are treated in a pulp and paper industry [62]. Also, the relative ease of operation and constant product characteristics combined with lower overall investment and operating costs is advantageous in a continuous mode of operation. The two main type of reactor configurations that are studied in continuous mode for lignin oxidation are [20, 63]: 1) Bubble Column Reactor (BCR) and 2) Structured Packed Bubble Column Reactor (SPBCR). The main advantages and disadvantages of BCR and SBCR are discussed in **Table 2.5 and 2.6** respectively.

Parameter	Advantages	Disadvantages
Mass transfer	Efficient liquid mixing, lower pressure drop and suitable for highly exothermic reactions	Lower mass transfer from gas to liquid phase due to absence of structured packing limiting product yields
Heat transfer and axial dispersion	High heat transfer coefficients providing uniform temperature distribution even with highly exothermic reactions	Radially non-uniform distribution of gas bubbles and lower initial temperature rise compared to SBCRs affecting vanillin formation
Lignin oxidation and vanillin formation	No shaft sealing is required, enabling the operation of aggressive substances at high temperatures and pressures which is crucial for lignin oxidation in alkaline medium	As vanillin yields are lower, catalysts in combination of BCR operation will be required. Significant problems are present with respect to catalyst separation and integrating into the pulp and paper mill
Cost of operation	Adaptable type of reactor, reasonable in price and can be built in large sizes	Relatively lower maximum vanillin yields compared to SPBCRs thereby limiting the scope for scale up of lignin oxidation to vanillin in pulp & paper industry

Table 2.5. Advantages and disadvantages of Bubble Column Reactor (BCR)

Parameter	Advantages	Disadvantages
Mass transfer	Reduced back-mixing of the liquid phase and improved overall mass transfer from gas to liquid phase enabling higher product yields	Reduced liquid hold up ε_L and higher gas hold up ε_G compared to BCRs.
Heat transfer and axial dispersion	Superficial velocity can be varied in a broad range without significant change in the axial dispersion accompanied by excellent radial dispersion and possibility of counter-current operation without flooding	Heat transfer, hydrodynamic and transport coefficients are altered by the presence of internals. Scope to develop reliable models for predicting large scale unit performance
Lignin oxidation and vanillin formation	Initial temperature increase is relatively higher compared to BCRs due large amounts of lignin degradation which may be accompanied by higher initial vanillin formation	Experimental validation of model predicted operating conditions for maximum vanillin yield is still under investigation
Cost of operation	Theoretical yield from model prediction is 1.8 g/L of vanillin (85% of max. vanillin yield in batch reactor) which has potential to overcome additional costs incurred due to structured packing	Relatively higher initial costs compared to BCRs due to the added cost of structured packing

Table 2.6. Advantages and disadvantages of Structured Packed Bubble Column Reactor (SPBCR)

A study was conducted to evaluate the performance of structured packed bubble column reactor (SPBCR) and bubble column reactor (BCR) on the oxidative conversion of kraft lignin to vanillin under similar operating conditions [20]. The nitrogen flow rate (Q_{N_2}), oxygen flow rate (Q_{O_2}), volumetric flow rate of the inlet stream (Q_L), concentration of lignin at the inlet (C_L^{in}), pH at the inlet (pH^{in}) and the total pressure inside the reactor (P) were kept constant as shown in **Table 2.7**. The steady state vanillin concentrations obtained were around 0.73 g/L and 0.56 g/L, for the SPBCR and BCR experiments respectively. It can be concluded that higher vanillin yields can be obtained in SPBCR compared to BCR under similar operating conditions. However, the vanillin concentration from SPBCR is still relatively low compared to the maximum vanillin concentration of 2.0 g/L that can be for the oxidation of the same kraft lignin in a batch reactor.

Parameters	**Bubble Column Reactor (BCR)**	**Structured Bubble Column Reactor (SPBCR)**
$C_L^{in}\ (g/l)$	60	60
pH^{in}	14	14
$Q_L\ (l/hr)$	2.12	2.12
$Q_{O_2}(ml_{NTP}/min)$	1000	1000
$Q_{N_2}(ml_{NTP}/min)$	1000	1000
$P\ (bar)$	10	10
Set point of thermostatic bath T_F^{set}	443 K (t < 2410 s) 440 K (t > 2410 s)	443 K
Type of packing used	N/A	Mellapak 750Y

Mass transfer coefficient, $k_L a$*	$6 \times 10^{-4}\ s^{-1}$	$8.1 \times 10^{-4}\ s^{-1}$
Steady state vanillin concentration	$0.56\ g/L$	$0.73\ g/L$
% of max. yield for the oxidation of same kraft lignin obtained in a batch reactor	28%	37%

Table 2.7. Experimental conditions and results of continuous oxidation of kraft lignin [20]

(*predicted by fitting experimental observations into equations)

To understand the effect of operating parameters to maximize the vanillin yield in a SPBCR, a mathematical model was developed by Araujo et al [63]. A new set of operating conditions was proposed to maximize the steady state vanillin concentration from 0.73 g/L to 1.8 g/L, close to 2.0 g/L that was the maximum concentration of vanillin obtained in batch experiments using kraft lignin. The following were the proposed operating conditions: $Q_L = 10\ l/hr$, $T_F^{set} = 433K$, oxygen partial pressure (P_{O_2}) $= 10\ bar$, $P = 10\ bar$, gas flow rate (Q_G) $= 40000\ ml_{NTP}/min$, and $k_L a = 1.5 \times 10^{-2} s^{-1}$. It was experimentally verified that the use of Mellapak 750Y modules increased the mass transfer coefficient by 35% comparted to BCR without the internals. It was observed that the liquid and gas flow rates should be adjusted to prevent excessive oxidative capacity of the media avoiding excessive vanillin oxidation. However, it can be concluded from this study that one of the most important tasks related to the continuous reactor unit that remain to be performed is a deeper experimental study about the hydrodynamics of the SPBCR configuration and its parameters (axial dispersion coefficient, gas and liquid hold-ups) and experimental

validation of the proposed operating conditions to achieve the model predicted steady state vanillin concentration of 1.8 g/L.

2.6. Thermodynamic and kinetic studies of kraft lignin and vanillin oxidation: The following sections briefly highlight the thermodynamic and kinetic parameters of kraft lignin and vanillin oxidation in batch and continuous reactors.

2.6.1. Kinetic laws for kraft lignin and vanillin oxidation:

The kinetic law for the production of vanillin from the oxidation of kraft lignin was determined in the literature [64] as:

$$r_1 = k_1 {C_{O_2}}^{1.75} C_L$$

The reaction constant (k_1) has an exponential dependence with temperature according to:

$$k_1 = k_1^0 \exp(-\frac{E_a}{RT})$$

From the slope of the lines from **Figure 2.18**, the activation energies (E_a) for the vanillin production (E_a^{NC}) and oxidation (E_a^{CI}) are calculated as 29.1 and 46.0 kJ/mol respectively.

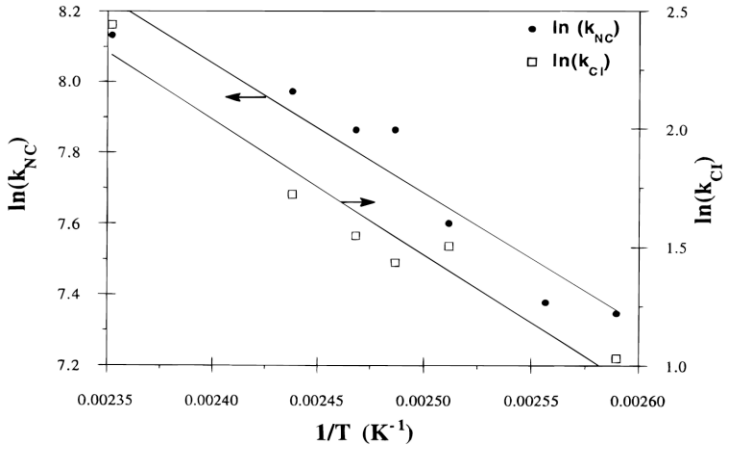

Figure 2.18. Arrhenius plots, k_{NC} and k_{CI}, versus $\frac{1}{T}$, for the calculation of the activation energy of lignin oxidation (eq 9; runs 1, 2, 4-7, and 9) and vanillin oxidation (eq.4; runs 1, 2 and 4-7) respectively [64] (Note*- k_{NC} and k_{CI} denote k_1 and k_2 respectively)

The kinetic constant for vanillin production (k_1) can then be expressed as:

$$k_1 = 1.376 \times 10^7 \exp\left(-\frac{3502}{T}\right)\left(\frac{l}{mol}\right)^{1.75} min^{-1}$$

For vanillin oxidation, the following kinetic law was found for two different mechanisms [65]:

(a) for pH ≥ 11.5 $$r_2 = k_2 \mathrm{C}_{O_2} \mathrm{C}_v$$

where, C_v is the concentration of vanillin and k_2 is expressed by [64]

$$\text{where, } k_2 = 4.356 \times 10^6 \exp\left(-\frac{5530}{T}\right)\left(\frac{l}{mol.min}\right)$$

(b) for pH < 11.5, $$r_2 = Af(pH)\mathrm{C}_v{}^2$$

where, $A = 4071 \exp(-\frac{3103.7}{T})$; $f(pH) = \left(\frac{B\times10^{-pH}}{1+B\times10^{-pH}}\right)^2$ and $B = 8.88 \times 10^{12} \exp(-\frac{1936.6}{T})$

2.6.2. Energy balance for kraft lignin and vanillin oxidation in a batch reactor:

In general the energy balance equation can be written as:

$$Q - W_s + \sum (F_i H_i)_{in} - \sum (F_i H_i)_{out} = \sum H_i \frac{dn_i}{dt} + \sum n_i \frac{dH_i}{dt}$$

To simplify the general energy balance, the following assumptions are made [20]:

1) perfectly mixed reactor, constant spatial values of all variables within the reactor system;

2) constant total pressure during the reaction;

3) mass transfer resistances are neglible (due to strong agitation);

4) irreversible oxidation reactions;

5) ideal behaviour of the gas phase

In general, the unsteady state energy balance to the system can then be written as [20, 65]:

$$Q - r_1 V_l \Delta H_{r,1} - r_2 V_l \Delta H_{r,2} = \lambda_{H_2O}^{vap} \left(\left[\frac{-B_0}{(C_0 + T)^2} - \frac{1}{T} \right] \frac{V_g P_{H_2O}}{RT} \frac{dT}{dt} + \frac{\Delta V_l}{\Delta t} \frac{P_{H_2O}}{RT} \right) + \sum n_i Cp_i \frac{dT}{dt}$$

The energy balance of the heat exchanged between the system and the surroundings can be expressed by

$$Q = U_1 A_1 (T_F - T) - U_2 A_2 (T - T_{amb})$$

in which the overall heat transfer coefficients U_1 and U_2 are defined as:

$$U_1 = \frac{1}{\left(\frac{1}{h_{gll}}\right) + A_1 \left(\frac{\ln\left(\frac{r_{ext1}}{r_{int}}\right)}{2\pi L k_{gl}} \right) + \left(\frac{1}{h_{fgl}}\right)\left(\frac{A_1}{A_{ext1}}\right)}$$

$$U_2 = \frac{1}{\left(\frac{1}{h_{sg}}\right) + \left(\frac{D_s}{k_s}\right) + \left(\frac{1}{h_{aus}}\right)} + \frac{1}{\left(\frac{1}{h_{sl}}\right) + \left(\frac{D_s}{k_s}\right) + \left(\frac{1}{h_{als}}\right)}$$

2.6.2.1. Estimation of heat of reaction of kraft lignin oxidation $\Delta H_{r,1}$

Considering that in the initial moments of reaction ($t = 0$) there is no vanillin oxidation, the energy balance equation can be reduced to:

$$Q^i - r_1^i V_l^i \Delta H_{r,1} = \lambda_{H_2O}^{vap} \left(\left[\frac{-B}{(C + T^i)^2} - \frac{1}{T^i} \right] \frac{V_g^i P_{H_2O}^i}{RT^i} \left(\frac{dT}{dt} \right)_{t=0} + \frac{\Delta V_l}{\Delta t} \frac{P_{H_2O}^i}{RT^i} \right) + (n_{N_2}^i Cp_{N_2} + n_{O_2}^i Cp_{O_2} + n_L^i Cp_L + n_{NaOH}^i Cp_{NaOH} + n_{H_2O}^i Cp_{H_2O} + m_{gl} Cp_{gl}) \left(\frac{dT}{dt} \right)_{t=0}$$

All the variables can be determined or calculated except $\left(\frac{dT}{dt}\right)_{t=0}$ and $\Delta H_{r,1}$.

The value of $\left(\frac{dT}{dt}\right)_{t=0}$ was determined by the temperature vs time data collected for the two experiments conducted in the study – one consisted of $P_{O_2}^i$ (4 bar) out of the total P (9 bar) and the

other consisted of $P_{O_2}^i$ (6.5 bar) out of the total P (9.5 bar) while the other operating conditions $C_{NaOH}^i = 80\ g/l, C_L^i = 60\ g/l, T^i = 123°C$ kept constant. Substituting the values in the equation, the value for the heat of reaction of vanillin formation from lignin oxidation $\Delta H_{r,1}$ was obtained as -29460 kJ mol^{-1} and -29913 kJ mol^{-1} for two the experiments conducted [20]. The average value of $\Delta H_{r,1}$ of -29687 kJ mol^{-1} or -12769 kJ kg^{-1} was used. The heat of reaction in the total combustion of pine wood is -19620 kJ kg^{-1} [66] and a heat value of -37143 kJ kg^{-1} for a kraft lignin extracted from black liquor was presented by P. Axegard [67]. These values were in the same order of magnitude of the $\Delta H_{r,1}$ determined above.

2.6.2.2. Estimation of heat of reaction of vanillin oxidation $\Delta H_{r,2}$

In a general assumption, the heat of reaction of vanillin oxidation in the literature is given as [20]:

$$\Delta H_{r,2}(140℃) = \Delta H_f^{140℃}(vanillin) - \Delta H_f^{140℃}(vanillic\ acid)$$

Based on the experimental results in the literature [22, 24, 58] , vanillic acid formation may not be necessary linked to vanillin formation. Therefore, the new modified version of heat of reaction of vanillin oxidation can be given as:

$$\Delta H_{r,2}(140℃) = \Delta H_f^{140℃}(vanillin) - \Delta H_f^{140℃}(others)^*$$

{*Note** - the modified equation represents that vanillin oxidation may result in the formation of vanillic acid and other by-products from ring opening.}

The enthalpy change when the temperature of aqueous vanillin is raised from 25°C to 140°C:

$$\Delta H_f^{140℃}(vanillin) = \Delta H_f^{25℃}(vanillin) + \Delta H_{sol}^{25℃}(vanillin) + \int_{25℃}^{140℃} Cp_v dT$$

The heats of solution of vanillin and vanillic acid are -21.8 kJ mol^{-1} and -21.59 kJ mol^{-1}, respectively as reported in the literature [68].

$$\Delta H_f^{140℃}(vanillin) = -485.7 - 21.8 + ([\int_{298.15K}^{413.15K}(0.6996T + 52.54)dT] \times \frac{1}{1000})$$

$$\Delta H_f^{140℃}(vanillin) = -472.84\ kJ/mol$$

$$\Delta H_f^{140℃}(vanillic\ acid) = \Delta H_f^{25℃}(vanillic\ acid) + \Delta H_{sol}^{25℃}(vanillic\ acid) + \int_{25℃}^{140℃} Cp_D dT$$

$$\Delta H_f^{140℃}(vanillic\ acid) = -755.6 - 21.59 + \left(\left[\int_{298.15K}^{413.15K}(0.8218T + 36.93)dT\right] \times \frac{1}{1000}\right)$$

$$\Delta H_f^{140℃}(vanillic\ acid) = -739.33\ kJ/mol$$

Estimated heat capacities of kraft lignin, vanillin and vanillic acid were found using the Missenard group activity method from the literature [20, 69] **Table 2.8**:

Source	**Heat capacity at 25°C** (J mol^{-1} K^{-1})	**Heat capacity at 50°C** (J mol^{-1} K^{-1})	**Heat capacity at 75°C** (J mol^{-1} K^{-1})	**Heat capacity at 100°C** (J mol^{-1} K^{-1})
Kraft lignin	N/A	3298.95	N/A	3700.42
Vanillin	261.30	N/A	296.23	313.60
Vanillic acid	281.80	N/A	324.27	342.89

Table 2.8. Predicted heat capacities of kraft lignin, vanillin and vanillic acid [20, 69]

Temperature (T_F^{set}) (°C)	$\Delta H_f^{T_F^{set}}(vanillin)$ (kJ mol^{-1})	$\Delta H_f^{T_F^{set}}(vanillic\ acid)$ (kJ mol^{-1})	$\Delta H_{r,2}(T_F^{set})$ (kJ mol^{-1})
120	-479.54	-746.70	-267.16
130	-476.23	-743.06	-266.83
140	-472.84	-739.33	-266.49
150	-469.39	-735.53	-266.13
160	-465.87	-731.64	-265.77

Table 2.9. Estimated heat of reaction of vanillin oxidation at different temperatures from 120°C to 160°C* (*Assumption – oxidation of vanillin is solely linked vanillic acid)

Based on thermodynamic concepts, reported literature and the above mentioned equations, the value of heat of reaction of vanillin oxidation $\Delta H_{r,2}$ was determined to be -266.49 kJ mol^{-1} at 140°C. However, it can be deduced from **Table 2.9** that the heat of reaction of vanillin oxidation decreases as the temperature of the reaction increases from 120°C to 160°C.

2.6.3. Energy balance for kraft lignin and vanillin oxidation in the column sections in SBCRs and BCRs

The energy balance for both the SBCRs and BCRs considering the axial dispersion model is made by considering the following assumptions [63]:

1) constant gas composition with the axial position and time; 2) isobaric reactor; 3) the oxygen gas-liquid mass transfer is dominated by the resistance in the liquid film: the resistance in the gas film is neglected and dissolved oxygen is in equilibrium with the gas at the interface; 4) ideal behavior of gas phase; 5) for the same axial position, the temperatures of the packing, gas and liquid phases are equal (pseudo-homogeneous model for the energy balance). 6) the external tube of the reactor jacket is thermally insulated from the surroundings, and the temperature of the outer tube of the column is equal to the temperature of the thermo-fluid flowing inside the jacket. 7) no heat losses in the thermo-fluid between the exit of the bath and the entrance of the reactor jacket.

The energy balance to the reaction media can be then simplified as:

$$\lambda_{ef}\frac{\partial^2 T}{\partial z^2}$$

$$= \left(u_{LS}\rho_L C_{P,L} + u_{GS}\rho_G C_{P,G}\right)\frac{\partial T}{\partial \mathrm{z}} - \varepsilon_L\left[\left(-\Delta H_{r,1}\right)r_1 + \left(-\Delta H_{r,2}\right)r_2\right] - \frac{2\pi R_2}{A_R}U(T_F - T)$$

$$+ \left(\varepsilon_L\rho_L C_{P,L} + \varepsilon_G\rho_G C_{P,G} + \varepsilon_S\rho_S C_{P,S} + \rho_W\frac{A_W}{A_R}C_{P,W}\right)\frac{\partial T}{\partial \mathrm{t}}$$

The energy balance to the fluid in the jacket can be given as:

$$\rho_F u_F C_{P,F}\frac{\partial T_F}{\partial \mathrm{z}} + \frac{2R_1}{R_3^2 - R_2^2}U(T_F - T) + \rho_F u_F C_{P,F}\frac{\partial T_F}{\partial \mathrm{t}} = 0$$

2.7. Conclusion

Alkaline hydrogen peroxide can be used at high temperatures for the peroxide degradation of kraft lignin using stabilization agents. It not only increases the amount of lignin oxidation but also improves peroxide utilization more efficiently [52]. pH control is crucial and should be maintained at pH 11.5 to prevent ionization of the hydroperoxy intermediates and maximize lignin oxidation [47]. Under these conditions, chromophoric groups are generated through Dakin and Dakin-like reaction pathways. In contrast, under acidic conditions aromatic compounds are not well preserved due to attack by HO^+ and other radicals [48].

Among the oxidizing agents used for degradation of lignin into aromatic aldehydes, nitrobenzene is the oxidant that gives the highest yields, followed by oxygen [20]. However, nitrobenzene is expensive and its reduction products are harmful and difficult to separate [70]. This makes industrial scale up of this process more complex. Another unresolved problems in oxidation of lignins into aromatic aldehydes in high consumption of oxygen – over 10 mol per mol

of obtained vanillin [42]. These challenges with oxygen and nitrobenzene remain to be addressed and hence, hydrogen peroxide can be an important oxidant to tackle these challenges.

The differences in oxidative chemistries between oxidizing agents such as hydrogen peroxide, oxygen and nitrobenzene do not allow for a straightforward comparison as represented by the yields. The extent of oxidation for each of these mechanisms can be weighed based on the amount of carboxylic acids produced in this process. Peroxide treatment also improves the carboxylic acid groups on lignin thereby enhancing its hydrophilicity and facilitating its dissolution. Since carboxylic acids are formed as the end products of aromatic ring degradation, the extent of oxidation can be evaluated based on their yields [10, 48].

Transition metals catalyze the decomposition of hydrogen peroxide into highly reactive radical species. Therefore, in order to utilize hydrogen peroxide and its corresponding anion on lignin and its model compound oxidation a sequestering agent is necessary. By using chelating agents, it is possible to use hydrogen peroxide at higher temperatures [46]. These conditions are also favorable for the reactions of non-phenolic lignin structures which are predominant in all different sources of lignin discussed above [29, 48, 59] and otherwise unreactive at conventional oxidation conditions.

2.8. Scope for future work

Vanillin, which is a high value-added product from oxidation of lignin is formed as a reaction intermediate, however, there is a scope to improve the yield of this product. A recent study showed that vanillin and vanillic acid were produced by hydrolysis in the absence of oxygen which started at 100°C [22]. Vanillic acid was formed in this process without the presence of oxygen, suggesting that vanillic acid was not the oxidation product of vanillin. The yield of vanillin by

hydrolysis in the absence of oxygen did not increase upon the addition of catalyst [22]. Based on this study, there is a scope to utilize hydrogen peroxide at lower temperatures to further develop the understanding of hydrolysis. The inclusion of molecular oxygen in combination with hydrogen peroxide has been shown to improve the extent of lignin degradation [52]. The optimum combination of both these oxidizing agents for degradation of lignin is still under investigation.

Another factor that can impact vanillin yield is the characteristics of lignin molecule that is used as a feedstock for oxidation treatment. The understanding of the lignin molecule should not be limited to mean molecular weight or ratio of lignin precursors but also details at the level of chemical structure which includes types and amounts of functional groups that deviate the purpose of oxidation of lignin molecule [20]. Technical lignins are obtained as byproducts from various conventional pulping routes such as kraft and sulphite processes [32]. The differences in these processes causes technical lignins to have different structures and impurities. Compared to native lignins, technical lignins have more condensed structures resulting in higher C-C linkages. Native lignins, on the other hand, have a higher proportion of C-O inter-unit linkages. This undesired condensation reactions occur during delignification process and efforts are being made by researchers to minimize condensations. Successful methods to address condensation reactions are split into two main categories: (1) strategies that are focused on *in situ* trapping of the reactive intermediates to convert them into stable molecules and (2) strategies that are focused on directly stabilizing the β-O-4 ether linkages (either physically or chemically) [71]. The use of phenolic compounds as additives during kraft pulping is also a promising approach to minimize condensation reactions. Addition of phenolic compounds such as 2, 4–xylenol during kraft pulping can reduce Kappa number by 13.9% [72]. There are other factors such as molecular weight, polydispersity, moisture, ash content, homogeneity, certain functional groups that should also be

taken into account for valorization of technical lignins [73, 74]. Biorefinery lignin which mainly consists of native lignin structures is an important feedstock to selectively utilize the uncondensed unit linkages for oxidation reactions. Lignosulfonates can produce higher yields phenolic aldehydes and acids due to the elimination of sulfonic group at C-α position under alkaline oxidative conditions. Due to the more severe conditions carried out in kraft pulping, the availability of reactive structures in the non-condensed fraction is comparatively lower in kraft lignins [35]. Hence, selective sulfonation of kraft lignin at the C-α position is a critical parameter to evaluate for improving vanillin yield from kraft lignins. Also, the treatment of lignosulfonates with hydrogen peroxide has not been reported in various literatures and there is a scope for investigation [10, 41, 47, 48, 52]. The results and mechanisms discussed provide details on developing processes for production of the aromatic aldehydes from hydrogen peroxide oxidation of lignin. Under optimized process conditions, there is a scope to develop value-added products using hydrogen peroxide as an oxidant.

2.9. References

[1] T. Werpy, and G. Petersen, "Top value added chemicals from biomass: volume I-results of screening for potential candidates from sugars and synthesis gas," National Renewable Energy Lab., Golden, CO, USA, 2004.

[2] S. G. Wettstein, D.M. Alonso, E.I. Gürbüz, and J.A. Dumesic, "A roadmap for conversion of lignocellulosic biomass to chemicals and fuels," *Curr. Opin. Chem. Eng*., vol. 1, pp. 218-224, 2012.

[3] H. L'udmila, J. Michal, S. Andrea, and H. Ales, "Lignin, potential products and their market value," *Wood. Res*., vol. 60, pp. 973-986, 2015.

[4] A. Sakakibara, “A structural model of softwood lignin,” *Wood. Sci. Tech*., vol. 14, pp. 89-100, 1980.

[5] B. Smith, R. Rice, and P. Ince, “Pulp capacity in the United States,” General Technical Report FPL-GTR-139. USDA Forest Service, 2000.

[6] H. Lange, S. Decina, and C. Crestini, “Oxidative upgrade of lignin–Recent routes reviewed,” *Eur. Polym. J*., vol. 49, pp. 1151-1173, 2013.

[7] J.J. Bozell, B.R. Hames, and D.R. Dimmel, “Cobalt-Schiff base complex catalyzed oxidation of para-substituted phenolics. Preparation of benzoquinones,” *J. Org. Chem.*, vol. 60, pp. 2398-2404, 1995.

[8] J. Zakzeski, P.C. Bruijnincx, A.L. Jongerius, and B.M. Weckhuysen, “The catalytic valorization of lignin for the production of renewable chemicals,” *Chem. Rev*., vol. 110, pp. 3552-3599, 2010.

[9] X. Zhang, M. Tu, and M. G. Paice, “Routes to potential bioproducts from lignocellulosic biomass lignin and hemicelluloses,” *Bioenerg. Res*., vol. 4, pp. 246-257, 2011.

[10] R. Ma, M. Guo, and X. Zhang, “Selective conversion of biorefinery lignin into dicarboxylic acids,” *ChemSusChem,* vol. 7, pp. 412-415, 2014.

[11] J. J. Bozell, J.O. Hoberg, and D.R. Dimmel, “Catalytic oxidation of para-substituted phenols with nitrogen dioxide and oxygen,” *Tetrahedron Lett*., vol. 39, pp. 2261-2264, 1998.

[12] J. L. Cole, P. A. Clark, and E.I. Solomon, “Spectroscopic and chemical studies of the laccase trinuclear copper active site: geometric and electronic structure,” *J. Am. Chem. Soc*., vol. 112, pp. 9534-9548, 1990.

[13] E.I. Solomon, and M.D. Lowery, “Electronic structure contributions to function in bioinorganic chemistry,” *Science*, vol. 259, pp.1575-1581, 1993.

[14] C. Crestini, R. Saladino, P. Tagliatesta, and T. Boschi, “Biomimetic degradation of lignin and lignin model compounds by synthetic anionic and cationic water soluble manganese and iron porphyrins,” *Bioorg. Med. Chemistry*., vol. 7, pp. 1897-1905, 1999.

[15] X.-p. Ouyang, Y.-d. Tan, and X.-q, Qiu, “Oxidative degradation of lignin for producing monophenolic compounds,” *J. Fuel. Chem. Technol*., vol. 42, no. 6, pp. 677-682, 2014.

[16] W. A. Herrmann, and R. W. Fischer, “Multiple bonds between main-group elements and transition metals. 136."Polymerization" of an organometal oxide: The unusual behavior of methyltrioxorhenium (VII) in water,” *J. Am. Chem. Soc*., vol. 117, pp. 3223-3230, 1995.

[17] H.S. Genin, K.A. Lawler, R. Hoffmann, W.A. Herrmann, R.W. Fischer, and W. Scherer, “Multiple bonds between main-group elements and transition metals. 138. Polymeric methyltrioxorhenium: some models for its electronic structure,” *J. Am. Chem. Soc*., vol. 117, pp. 3244-3252, 1995.

[18] B. Moodley, D. Mulholland, and H. Brookes, “The chemical oxidation of lignin found in Sappi Saiccor dissolving pulp mill effluent,” *Water S.A*., vol. 38, pp. 1-8, 2012.

[19] Y. Ni, A. Van Heiningen, and G. Kubes, “Mechanism of formation of chloro-organics during chlorine dioxide pre bleaching of kraft pulp,” *Nord. Pulp. Pap. Res. J*., vol. 8, pp. 350-351, 1993.

[20] J.D.P. Araújo, “Production of vanillin from lignin present in the Kraft black liquor of the pulp and paper industry,” Ph.D. thesis, University of Porto, Porto, Portugal, 2008 [accessed 1 June 2022].

[21] https://www.solvay.com/en/article/natural-vanillin-ensures-resource-efficiency

[22] A.W. Pacek, P. Ding, M. Garrett, G. Sheldrake, and A.W. Nienow, "Catalytic conversion of sodium lignosulfonate to vanillin: engineering aspects. Part 1. Effects of processing conditions on vanillin yield and selectivity," *Ind. Eng. Chem. Res*., vol. 52, pp. 8361-8372, 2013.

[23] https://www.vanillin.com/Products/eurovanillin-plus

[24] P.C.R. Pinto, E.A.B. da Silva, and A.E. Rodrigues, "Lignin as source of fine chemicals: vanillin and syringaldehyde," Biomass Conversion; C. Baskar, S. Baskar, R.D. Dhillon, Eds; Springer: London, pp. 381-420, 2012.

[25] M. Fache, B. Boutevin, and S. Caillol, "Vanillin production from lignin and its use as a renewable chemical," *ACS. Sustain. Chem. Eng*., vol. 4, pp. 35-46, 2016.

[26] T.Q. Hu, "Chemical modification, properties, and usage of lignin," New York: Kluwer Academic/ Plenum Publisher pp. 291, 2002.

[27] V.E. Tarabanko, and N. Tarabanko, "Catalytic oxidation of lignins into the aromatic aldehydes: general process trends and development prospects," *Int. J. Mol. Sci*., vol. 18, pp. 2421, 2017.

[28] W. He, W. Gao, and P. Fatehi, "Oxidation of kraft lignin with hydrogen peroxide and its application as a dispersant for kaolin suspensions," *ACS. Sustain. Chem. Eng*., vol. 5, pp. 10597-10605, 2017.

[29] J.F. Kadla, and H. Chang, "The reactions of peroxides with lignin and lignin model compounds," ACS Publications: Columbia, DC, USA, 2001.

[30] R. Ma, Y. Xu, and X. Zhang, "Catalytic oxidation of biorefinery lignin to value-added chemicals to support sustainable biofuel production," *ChemSusChem*, vol. 8, pp. 24-51, 2015.

[31] S. Guadix-Montero, and M. Sankar, “Review on catalytic cleavage of C–C inter-unit linkages in lignin model compounds: towards lignin depolymerization,” *Top. Catal*., vol. 61, pp. 183-198, 2018.

[32] https://sg.inflibnet.ac.in/bitstream/10603/124826/8/08chapter%204.pdf.

[33] F.G. Calvo-Flores, J.A. Dobado, J. Isac-García, and F.J. Martín-Martínez, “Lignin and Lignans as Renewable Raw Materials: Chemistry, Technology and Applications,” John Wiley & Sons, 2015.

[34] R. Rinaldi, R. Jastrzebski, M.T. Clough, J. Ralph, M. Kennema, P.C. Bruijnincx, and B.M. Weckhuysen, “Paving the way for lignin valorisation: recent advances in bioengineering, biorefining and catalysis,” *Angew. Chem. Int. Ed*., vol. 55, pp. 8164-8215, 2016.

[35] P.C.R. Pinto, C.E. Costa, and A.E. Rodrigues, “Oxidation of Lignin from Eucalyptus globulus Pulping Liquors to Produce Syringaldehyde and Vanillin,” *Ind. Eng. Chem. Res*., vol. 52, pp. 4421-4428, 2013.

[36] J. Huang, S. Fu, and L. Gan, “Structure and characteristics of lignin,” Lignin Chemistry and Applications. Elsevier, pp. 25-50, 2019.

[37] Kirk-Othmer Encyclopedia of Chemical Technology, John Wiley & Sons: New York, vol. 11, 2005.

[38] T.R. Nunn, J.B. Howard, J.P. Longwell, and W.A. Peters, “Product compositions and kinetics in the rapid pyrolysis of milled wood lignin,” *Ind. Eng. Chem. Process. Des. Dev*., vol. 24, pp. 844-852, 1985.

[39] R. Ma, X. Zhang, Y. Wang, and X. Zhang, “New insights toward quantitative relationships between lignin reactivity to monomers and their structural characteristics,” *ChemSusChem*, vol. 11, pp. 2146-2155, 2018.

[40] J. Gierer, “Formation and involvement of superoxide (O_2^-/HO_2·) and hydroxyl (OH·) radicals in TCF bleaching processes: A review,” *Holzforschung*, vol. 51, pp. 34-46, 1997.

[41] R. Agnemo, and G. Gellerstedt, “The reactions of lignin with alkaline hydrogen peroxide. Part II. Factors influencing the decomposition of phenolic structures,” *Acta Chem. Scand*., vol. B33, pp. 337-342, 1979.

[42] Tarabanko, V.E., and Petukhov, D. “Study of mechanism and improvement of the process of oxidative cleavage of lignins into the aromatic aldehydes,” *Chem. Sustain. Dev*., vol. 11, pp. 655-667, 2003

[43] Ralph, J., Schatz, P.F., Lu, F., Kim, H., Akiyama, T. and Nelsen, S.F. “Quinone methides in lignification,” In: Quinone methides; Rokita, S., ed. (Hoboken, NJ: Wiley-Blackwell), pp. 385-420, 2009.

[44] S.G. Santos, A.P. Marques, D.L. Lima, D.V. Evtuguin, and V.I. Esteves, “Kinetics of eucalypt lignosulfonate oxidation to aromatic aldehydes by oxygen in alkaline medium,” *Ind. Eng. Chem. Res.*, vol. 50, pp. 291-298, 2011.

[45] P. Sharma, A.B. Jha, R.S. Dubey, and M. Pessarakli, “Reactive oxygen species, oxidative damage, and anti-oxidative defense mechanism in plants under stressful conditions,” *J. Bot.*, vol. 2012, pp. 1-26, 2012.

[46] G. Gellerstedt, and R. Agnemo, “The reactions of lignin with alkaline hydrogen peroxide. Part III. The oxidation of conjugated carbonyl structures,” *Acta Chem. Scand*., vol. B34, pp. 275-280, 1980.

[47] J.F. Kadla, H.-m. Chang, and H. Jameel, “The reactions of lignins with hydrogen peroxide at high temperature. Part I. The oxidation of lignin model compounds,” *Holzforschung*, vol. 51, pp. 428-434, 1997.

[48] Q. Xiang, and Y. Lee, “Oxidative cracking of precipitated hardwood lignin by hydrogen peroxide,” *Appl. Biochem. Biotechnol*., vol. 84, pp. 153-162, 2000.

[49] S. Zeronian, and M. K. Inglesby, “Bleaching of cellulose by hydrogen peroxide,” *Cellulose*, vol. 2, pp. 265-272, 1995.

[50] D. Johnson, S. Park, J. Genco, A. Gibson, M. Wajer, and B. Branch, “Hydrogen peroxide bleaching of TMP pulps using $Mg(OH)_2$,” TAPPI Pulping Conference Proceedings, TAPPI Fall Conference and Trade Fair, Atlanta, GA, USA, 2002.

[51] M. B. Hocking, and J. P. Crow, “On the mechanism of alkaline hydrogen peroxide oxidation of the lignin model *p*-hydroxyacetophenone,” *Can. J. Chem*., vol. 72, pp. 1137-1142, 1994.

[52] J. Kadla, , H. Chang, and H. Jameel, “The reactions of lignins with hydrogen peroxide at high temperature. Part 2. The oxidation of kraft lignin,” *Holzforschung*, vol. 53, pp. 277-284, 1999.

[53] H. Schwarz, and R. Dodson, “Equilibrium between hydroxyl radicals and thallium (II) and the oxidation potential of hydroxyl (aq),” *J. Phys. Chem*., vol. 88, pp. 3643-3647, 1984.

[54] U. K. Kläning, K. Sehested, and J. Holcman, “Standard gibbs energy of formation of the hydroxyl radical in aqueous solution. Rate constants for the reaction $ClO_2^- + O_3 \rightleftharpoons O_3^- + ClO_2$,” *J. Phys. Chem*., vol. 89, pp. 760-763, 1985.

[55] R. Barkhau, J. Bastian, and N. Thompson, “The reaction of model lignins with oxygen radicals,” *TAPPI. J*., vol. 68, no. 10, pp. 110, 1985.

[56] A. Mathias, and A. Rodrigues, “Production of vanillin by oxidation of pine kraft lignins with oxygen,” *Holzforschung*, vol. 49, pp. 273-278, 1995.

[57] J. Villar, A. Caperos, and F. García-Ochoa, “Oxidation of hardwood kraft-lignin to phenolic derivatives. Nitrobenzene and copper oxide as oxidants,” *J. Wood. Chem. Technol*., vol. 17, pp. 259-285, 1997.

[58] P.C. Rodrigues Pinto, E.A. Borges da Silva, and A.E. Rodrigues, “Insights into oxidative conversion of lignin to high-added-value phenolic aldehydes,” *Ind. Eng. Chem. Res*., vol. 50, pp. 741-748, 2011.

[59] J. Villar, A. Caperos, and F. García-Ochoa, “Oxidation of hardwood kraft-lignin to phenolic derivatives with oxygen as oxidant,” *Wood Sci. Technol*., vol. 35, pp. 245-255, 2001.

[60] V. E. Tarabanko, N. V. Koropatchinskaya, A. V. Kudryashev, and B. N. Kuznetsov, “Influence of lignin origin on the efficiency of the catalytic oxidation of lignin into vanillin and syringaldehyde,” *Russ. Chem. Bull*., vol. 44, no. 2, pp. 367-371, 1995.

[61] H. R. Bjorsvik, and F. Minisci, “Fine chemicals from lignosulfonates. 1. Synthesis of vanillin by oxidation of lignosulfonates,” *Org. Process. Res. Dev*., vol. 3, no. 5, pp. 330-340, 1999.

[62] E. B. da Silva, M. Zabkova, J. Araújo, C. Cateto, M. Barreiro, M. Belgacem, and A. Rodrigues, “An integrated process to produce vanillin and lignin-based polyurethanes from Kraft lignin,” *Chem. Eng. Res. Des*., vol. 87, no. 9, pp. 1276-1292, 2009.

[63] J. D. P Araujo, C. A. Grande and A. Rodrigues, “Structured packed bubble column reactor for continuous production of vanillin from kraft lignin oxidation,” *Catal. Today*, vol. 147, pp. S330-S335, 2009.

[64] C. Fargues, A. Mathias, and A. Rodrigues, “Kinetics of vanillin production from kraft lignin oxidation,” *Ind. Eng. Chem. Res*., vol. 34, pp. 28-36, 1996.

[65] J. D. Araújo, C. A. Grande, and A. E. Rodrigues, "Vanillin production from lignin oxidation in a batch reactor," *Chem. Eng. Res. Des.*, vol. 88, no. 8, pp. 1024-1032, 2010.

[66] A. Berlin, N. A. Khalturinskiy, I. A. Novikov, and G. E. Zaikov, "Chemical physics of pyrolysis, combustion and oxidation," Nova Publishers, 2005.

[67] P. Axegard, "The kraft pulp mill as a biorefinery," ICEP4 Conference, *Belo Horizonte,* Brazil, March 5-8, 2007.

[68] E. W. Washburn, "International critical tables of numerical data, physics, chemistry and technology," (1st electronic edition), Knovel, 2003.

[69] B. E. Poling, J. M. Prausnitz, and J. P. O'Conell, "The properties of gases and liquids", (5th edition), McGraw Hill, USA, 2001.

[70] G. Wu, M. Heitz, and E. Chornet, "The depolymerization of lignin via aqueous alkaline oxidation," Advances in Thermochemical Biomass Conversion; Bridgewater, A.V., Ed; Springer: Cham, Switzerland pp. 1558-1571, 1993.

[71] W. Lan, and J. S. Luterbacher, "Preventing lignin condensation to facilitate aromatic monomer production," *CHIMIA Int. J. Chem.*, vol. 73, pp. 591-598, 2019.

[72] Z. Jiang, B. Aksoy, and The Auburn University, "Phenols as additives in kraft pulping," US Patent No. 20190112757A1, 2019.

[73] A.G. Vishtal, and A. Kraslawski, "Challenges in industrial applications of technical lignins," *BioResources*, vol. 6, pp. 3547-3568, 2011.

[74] Y. Matsushita, "Conversion of technical lignins to functional materials with retained polymeric properties," *J. Wood. Sci.*, vol. 61, pp. 230-250, 2015.

Chapter 3 | Towards bio-based vitrimers from lignocellulosic feedstock

Vitrimers are novel materials that exhibit permanent molecular networks which can change their molecular configuration through segmental diffusion simultaneously preserving network integrity. This allows vitrimers to have interesting properties such as self-healing, shape memory and solvent swelling. Bio-based vitrimers developed from lignocellulosic feedstock have shown excellent shape memory and repairing properties. The development of bio-based technologies is interesting since it allows to address the major limitations in valorization of lignocellulosic feedstock. This review addresses the current technologies for producing bio-based vitrimers in an integrated biorefinery.

3.1. Introduction

Currently, disposal of thermoset waste in our environment is one of the most challenging problems that needs to be addressed [1]. The available technologies focused on recycling can be classified into mechanical, thermal and chemical methods. However, these processes are not energy efficient and do not consider the recycling of the thermoset matrix. The modification of thermosetting polymers is, hence, crucial to address this issue. Novel development of vitrimer chemistries have the potential to tackle this challenge due to their repairing and recycling properties [2, 3]. These properties are a result of permanent network integrity that remains unchanged at all temperatures and during the entire experimental time.

Currently reported vitrimers are mainly derived from petrochemical feedstock. Hence, the use of bio–based vitrimers seems to be attractive in a sustainable biorefinery. Bio–based vitrimers are promising in industrial contexts due their preparation from commercially available monomers. These monomers include hemicellulose, cellulose and lignin which are readily available from pulp and paper industries.

Lignin is an amorphous high molecular mass biopolymer with a chemical structure distinct from the other constituents of wood. The chemical structure of the lignin is made up of phenyl-propane units that are not linked to each other in any systematic order [4]. The byproduct lignin obtained from pulping routes such as kraft, soda, organosolv, hydrolysis and sulphite processes are often called as technical lignins. Kraft lignin accounts for 85% of all the lignin produced in the world. Approximately, 45 million metric tons/year of kraft lignin is produced worldwide, however the majority of it is used as a low-grade fuel in the kraft pulping operation [5]. Due to the large commercial production scale of kraft lignin, there is a tremendous opportunity and economic incentive to find value-added uses.

Cellulose is the most abundant organic compound in the world which is produced by plants [6]. It is the predominant component of wood making up about 40 – 44% by dry weight [7]. It is hydrophilic in nature and insoluble in most organic solvents [8]. It is mainly obtained from wood pulp and cotton for industrial applications such as paper products. Cellulose extracted by chemical solubilization such as pulping has a refined structure. Cellulose nanofibrils (CNF) and cellulose nanocrystals (CNC) have a tremendous potential as components in bio-based vitrimers.

Hemicelluloses belong to a group of hetero-polysaccharides containing glucose, mannose, galactose, xylose and arabinose [9, 10]. In the process of converting wood into pulp, significant changes in the amounts, locations and structure of hemicellulose takes place. Compared to cellulose, they have a higher tendency toward degradation and dissolution. The sugars present in hemicellulose can be converted into value added products such as furfural, xylitol, ethanol, and arabitol. There are also opportunities to utilize these products from hemicelluloses for bio-based vitrimers.

3.2. Chemistry of vitrimers

Vitrimers are derived from thermosetting polymers (thermosets) and are very similar in nature to them. Vitrimer are based on dynamic associative bond-exchange reactions which allows them to retain the integrity of the crosslinked structure and impart self-healing properties. Due to their permanent network at all temperatures except their degradation temperatures, they usually swell in chemically inert solvents but do not dissolve when heated. The distinct properties of vitrimers are a result of bond-exchange reactions which are discussed briefly in the following sections.

3.2.1. Concerted type network rearrangement

In an ideal scenario for molecular network rearrangement, a new network bond can be formed at the same time as the old network bond is broken without a reactive intermediate as shown in **Figure 3.1**. The transition involves a temporary more cross-linked stage which is thermodynamically unstable [11]. In this case, the network integrity is maintained as the network exhibits same number of bonds at any given time. The permanent nature of crosslinking also avoids the possibility of side reactions. However, a single step molecular network rearrangement in a polymer is less likely and an actual polymer will more likely feature a multi-step pathway.

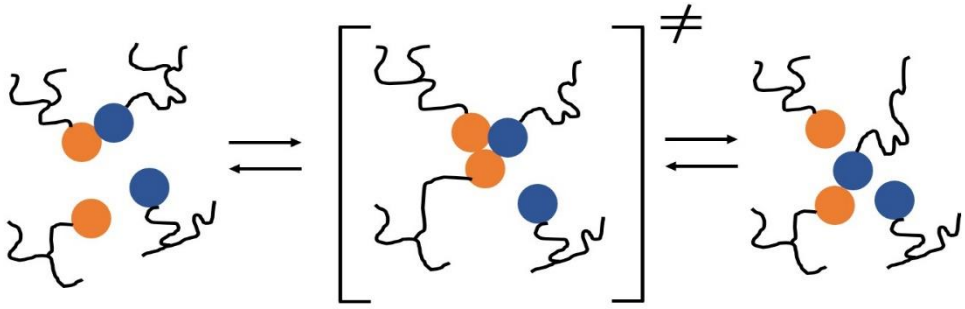

Figure 3.1. Concerted type molecular network rearrangement (Reproduced from open access article published by Royal Society of Chemistry)

3.2.2. Dissociative type network rearrangement

In the dissociative stepwise molecular network re-arrangement, the polymer chain undergoes formation of a temporarily de-crosslinked intermediate state as shown in **Figure 3.2**. In this case bonds are broken and formed again at another place. This results in temporary disruption of network integrity which results in a sudden viscosity drop. Upon cooling, the extent of crosslinking can be restored enabling the desirable thermosetting properties.

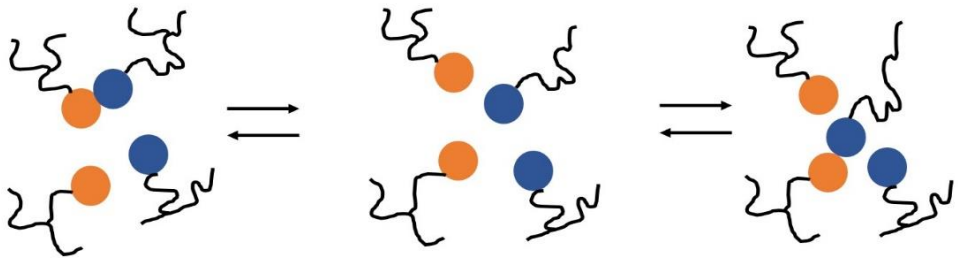

Figure 3.2. Dissociative type molecular network rearrangement (Reproduced from open access article published by Royal Society of Chemistry)

3.2.3. Associative type network rearrangement

In the case of associative stepwise molecular network re-arrangement, the original cross-link is only broken when a new covalent bond at another point takes place. This type of rearrangement is expected to meet the ideal vitrimer requirements. In this case, a reactive intermediate is involved during the bond breaking and reforming as shown in **Figure 3.3**. The transition to reactive intermediate causes temporary increase in cross-link density however, this effect is negligible since the new bond is formed soon after the former is cleaved [11].

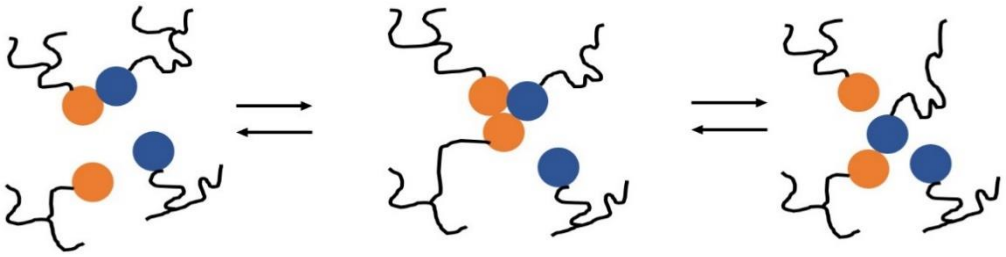

Figure 3.3. Associative type molecular network rearrangement (Reproduced from open access article published by Royal Society of Chemistry)

3.3. Bio-based vitrimers

Lignocellulosic materials which are widely available from pulp and paper industry can be used as monomers for preparation of 'green' vitrimers. However, there are technical and economic challenges for valorization limiting their application. For this reason, development of technologies which are sustainable and techno-economically feasible is crucial in an integrated biorefinery approach. Bio-based vitrimers are novel materials which have the potential to address these challenges. The following section highlights the current development of bio-based vitrimers from the point of view of an integrated biorefinery.

3.3.1. Lignin-based vitrimers

In general, vitrimers can be prepared by different chemistries such as transesterification, transamination, transalkylation, olefin metathesis exchange, disulfide exchange and imine amine exchange [2, 12-18]. Preparation of lignin based vitrimers from a transesterification exchange reaction is commonly studied in literature. The reaction involves initial nucleophilic attack by the hydroxyl of carboxylic acid groups on the electron deficient carbon on the epoxy group of a polymer. Further proton transfer from the oxygen of the hydroxyl group to the electron rich oxygen on the epoxy takes place to form a polymer containing both an ester and a hydroxyl function (**step 1**). This is followed by exchange of alkyl groups among the alcohol and ester at higher

temperatures and in the presence of catalysts (**step 2**) known as transesterification exchange reaction (TER). It is critical to note that the alcohol groups within the epoxy matrix can be self-sufficient to create TERs. This is highlighted in the reaction scheme shown in **Figure 3.4**.

Reaction scheme

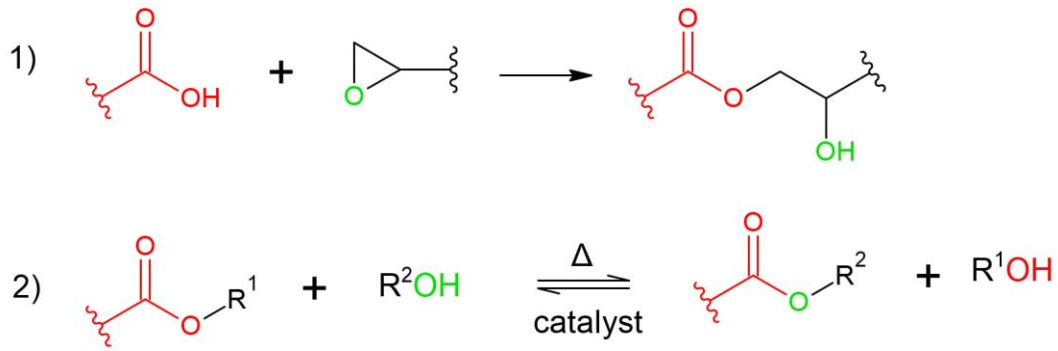

Figure 3.4. Transesterification reaction for lignin-based vitrimers (Reproduced from open access article published by Royal Society of Chemistry)

It is critical to note that untreated lignin contains a low amount of carboxyl groups [19]. To utilize lignin as a feedstock for transesterification reaction, the content of carboxylic acid groups should be increased within the lignin macromolecule. The carboxyl content in lignin can be increased by oxidizing agents such as oxygen, hydrogen peroxide and ozone. The oxidation of lignin results in formation of carboxylic acid via number of pathways either as monomer fragments or functional groups at the end of side chains of lignin. The side chain elimination of lignin results in phenolic compounds such as vanillin and vanillic acid which can further degrade to monomeric carboxylic acid fragments [20, 21]. Another pathway involves electrophilic attack at electron rich centers on the aromatic ring of lignin resulting in a four membered cyclic peroxide intermediate termed as dioxetane. This dioxetane can rearrange causing efficient cleavage of C–C bonds. The strategy for oxidation of lignin should target higher carboxylation on the lignin since more carboxyl groups induce efficient TERs and lignin content can be reduced less than the critical limit.

Table 3.1 shows the effect of oxidation treatments on the carboxyl content of lignin macromolecule.

Source	Oxidizing agent	Temp (°C)	Time (min)	Carboxyl content (mmol/g)	Literature source
Residual kraft lignin	O_2	140	80	1.50	[19]
Kraft lignin	O_3	80	360	4.20	[22]
Kraft lignin	H_2O_2	90	60	1.65	[23]
Alkali lignin	$(NH_4)_2S_2O_8$	90	120	1.62	[24]
Alkali lignin	CuO	90	120	1.87	

Table 3.1. Effect of oxidation treatments on carboxyl content of kraft lignins

The amount of lignin in the vitrimer has a profound effect on various tensile properties. The glass transition temperature and modulus usually increase with increasing lignin content. However, the epoxy polymer matrix also governs these tensile properties and the final tensile properties of the vitrimer are usually a combination effect of epoxy and lignin. A higher lignin content results in a denser cross-linked vitrimer and provides a rigid backbone. As a result, the glass transition temperature tends to increase with increasing lignin content provided the epoxy content is kept constant. Usually, a higher glass transition temperature will benefit the vitrimer stability since the segmental motions occur only after reaching this temperature. However, the viscoelastic liquid flow will only occur at temperatures higher than the topology freezing transition temperature 'T_v' [2, 25-27].

Among the various properties of vitrimers, self-healing is a unique property compared to conventional polymers [28-30]. The dynamic covalent network allows vitrimers to have molecular

rearrangements and topology fluctuations. The network segments can diffuse preserving the network integrity and as a result self-healing can be achieved. It is critical to note that higher cross-linking arising from lignin can restrict this segmental mobility and limit the self-healing ability. In this case, the abundance of ester bonds will be present however, to improve the efficiency of transesterification reaction additional measures are necessary. One way to address this challenge is to consider additional alcohol moieties from an external source. For example, the addition of ethylene glycol (EG) to a vitrimer composed of polyethylene glycol epoxy (PEG-epoxy) and carboxylated lignin (L-COOH) with 47.2% (wt.) lignin content allowed for over 80% healing of a crack in just 15 mins [31]. Another way to address the efficiency of TER is by heating the sample significantly higher than the glass transition temperature while simultaneously applying some pressure (~ 0.14 MPa). The application of pressure initiates deformation in the sample whereas, higher temperatures enable the sample to achieve thermal-responsive shape changing with efficient TERs [32].

The elongation at break of vitrimer can also be optimized by adjusting the amount of lignin charged in the reaction. A lower lignin content tends to allow considerable flexibility in the vitrimer because the rigidity and crosslinking tend to decrease and the amount of epoxy in the matrix increases. It has been observed that adjusting lignin content from 50% (wt.) to 66.6% (wt.) can reduce the elongation at break from 40.7% to 10.8% which represents a significant change [32]. It was also seen that lignin content can reduce the relaxation time significantly. The relaxation time for a vitrimer is related to the amount of elastic energy being stored by the fluid. Polymers in general can have a wide spectrum of relaxation times governing the relaxation process within and outside the polymer chain [33, 34]. For a sample with 66.6% (wt.) lignin content, the relaxation time of only 81 seconds was obtained compared to 1290 seconds obtained for 50% (wt.) lignin

content. This is because of the higher carboxyl content in the lignin which allows for increase in ester bonds with efficient TERs.

3.3.2. Cellulose-based vitrimers

Recent studies show tremendous research efforts in preparation of cellulose nanofibers (CNFs) from cellulose since they are one of the stiffest, strongest and most lightweight sustainable nanomaterials [18, 35-43]. One of the main limitations in CNFs produced from lignocellulosic materials is their hydrophilicity which results in poor water barrier properties [44]. The incorporation of vitrimer nanoparticles in CNFs is a promising approach to address this challenge.

Reaction scheme

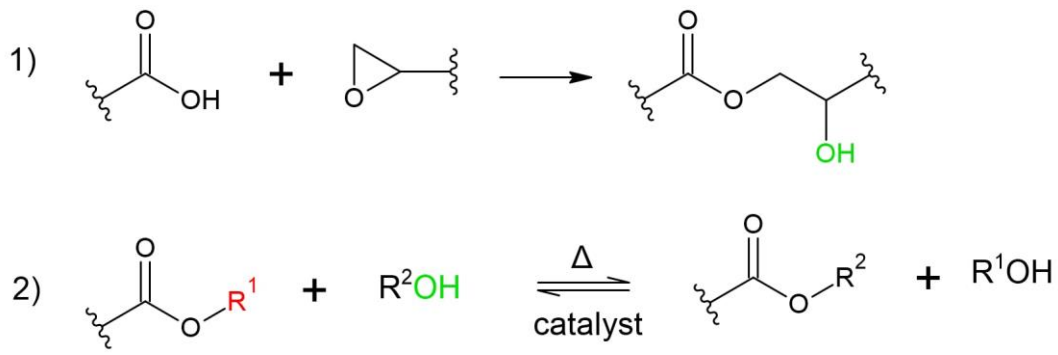

Figure 3.5. Transesterification reaction for CNF based vitrimers (Reproduced from open access article published by Royal Society of Chemistry)

Based on the reaction scheme mentioned in **Figure 3.5**, the initial vitrimer formation takes place between an epoxy and a fatty dimer acid (**Step 1**). The vitrimer formed in this step is rather uncured and the curing happens between carboxylate and alcohol groups in **Step 2** at higher temperatures in presence of catalysts. Nanocomposites can be further developed by incorporating these vitrimer nanoparticles into CNF. The role of CNF here is to react further with the alcohol moieties present in vitrimer nanoparticles again via transesterification exchange reaction (**step 2**). Hence, sufficient amount of carboxylic acid groups in CNFs are necessary. To improve the

carboxyl content in CNF, oxidation strategies such as TEMPO-mediated and ammonium persulfate (APS) oxidation can be used. TEMPO-mediated oxidation results in carboxyl content of 1.49 mmol/g whereas APS oxidation can result up to 1.33 mmol/g depending on the conditions used [45]. Hence, it is evident that there are differences in the way carboxylic acid groups perform TERs in lignin and CNF based vitrimers.

Pure CNFs, due to their hydrophilic nature, show considerable water absorption of more than 2500% in just 1 day. Also, prolonged exposure to water leads to disengagement of the network and redispersion of the CNFs leading to loss of mass. However, the incorporation of vitrimers into the CNF matrix can alter the physical properties significantly. Since, vitrimers are usually hydrophobic in nature, the nanocomposites made up of CNF and vitrimer result in 3 times lower water uptake compared to conventional CNF. Compared to uncured nanocomposites, the cured nanocomposites show lower uptake because the transesterification reaction decreases the hydrophilic groups such as hydroxyl and carboxylic acid. Also, curing eliminates the hydrophilic inter layer which promotes the interstitial migration of water within the material.

The nanocomposites also can address the wettability properties. Pure CNF nanopapers undergo an increase in ductility as humidity increases which affects hydrogen bonding [18, 46]. Hydrogen bonding is stronger in absence of humidity which helps prevent inelastic deformation. As the water molecules in the matrix increases, the amount of interfibrillar hydrogen bonds decrease and as a result, the binding strength is negatively affected. Hence, this challenge can be addressed by vitrimer based nanocomposites which facilitate inelastic behavior and allows the polymer composite to undergo higher deformation under proper conditions. Cured CNF/vitrimer nanocomposites showed stiffer and stronger tensile properties under different humidity scenario compared to non-cured samples.

In another study, polycarbonate chemistry **(Figure 3.6)** was utilized to synthesize a vitrimer-paper based composite [47, 48]. The porous structure of cellulose fiber paper network can be penetrated by vitrimers made from polyols and bicyclic carbonates via trans-carbonation exchange reactions. The hydrogen bonding interactions between natural cellulose fibers and the dynamical covalent bonds results in enhanced mechanical properties and smart properties such as shape-memory, self-healing, re-shaping and reprocessing. Notably, the vitrimer paper composites formed are totally recyclable. Based on the abundant nature of cellulose paper and excellent mechanical properties, vitrimer-paper represents a new class of sustainable composite materials with superior performance compared to the current thermoset based polymer composites.

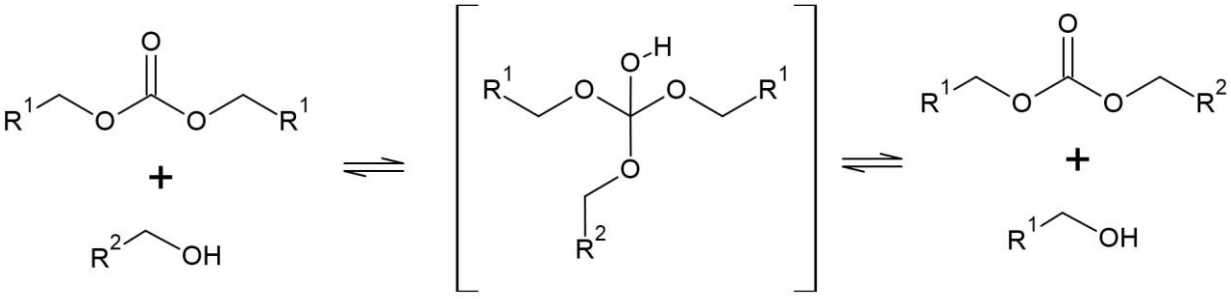

Figure 3.6. Transcarbonation exchange reaction for vitrimer based papers (Reproduced from open access article published by ACS)

3.3.3. Hemicellulose-based vitrimers

In an integrated biorefinery approach, the production of dissolving pulp is environmentally sustainable and suitable for pulp and paper mills. In contrast to conventional paper making which is mainly dependent on the kraft pulping process, 65% of the total dissolving pulp is produced by the acid sulfite method and 25%, by the prehydrolysis kraft (PHK) process, with the remaining 10% derived from cotton linters [10, 49-51]. During the PHK process, large amounts of hemicelluloses are dissolved in the prehydrolysis liquor. The presence of high amounts of hemicellulose in dissolving pulp is detrimental in further processing to end-uses [52, 53].

Therefore, the hemicelluloses in the prehydrolysis liquor are a source of hexose and pentose sugars which can be further converted to value added products such as furfural, xylitol, ethanol, and arabitol.[54].

From the point of view of bio-based vitrimers, the conversion of hemicellulose into furfural is of principal interest. Furfural is obtained by acid hydrolysis of hemicelluloses followed by dehydration of the pentose mono-sugars (xylose and arabinose) [55, 56]. Hydroxy-methylation of furfural can be performed to produce 5-hydroxy methyl furaldehyde (HMF) [57]. The chemistry of forming HMF based vitrimers follows imine-amine exchange reactions [58] as shown in **Figure 3.7**. In **step 1**, nucleophilic attack by an amine group takes place at the electron deficient carbon atom of the aldehyde. Further, proton transfer from the amine group to the electron rich oxygen atom takes place followed by the protonation of this OH group. The imine formation takes place in this case with subsequent elimination of water. The formed imine group is prone to nucleophilic attack by another amine group in as shown in **step 2**. Finally, metathesis takes place between the formed imines in **step 1** and **step 2** as shown in **step 3**.

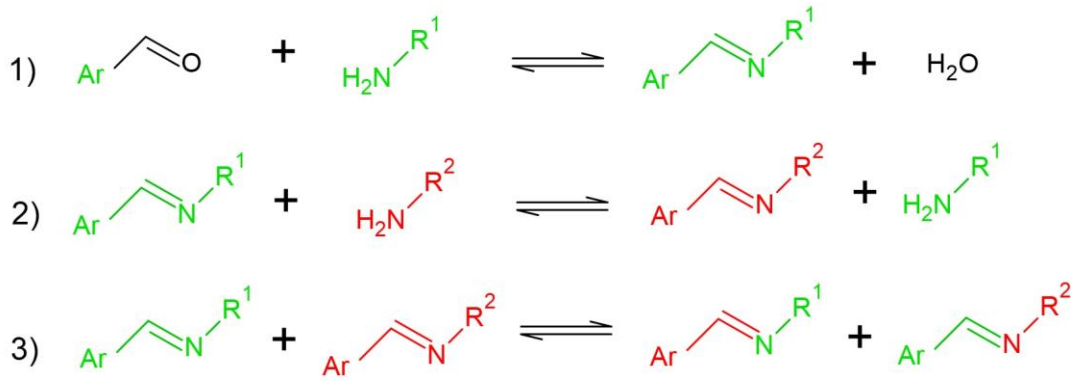

Figure 3.7. Imine-amine exchange chemistry 1) equilibrium of imine formation 2) transamination between imines and amines 3) imine metathesis

Direct synthesis of 2,5-furandicarboxaldehyde (FDC) from HMF is an active research topic in green chemistry [58-64]. FDC can be reacted with trimeric amine bio-based mixture (DTA) to

form vitrimers using imine – amine exchange chemistry. At various temperatures ranging from 40°C to 80°C, the vitrimer showed full stress relaxation because of reversibility of the imine bonds which was enhanced by an excess of amines. The vitrimer also showed almost constant tensile properties after three recycling cycles. The investigation of solubility studies also revealed that the vitrimer was undissolved in all the solvents examined such as THF, ethyl alcohol, DMF. The hydrolytic stability was also observed in neutral, acidic and basic water due to the hydrophobic nature of the amines used. Interestingly, when butyl amine was used, the vitrimer was completely dissolved due to the complete depolymerization of the network by dynamic amine exchange reactions.

3.4. Conclusions

In this review, we highlight potential strategies to produce bio-based vitrimers from lignin, cellulose and hemicellulose in an integrated biorefinery approach. The steady growth in demand for pulp and paper products calls for diversifying product profiles to meet consumer needs. Lignin-based vitrimers from can be produced by utilizing part of the black liquor stream since it contains significant amount of lignin. Cellulose based vitrimers can be produced by treating pulp to manufacture CNFs. In dissolving pulp producing mills, hemicellulose-based vitrimers can be integrated in the prehydrolysis stage since it is a major by-product obtained. It is also critical to note that the disadvantages in integrating to current pulp and paper mill operations cannot be avoided. However, in the scope of diversifying product profile for future demands, the advantages of valorizing lignocellulosic feedstock are more compared to the disadvantages.

One of the key developments of bio-based vitrimers is the tunable chemistry of bond exchange reactions. The efficiency of transesterification exchange reaction can be improved by addition of compounds containing alcohol groups, carboxylic acid groups or by adjusting the

reaction conditions using temperature, pressure. This is also applicable to other chemistries involved in vitrimer formation since the bond exchange reactions are reversible. In addition, this allows vitrimers to possess novel shape changing and self-healing properties. As they can be reprocessed, recycled and repaired these polymers have a potential to evolve as versatile light weight raw materials with high intrinsic value.

The major limitations of valorizing lignocellulosic feedstock can also be addressed using this pathway. For example, the current strategies of lignin valorization have lower yield of value-added products and majority of lignin remains unutilized. The current strategies of lignin based vitrimers consider more than 60% (by weight) conversion of lignin. In case of cellulose, hydrophilicity of CNFs is one of the main challenges limiting its application. However, this can be addressed by CNF/vitrimer composites which show significantly lower hydrophilicity. The conversion of hemicellulose into vitrimers is also an attractive approach since it is an underutilized feedstock for valorization. Therefore, the development of bio-based vitrimers is significant in an integrated biorefinery approach.

3.5. References

[1] W. Post, A. Susa, R. Blaauw, K. Molenveld, and R. J. Knoop, “A review on the potential and limitations of recyclable thermosets for structural applications,” *Polym. Rev.*, vol. 60, no. 2, pp. 359-388, 2020.

[2] W. Denissen, J.M. Winne, and F.E. Du Prez, “Vitrimers: permanent organic networks with glass-like fluidity,” *Chem. Sci.*, vol. 7, no. 1, pp. 30-38, 2016.

[3] J. M. Winne, L. Leibler, and F.E. Du Prez, “Dynamic covalent chemistry in polymer networks: a mechanistic perspective,” *Polym. Chem.*, vol. 10, no. 45, pp. 6091-6108, 2019.

[4] F. G. Calvo-Flores, J. A. Dobado, J. Isac-García, and F. J. Martín-Martínez, “Lignin and lignans as renewable raw materials: chemistry, technology and applications,” John Wiley & Sons, 2015.

[5] T. Q. Hu, “Chemical modification, properties, and usage of lignin,” Kluwer Academic/Plenum Publisher, 2002.

[6] D. P. Delmer, and C. H. Haigler, “The regulation of metabolic flux to cellulose, a major sink for carbon in plants,” *Metab. Eng*., vol. 4, no. 1, pp. 22-28, 2002.

[7] P. Basu, “Biomass gasification, pyrolysis and torrefaction: practical design and theory,” Academic press, 2018.

[8] M. He, A. Lu, and L. Zhang, “Advances in cellulose hydrophobicity improvement, Food Additives and Packaging,” *ACS Symp. Ser. Am. Chem. Soc*., pp. 241-274, 2014.

[9] G. A. Smook, and M.J. Kocurek, “Handbook for pulp & paper technologists,” Canadian Pulp and Paper Association, 1982.

[10] H. Kumar, and L. P. Christopher, “Recent trends and developments in dissolving pulp production and application,” Cellulose, vol. 24, no. 6, pp. 2347-2365, 2017.

[11] W. Alabiso, and S. Schlögl, “The impact of vitrimers on the industry of the future: Chemistry, properties and sustainable forward-looking applications,” *Polymers*, vol. 12, no. 8, pp. 1660, 2020.

[12] W. Denissen, G. Rivero, R. Nicolaÿ, L. Leibler, J. M. Winne, and F. E. Du Prez, “Vinylogous urethane vitrimers,” *Adv. Funct. Mater*., vol. 25, no. 16, pp. 2451-2457, 2015.

[13] D. J. Fortman, J. P. Brutman, C. J. Cramer, M. A. Hillmyer, and W. R. Dichtel, “Mechanically activated, catalyst-free polyhydroxyurethane vitrimers,” *J. Am. Chem. Soc*., vol. 137, no. 44, pp. 14019-14022, 2015.

[14] A. Rekondo, R. Martin, A. R. de Luzuriaga, G. Cabañero, H. J. Grande, and I. Odriozola, "Catalyst-free room-temperature self-healing elastomers based on aromatic disulfide metathesis," *Mater. Horiz.*, vol. 1, no. 2, pp. 237-240, 2014.

[15] M. M. Obadia, B.P. Mudraboyina, A. Serghei, D. Montarnal, and E. Drockenmuller, "Reprocessing and recycling of highly cross-linked ion-conducting networks through transalkylation exchanges of C–N bonds," J. Am. Chem. Soc., vol. 137, no. 18, pp. 6078-6083, 2015.

[16] W. Zou, J. Dong, Y. Luo, Q. Zhao, and T. Xie, "Dynamic covalent polymer networks: from old chemistry to modern day innovations," Adv. Mater., vol. 29, no. 14, pp. 1606100, 2017.

[17] M. M. Obadia, A. Jourdain, P. Cassagnau, D. Montarnal, and E. Drockenmuller, "Tuning the Viscosity Profile of Ionic Vitrimers Incorporating 1, 2, 3-Triazolium Cross-Links," *Adv. Funct. Mater*., vol. 27, no. 45, pp. 1703258, 2017.

[18] F. Lossada, J. Guo, D. Jiao, S. Groeer, E. Bourgeat-Lami, D. Montarnal, and A. Walther, "Vitrimer chemistry meets cellulose nanofibrils: bioinspired nanopapers with high water resistance and strong adhesion," *Biomacromolecules*, vol. 20, no. 2, pp. 1045-1055, 2018.

[19] F. Asgari, and D.S. Argyropoulos, "Fundamentals of oxygen delignification. Part II. Functional group formation/elimination in residual kraft lignin," *Can. J. Chem*., vol. 76, no. 11, pp. 1606-1615, 1998.

[20] R. Ma, M. Guo, and X. Zhang, "Selective conversion of biorefinery lignin into dicarboxylic acids," *ChemSusChem*, vol. 7, no. 2, pp. 412-415, 2014.

[21] J. Gierer, "Formation and involvement of superoxide (O_2-/HO_2·) and hydroxyl (OH·) radicals in TCF bleaching processes: A review," *Holzforschung*, vol. 51, no. 1, pp. 34-46, 1997.

[22] O. Musl, M. Holzlechner, S. Winklehner, G. Gübitz, A. Potthast, T. Rosenau, and S. Böhmdorfer, “Changing the Molecular Structure of Kraft Lignins-Ozone Treatment at Alkaline Conditions,” *ACS Sustain. Chem. Eng*., vol. 7, no. 18, pp. 15163-15172, 2019.

[23] F. Kong, S. Wang, W. Gao, and P. Fatehi, “Novel pathway to produce high molecular weight kraft lignin–acrylic acid polymers in acidic suspension systems,” *RSC Adv*., vol. 8, no. 22, pp. 12322-12336, 2018.

[24] Z. Q. Zhao, and X. P. Ouyang, “Effect of oxidation on the structures and properties of lignin,” *Adv. Mater. Res*., Trans Tech Publ, pp. 1208-1213, 2012.

[25] D. Montarnal, M. Capelot, F. Tournilhac, and L. Leibler, “Silica-like malleable materials from permanent organic networks,” *Science*, vol. 334, no. 6058, pp. 965-968, 2011.

[26] J. C. Dyre, “Colloquium: The glass transition and elastic models of glass-forming liquids,” *Rev. Mod. Phys*., vol. 78, no. 3, pp. 953, 2006.

[27] Y. Yang, S. Zhang, X. Zhang, L. Gao, Y. Wei, and Y. Ji, “Detecting topology freezing transition temperature of vitrimers by AIE luminogens,” *Nat. Commun*., vol. 10, no. 1, pp. 1-8, 2019.

[28] T. Liu, C. Hao, L. Wang, Y. Li, W. Liu, J. Xin, and J. Zhang, “Eugenol-derived biobased epoxy: shape memory, repairing, and recyclability,” *Macromolecules*, vol. 50, no. 21, pp. 8588-8597, 2017.

[29] Z. Pei, Y. Yang, Q. Chen, E.M. Terentjev, Y. Wei, and Y. Ji, “Mouldable liquid-crystalline elastomer actuators with exchangeable covalent bonds,” *Nat. Mater*., vol. 13, no. 1, pp. 36-41, 2014.

[30] X. Yang, L. Guo, X. Xu, S. Shang, and H. Liu, “A fully bio-based epoxy vitrimer: Self-healing, triple-shape memory and reprocessing triggered by dynamic covalent bond exchange,” *Mater. Des.*, vol. 186, pp. 108248, 2020.

[31] C. Hao, T. Liu, S. Zhang, L. Brown, R. Li, J. Xin, T. Zhong, L. Jiang, and J. Zhang, “A High-Lignin-Content, Removable, and Glycol-Assisted Repairable Coating Based on Dynamic Covalent Bonds,” *ChemSusChem*, vol. 12, no. 5, pp. 1049-1058, 2019.

[32] S. Zhang, T. Liu, C. Hao, L. Wang, J. Han, H. Liu, and J. Zhang, “Preparation of a lignin-based vitrimer material and its potential use for recoverable adhesives,” Green Chem., vol. 20, no. 13, pp. 2995-3000, 2018.

[33] M. Rubinstein, and R. H. Colby, *Polymer physics*, Oxford University Press New York, 2003.

[34] F. Del Giudice, S. J. Haward, and A. Q. Shen, “Relaxation time of dilute polymer solutions: A microfluidic approach,” *J. Rheol.*, vol. 61, no. 2, pp. 327-337, 2017.

[35] T. Saito, S. Kimura, Y. Nishiyama, and A. Isogai, “Cellulose nanofibers prepared by TEMPO-mediated oxidation of native cellulose,” *Biomacromolecules*, vol. 8, no. 8, pp. 2485-2491, 2007.

[36] K. Abe, S. Iwamoto, and H. Yano, “Obtaining cellulose nanofibers with a uniform width of 15 nm from wood,” *Biomacromolecules*, vol. 8, no. 10, pp. 3276-3278, 2007.

[37] A. Isogai, T. Saito, and H. Fukuzumi, “TEMPO-oxidized cellulose nanofibers,” Nanoscale, vol. 3, no. 1, pp. 71-85, 2011.

[38] W. Chen, H. Yu, Y. Liu, P. Chen, M. Zhang, and Y. Hai, “Individualization of cellulose nanofibers from wood using high-intensity ultrasonication combined with chemical pretreatments,” *Carbohydr. Polym.*, vol. 83, no. 4, pp. 1804-1811, 2011.

[39] F. Jiang, and Y.-L. Hsieh, “Chemically and mechanically isolated nanocellulose and their self-assembled structures,” *Carbohydr. Polym.*, vol. 95, no. 1, pp. 32-40, 2013.

[40] S. Kalia, S. Boufi, A. Celli, and S. Kango, “Nanofibrillated cellulose: surface modification and potential applications,” *Colloid Polym. Sci*., vol. 292, no. 1, pp. 5-31, 2014.

[41] M. Jonoobi, R. Oladi, Y. Davoudpour, K. Oksman, A. Dufresne, Y. Hamzeh, and R. Davoodi, “Different preparation methods and properties of nanostructured cellulose from various natural resources and residues: a review,” *Cellulose*, vol. 22, no. 2, pp. 935-969, 2015.

[42] O. Nechyporchuk, M.N. Belgacem, and J. Bras, “Production of cellulose nanofibrils: A review of recent advances,” *Ind. Crops Prod*., vol. 93, pp. 2-25, 2016.

[43] M. Pääkkö, M. Ankerfors, H. Kosonen, A. Nykänen, S. Ahola, M. Österberg, J. Ruokolainen, J. Laine, P.T. Larsson, and O. Ikkala, “Enzymatic hydrolysis combined with mechanical shearing and high-pressure homogenization for nanoscale cellulose fibrils and strong gels,” *Biomacromolecules*, vol. 8, no. 6, pp. 1934-1941, 2007.

[44] M. Borrega, and H. Orelma, “Cellulose nanofibril (CNF) films and xylan from hot water extracted birch kraft pulps,” *Appl. Sci*., vol. 9, no. 16, pp. 3436, 2019.

[45] I. Filipova, F. Serra, Q. Tarrés, P. Mutjé, and M. Delgado-Aguilar, “Oxidative treatments for cellulose nanofibers production: a comparative study between TEMPO-mediated and ammonium persulfate oxidation,” Cellulose, pp. 1-18, 2020.

[46] A.J. Benítez, J. Torres-Rendon, M. Poutanen, and A. Walther, “Humidity and multiscale structure govern mechanical properties and deformation modes in films of native cellulose nanofibrils,” Biomacromolecules, vol. 14, no. 12, pp. 4497-4506, 2013.

[47] W. Zhao, Z. Feng, Z. Liang, Y. Lv, F. Xiang, C. Xiong, C. Duan, L. Dai, and Y. Ni, "Vitrimer-Cellulose Paper Composites: A New Class of Strong, Smart, Green, and Sustainable Materials," *ACS Appl. Mater. Interfaces*., vol. 11, no. 39, pp. 36090-36099, 2019.

[48] R. L. Snyder, D. J. Fortman, G. X. De Hoe, M. A. Hillmyer, and W. R. Dichtel, "Reprocessable acid-degradable polycarbonate vitrimers," *Macromolecules*, vol. 51, no. 2, pp. 389-397, 2018.

[49] M. Marinova, E. Mateos-Espejel, N. Jemaa, and J. Paris, "Addressing the increased energy demand of a Kraft mill biorefinery: The hemicellulose extraction case," *Chem. Eng. Res. Des*., vol. 87, no. 9, pp. 1269-1275, 2009.

[50] C. Mendes, M. Carvalho, C. Baptista, J. Rocha, B. Soares, and G. Sousa, "Valorisation of hardwood hemicelluloses in the kraft pulping process by using an integrated biorefinery concept," *Food Bioprod. Process*., vol. 87, no. 3, pp. 197-207, 2009.

[51] H. Sixta, A. Potthast, and A.W. Krotschek, "Chemical Pulping Processe: Sections 4.1–4.2.5," Handbook of pulp, pp. 109-229, 2006.

[52] J. Behin, and M. Zeyghami, "Dissolving pulp from corn stalk residue and waste water of Merox unit," *Chem. Eng. J*., vol. 152 no. 1 pp. 26-35, 2009.

[53] D. Ibarra, V. Köpcke, P.T. Larsson, A.-S. Jääskeläinen, and M. Ek, "Combination of alkaline and enzymatic treatments as a process for upgrading sisal paper-grade pulp to dissolving-grade pulp," *Bioresour. Technol*., vol. 101, no. 19, pp. 7416-7423, 2010.

[54] I. Kaur, and Y. Ni, "A process to produce furfural and acetic acid from pre-hydrolysis liquor of kraft based dissolving pulp process," *Sep. Purif. Technol*., vol. 146, pp. 121-126, 2015.

[55] P. Bhaumik, and P.L. Dhepe, “Efficient, stable, and reusable silicoaluminophosphate for the one-pot production of furfural from hemicellulose,” *ACS Catal*., vol. 3, no. 10, pp. 2299-2303, 2013.

[56] A. S. Mamman, J.M. Lee, Y. C. Kim, I. T. Hwang, N. J. Park, Y. K. Hwang, J.S. Chang, and J. S. Hwang, “Furfural: Hemicellulose/xylose derived biochemical,” *Biofuel. Bioprod. Biorefin*., vol. 2, no. 5, pp. 438-454, 2008.

[57] S. Nishimura, and A. Shibata, “Hydroxymethylation of Furfural to HMF with Aqueous Formaldehyde over Zeolite Beta Catalyst,” *Catalysts*, vol. 9, no. 4, pp. 314, 2019.

[58] S. Dhers, G. Vantomme, and L. Avérous, “A fully bio-based polyimine vitrimer derived from fructose,” *Green Chem*., vol. 21, no. 7, pp. 1596-1601, 2019.

[59] M. Chatterjee, T. Ishizaka, A. Chatterjee, and H. Kawanami, “Dehydrogenation of 5-hydroxymethylfurfural to diformylfuran in compressed carbon dioxide: an oxidant free approach,” *Green Chem*., vol. 19, no. 5, pp. 1315-1326, 2017.

[60] A. Rapeyko, K.S. Arias, M.J. Climent, A. Corma, and S. Iborra, “Polymers from biomass: one pot two-step synthesis of furilydenepropanenitrile derivatives with MIL-100 (Fe) catalyst,” *Catal. Sci. Technol*., vol. 7, no. 14, pp. 3008-3016, 2017.

[61] E. Giglio, “Tunable mixed oxides based on CeO_2 for the selective aerobic oxidation of 5-(hydroxymethyl) furfural to FDCA in water,” *Green Chem*., vol. 20, no. 17, pp. 3921-3926, 2018.

[62] Y. Ren, Z. Yuan, K. Lv, J. Sun, Z. Zhang, and Q. Chi, “Selective and metal-free oxidation of biomass-derived 5-hydroxymethylfurfural to 2, 5-diformylfuran over nitrogen-doped carbon materials,” *Green Chem*., vol. 20, no. 21, pp. 4946-4956, 2018.

[63] J. Ma, Z. Du, J. Xu, Q. Chu, and Y. Pang, “Efficient aerobic oxidation of 5-hydroxymethylfurfural to 2, 5-diformylfuran, and synthesis of a fluorescent material,” *ChemSusChem*, vol. 4, no. 1, pp. 51-54, 2011.

[64] M. Kompanets, O. Kushch, Y.E. Litvinov, O. Pliekhov, K. Novikova, A. Novokhatko, A. Shendrik, A. Vasilyev, and I. Opeida, “Oxidation of 5-hydroxymethylfurfural to 2, 5-diformylfuran with molecular oxygen in the presence of N-hydroxyphthalimide,” *Catal. Commun*., vol. 57, pp. 60-63, 2014.

Chapter 4 | Towards a new understanding of the retro-aldol reaction for oxidative conversion of lignin to aromatic aldehydes and acids

The retro-aldol reaction is one of the key steps involved in the oxidative conversion of lignin to aromatic aldehydes and acids. In principle, the retro-aldol reaction can proceed in the absence of oxygen. In this work, a new approach based on the influence of oxygen on the oxidation of lignin was investigated. In this approach, the duration of oxygen charged during the reaction was optimized to, for the first time, improve the yield of aromatic aldehydes and acids. The effect of reaction chemistry, time, temperature, and lignin feedstock plays a key role on the yield of aromatic aldehydes and acids. At 140°C, oxidation of softwood kraft lignin (SKL) for 40 minutes results in combined maximum yield of 5.17% w/w of vanillin and vanillic acid. In comparison, using the new approach in which oxygen was charged for only 20 minutes during the 40 minute reaction improved this yield considerably to 6.95%. Further, yield improvement was obtained when applying this approach to different lignin feedstocks. Oxidation also increased the carboxyl content in lignin to 1.41 mmol/g at 130°C which represents a marked improvement. The current study provides new evidence showing that the oxidation reaction is a crucial pathway for lignin valorization.

4.1. Introduction

Lignin is the most abundant natural biopolymer after cellulose and accounts for about 30% of non-fossil carbon on earth [1, 2]. The distinct aromatic nuclei representing *p*-hydroxyphenyl (H), guaiacyl (G), and syringyl nuclei (S) in the lignin structure arise from the monomers *p*-hydroxycoumaryl alcohol, coniferyl alcohol, and sinapyl alcohol respectively [3, 4]. The ratio of these monomers influence the degree of branching and the reactivity of lignin [5]. During pulping processes, delignification of the wood matrix takes place by chemically degrading the lignin to

liberate cellulose. The lignin obtained from technical processes has different structural characteristics based on the origin of wood species, delignification type and recovery process of lignin from pulping liquors [6, 7]. The structural details of one fragment of technical kraft lignin is highlighted in **Figure 4.1**.

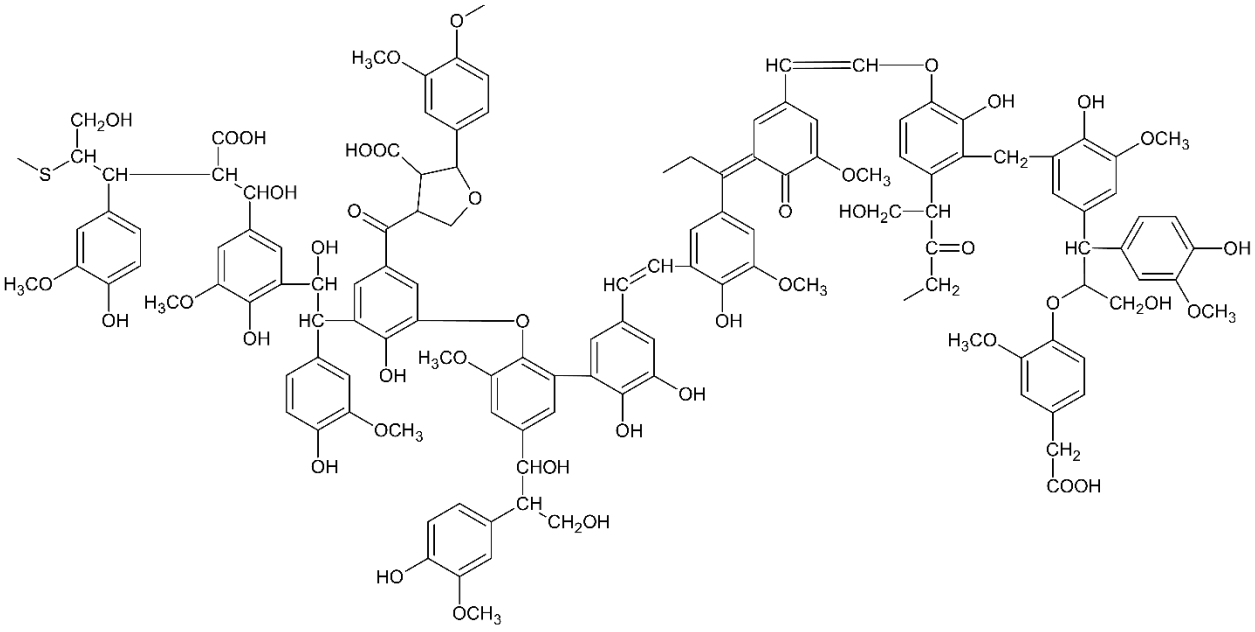

Figure 4.1. Structure of kraft lignin [8] (reproduced with permission from Elsevier)

In an integrated approach, the oxidative conversion of lignin to aromatic aldehydes and acids such as vanillin and vanillic acid is widely proposed [9-12]. Currently, only lignosulfonates are used for the industrial production of vanillin due to higher yields ranging from 5-7% in the presence of transition metal catalysts. However, lignosulfonates represent less than 10% of total lignins extracted [13, 14]. Kraft lignin represents the majority of lignin produced worldwide and accounts for 85% of all the lignin produced, corresponding to around 45 million metric tons/year. However, lignin which is an abundant aromatic biopolymer, is underutilized and is considered as a non-valorized waste [15]. Currently, it is mainly used as a source of low grade fuel in the pulping operation and only about 100,000 tons of kraft lignins available are valorized per year [16, 17]. Therefore, valorization of kraft lignin into high value-added products is an important goal.

Pine kraft lignin has been commercially available as ‘Indulin’ from Mead-Westvaco since the 1950s. Indulin represented the main source of commercial kraft lignin for a long time. However, the conventional process of lignin precipitation and separation from kraft black liquors causes serious problems related to complete or partial plugging of the filter cake and of the filter medium. In 2013, the Domtar Plymouth Mill in North Carolina (USA) installed the ‘Lignoboost’ process to address the problems associated with traditional processes of lignin separation from kraft black liquors. In the following year, West Fraser Company installed the ‘Lignoforce’ process at the Hinton Pulp Mill in Alberta, Canada. Due to the differences in the process of lignin precipitation and separation from kraft black liquors, these three kraft lignins have quite different properties [18, 19].

The oxidation of lignin produces vanillin (4-hydroxy-3-methoxybenzaldehyde, $C_8H_8O_3$), which is a high value product having applications in a variety of industries. It is useful due to its aromatic nature and reactive functional groups, methoxy, aldehyde and phenol. It is the highest volume aromatic aldehyde produced worldwide [13]. It has various applications in food, cosmetic, chemical and pharmaceuticals industries. The importance of vanillin is also growing because of its antioxidant and anti-cancer properties and also its involvement in bacterial cell to cell signaling [20, 21]. Other applications of vanillin are as a ripening agent to increase the sucrose content in sugar cane or in the preparation of sunscreen [22]. Vanillic acid (4-hydroxy-3-methoxybenzoic acid) is another value added product generated in the process of lignin oxidation which is used as a flavoring agent. Recently, vanillic acid has received considerable attention due to its role in preventing human diseases. It is of importance due to its antibacterial, antimicrobial and chemo-preventive properties [23]. Vanillin and vanillic acid have both been obtained as major products from the alkaline oxidation of softwood and hardwood lignin [24, 25].

The oxidative conversion of lignin to vanillin and vanillic acid in an alkaline medium using oxygen has been widely discussed in the literature [14, 26-31]. Oxygen is the preferred oxidizing agent due to its environmental friendliness, high atom economy and low price. However, due to the lower yields obtained in this process, catalysts in combination with oxygen are required to improve the yields by a factor of 1.5-2. To produce vanillin and vanillic acids in the kraft pulping process, it is crucial to avoid the use of catalysts to allow for downstream processing of kraft liquor in evaporators and recovery boilers. The high consumption of oxygen – over 10 mol per mol of vanillin obtained is also an unresolved problem [12]. Another limitation of this process is the use of large amount of acids, organic solvents and energy which have environmental consequences [13]. Therefore, the development of technologies which are sustainable and easily integrable in the current pulp and paper industrial processes are needed. The work reported here is focused on addressing this problem in the oxidative conversion of lignin to vanillin and vanillic acid using a sustainable approach. In this approach, more lignocellulosic biomass can be converted to value-added products with lower consumption of oxygen improving the overall economic and environmental viability of this process.

The formation of vanillin and vanillic acid from the oxidation of lignin using oxygen under alkaline conditions depends on reaction chemistry, time, temperature, oxygen partial pressure, lignin concentration, and feedstock. Among the various oxidation pathways proposed in the literature, the retro-aldol reaction is the most promising pathway for explaining the production of vanillin and acetovanillone. In alkaline conditions, the reaction begins with dehydration of the C_α-C_β bond proceeded by electron abstraction from the phenoxyl anion. The oxygen oxidation then results in single-electron abstraction from phenoxyl anion resulting in the formation of the superoxide anion radical and phenoxyl radical (Step 1) (**Figure 4.2**). The major steps that follow

are the formation of a quinone methide from the phenoxyl radical (Step 2a & 2b), and nucleophilic attack of a hydroxyl ion at γ position which is under thermodynamic control (Step 3). The hydroxyl group at the γ position is oxidized to a γ-carbonyl group (coniferaldehyde type structure) (Step 4). The retro-aldol reaction proceeds by alkaline hydrolysis of this structure to form an α-hydroxy-γ-carbonyl structure (Step 5). Further, alkaline dissociation of this α- hydroxy-γ-carbonyl structure takes place at C_β position (Step 6) followed by retro-aldol cleavage to form vanillin as shown in (Step 7). Under kinetic control, nucleophilic attack of hydroxyl ion takes place at the α-position. Subsequent oxidation and eventual retro-aldol reaction of the resulting α-oxo-β-unsaturated structure results in acetovanillone.

Step 1: Dehydration followed by initiation of phenoxyl anion

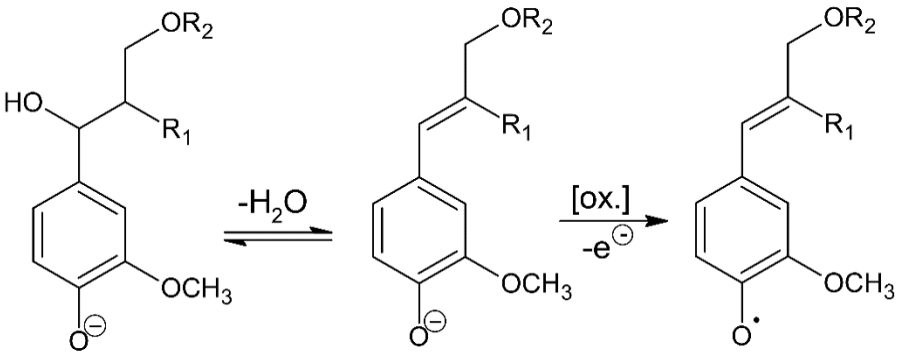

Step 2a: Disproportionation of phenoxyl radical to form quinone methide

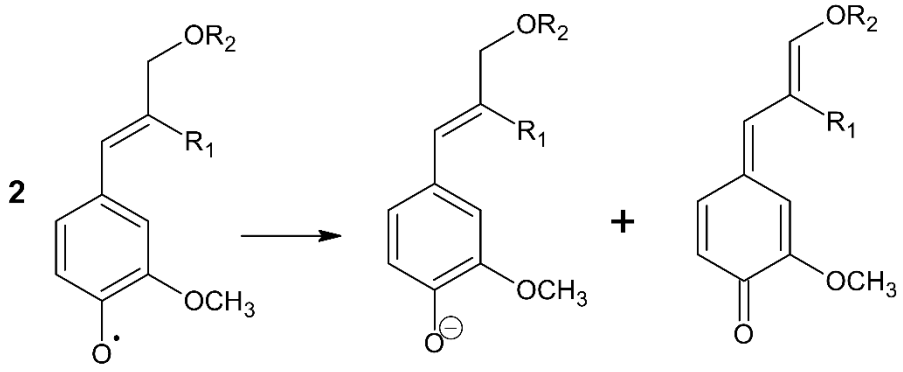

Step 2b: Oxidation of phenoxyl radical preceded by proton detachment

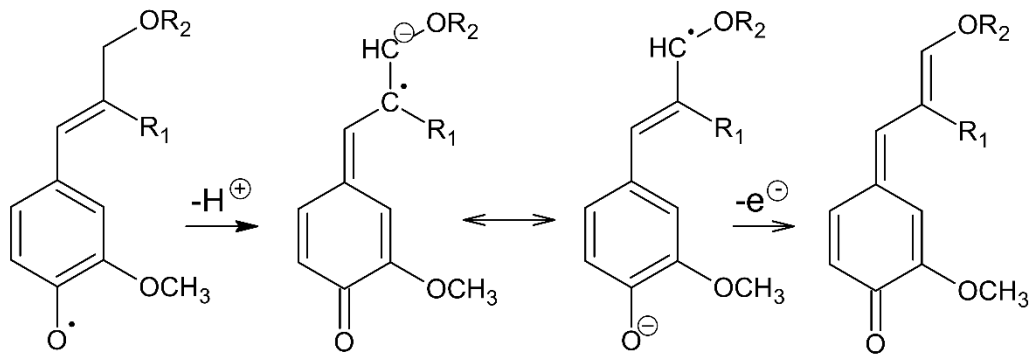

Step 3: Nucleophilic addition of hydroxide ion to form coniferyl alcohol structure

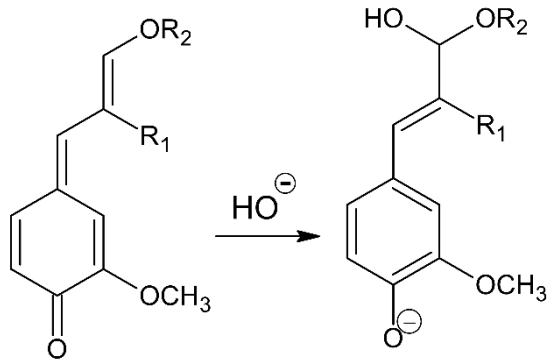

Step 4: Oxidation of coniferyl alcohol structure to *γ*-carbonyl group

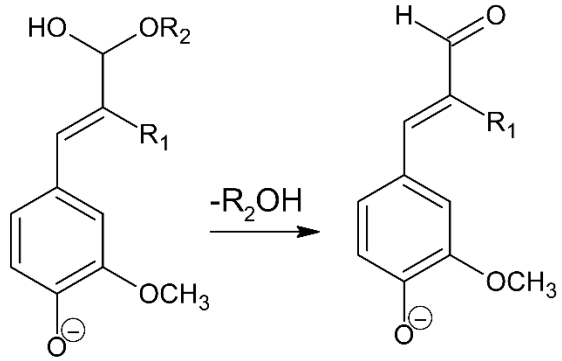

Step 5: Alkaline hydrolysis of *γ*-carbonyl coniferyl structure

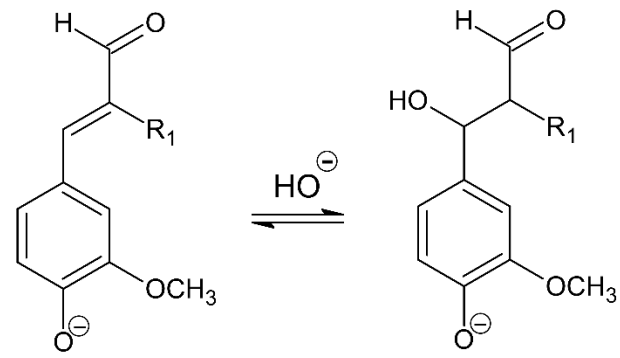

Step 6: Alkaline dissociation of α- hydroxy-γ-carbonyl structure

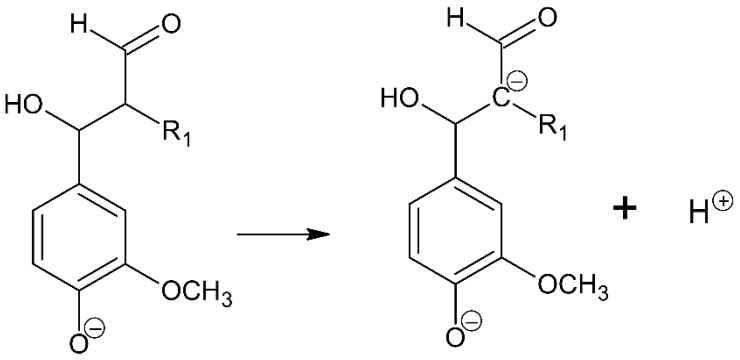

Step 7: Retro-aldol cleavage of C_α-C_β bond to form vanillin

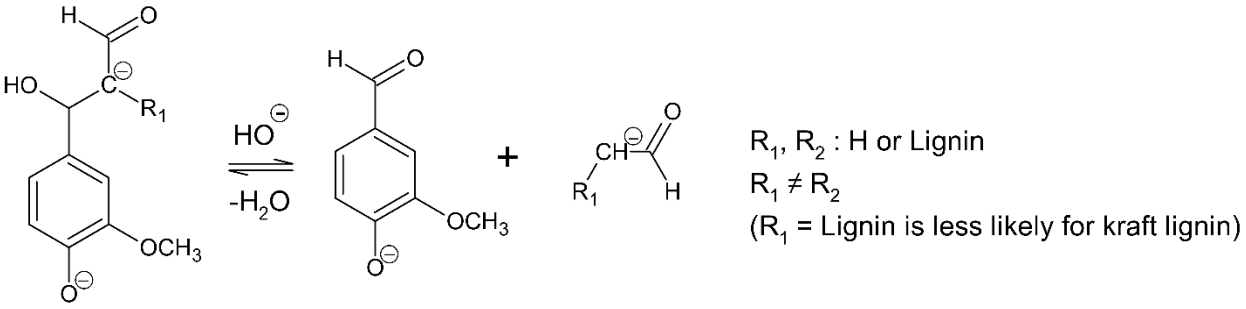

Figure 4.2. Mechanism of alkaline oxidation of lignin using oxygen [31]

In principle, the retro-aldol reaction (Steps 5, 6 and 7) proceeds in the absence of oxygen. Also, the degradation of vanillin and vanillic acid occurs at severe oxidation conditions if oxygen is charged beyond this final phase of product formation [6, 14, 32]. To confirm the role of the retro-aldol reaction, a model compound study was performed using vanillidenacetone (α-β-

unsaturated-γ-carbonyl type structure) in the literature [30]. In this study, the model compound was formed by the aldol condensation of vanillin and acetone as shown in **Figure 4.3**.

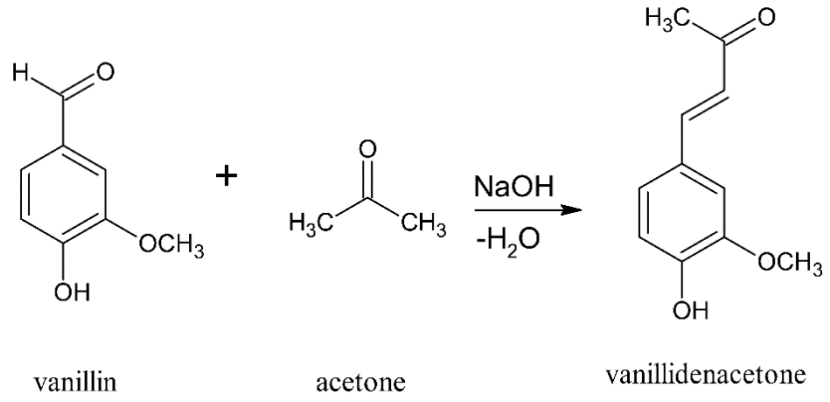

Figure 4.3. Aldol condensation of vanillin and acetone resulting in vanillidenacetone* according to the literature [30]

***Note –** The term 'vanillidenacetone' used here to be consistent with the literature and it refers to the compound 'dehydrozingerone' (4-(4-hydroxy-3-methoxyphenyl)-3-buten-2-one)

It was observed that under an argon atmosphere, vanillidenacetone is hydrolyzed with the formation of vanillin at pH 10 and 160°C for 30-50 min, with vanillin selectivity of about 90%. In the presence of oxygen and a catalyst, vanillidenacetone is consumed faster and the vanillin yield decreases by a factor of 3-5. Therefore, the rate of the retro-aldol reaction decreases with the introduction of oxygen which decreased vanillin yield substantially at pH 10. However, increasing the pH to 11, increased the rate of the retro-aldol reaction, since it is directly proportional to the concentration of hydroxide ion. In this case, vanillin yield does not decrease under the action of oxygen prior to reaching its maximum. A decrease in vanillin yield after reaching its maximum is likely due to its subsequent oxidation. Therefore, this study confirms the occurrence of the retro-aldol reaction in the formation of vanillin from the oxidation of lignin model compounds. It can also be deduced from this study that the retro-aldol reaction can proceed in the absence of oxygen

and the introduction of oxygen in this phase is likely to contribute negatively to vanillin yield due to its subsequent oxidation after reaching its peak yield.

In another study, vanillin, vanillic acid and traces of acetovanillone were formed from sodium lignosulfonate in the absence of oxygen solely by the hydrolysis reaction [14]. In this study, hydrolysis was observed at much lower temperatures (120°C) compared to the previous study in which it was carried out at 160°C. The formation of vanillic acid in this case also suggests that it is not a product of only the oxidation of vanillin. It was also observed in this study that the increase in oxygen partial pressure led to an increase in the vanillin oxidation rate after the maximum vanillin concentration was reached. This study supports the presence of the retro-aldol reaction and the role of oxygen in the oxidative conversion of lignins to aromatic aldehydes and acids. Therefore, yields may be improved in this final phase of the reaction sequence and degradation of high-value added products can be inhibited by controlling the amount of oxygen charged in the reaction after reaching the peak yields from oxidation. The objective of this work is to analyze the effect of controlling the amount of oxygen charged during the reaction on the yield of vanillin and vanillic acid. The optimum conditions based on time and temperature were established and then optimization based on the effect of oxygen addition was performed. Further, based on these experiments for softwood kraft lignin (SKL), other lignin feedstocks were then analyzed to determine if similar yield improvements can be observed.

4.2. Materials and methods

4.2.1. Chemicals: Oxygen and nitrogen of ultra-high purity were supplied by Airgas, USA. Sodium hydroxide beads (purity ≥ 97%), sulfuric acid and hydrochloric acid (1.0 N laboratory reagent grade), HPLC grade acetonitrile (assay ≥ 99.95%) were purchased from VWR Chemicals,

USA. Sodium chloride (assay ≥ 99%) was supplied by Fisher Chemical™, USA. Vanillin and vanillic acid, both with a purity higher than 99% were supplied by Sigma-Aldrich, USA.

4.2.2. Raw materials: In this work, four different lignins were used to study the effect of their different processing conditions. They are: 1) Softwood kraft lignin (*SKL*); 2) Indulin AT from Sigma-Aldrich *LInAT*; 3) *H-lignin* (enzymatic hydrolysis lignin) from FPInnovations; 4) Marasperse AG from Borregaard Lignotech *LMarAG*. All lignins were analyzed for moisture content and used without further purification. The structural features of the lignins have been characterized in the literature [18, 33] and shown in **Table 4.1** as follows:

Note*-includes condensed and uncondensed phenolic OH groups, n.d: not detected

Lignin properties	SKL	Indulin AT	H-lignin	Marasperse AG
molecular weight, g/mol	M_w: 6772	M_w: 6549	M_w: 5840-7580	M_n: 534.5
carboxylic OH, mmol/g	0.35	0.40	0.10-0.15	n.d
aliphatic OH, mmol/g	2.02	2.19	4.8-6.3	n.d
total phenolic OH*, mmol/g	4.28	3.43	0.62-0.92	1.42

Table 4.1. Structural characterization of different lignins

4.2.3. Oxidation of lignin: Oxidation experiments were carried out in a Parr reactor with a capacity of 1L (Series 4520). The heating and temperature were controlled with a Parr 4848 reactor controller. Temperature and total pressure inside the reactor were measured using a Type J (iron-constantan) thermocouple and a pressure gauge respectively. The agitator speed was kept constant

at 400 RPM for all runs. The procedure for oxidation of lignin using oxygen was carried out in accordance with the literature [3]. 20 g of lignin were dissolved in 200 mL of alkaline solution containing 26.67 g of NaOH. After complete dissolution, the resulting mixture was diluted to a final volume of 333 mL. This concentration of lignin (20 g in 333 mL of solution) was kept constant for all experiments performed. The resulting solution was introduced into the reactor and initially pressurized to 30 psi using nitrogen. The reactor was then heated until the temperature set point was reached. After the temperature set point was reached, oxygen was introduced to the reactor and the reaction time was monitored from the point of admission of oxygen. The reactor was pressurized with 50 psi of oxygen for all experiments based on optimized conditions for oxygen pressure in the literature [3]. The solubility of oxygen in the reaction medium is dependent on the oxygen partial pressure (P_{O_2}), temperature of the reaction (T) and the ionic strength of the liquid medium (I). The concentration of dissolved oxygen $[O_2^{liq}]$ can be obtained with the following empirical correlation which is valid for temperatures ≤ 150°C and oxygen partial pressures ≤ 5 MPa [14, 32, 34]:

$$[O_2^{liq}] = \left(3.559 - 6.659 \times 10^{-3} \times T - 5.606 \times P_{O_2} + 1.594 \times 10^{-5} \times P_{O_2} \times T^2 + 1.498 \times 10^3 \times \frac{P_{O_2}}{T}\right) \times (10^{-0.144 \times I}) \times (10^{-3})$$

$$where\ P_{O_2}\ is\ in\ bar, I\ and\ [O_2^{liq}]\ is\ in\ mol\ per\ liter, and\ T\ is\ in\ Kelvin$$

The water partial pressure above the NaOH solution, P_{NaOH} (bar) can be calculated as follows:

$$\log P_{NaOH} = a + b \log p^0$$

$$the\ parameters\ a\ and\ b\ depend\ only\ on\ the\ concentration\ of\ NaOH\ (M)$$

$$and\ p^0\ (bar)\ represents\ the\ equilibrium\ partial\ pressure\ of\ water\ vapor\ over\ pure\ water\ as\ a\ function\ of\ temperature$$

$$a = -0.010986M - 1.461 \times 10^{-3}M^2 + 2.03528 \times 10^{-5}M^3$$

$$b = 1 - 1.34141 \times 10^{-3}M + 7.07241 \times 10^{-4}M^2 - 9.5362 \times 10^{-6}M^3$$

$$and \log p^0 = 35.4462 - \frac{3343.93}{T} - 10.9 \log T + 0.0041645T \; where \; T \; is \; in \; Kelvin \quad [14, 35]$$

Since the reaction is exothermic, the reaction was monitored using the initial temperature (T_i). The effect of temperature on the yield of vanillin and vanillic acid and the carboxyl content of lignin was studied at 120°C, 130°C, 140°C, 150°C and 160°C at a constant reaction time of 40 minutes. The effect of time at 0, 20, 40 and 60 minutes was studied by keeping the temperature of the reactor constant at 140°C. The effect of controlling the amount of oxygen charged during the reaction was studied by introducing oxygen for 0, 5, 20 and 30 minutes out of the 40 minute reaction time at 140°C. *SKL*, *LInAT*, *H-lignin* and *LMarAG* were then used to compare the conventional strategy (oxygen introduction = 40 minutes) against a new proposed strategy (oxygen introduction = 20 minutes out of 40 minutes)

4.2.4. Quantification of yield using High-Performance Liquid Chromatography: The low molecular weight aromatic aldehydes and acids produced by lignin oxidation with oxygen were quantified by high performance liquid chromatography (HPLC). The details on the extraction procedure and HPLC conditions were in accordance with the literature [34]. Quantification of all compounds was done based on calibration curves prepared from standard solutions in the required concentration range. The HPLC system was equipped with an Alcott 708 auto-sampler, an online degasser, a Lab Alliance Series III pump and a Waters 2487 Dual λ Absorbance Detector. The detection wavelength was set to 280 nm and the injection volume was 10 µL. Chromatograms were acquired at 60°C with a flow rate of 0.6 mL/min using a mobile phase composed of two eluents (A) 5 mM sulphuric acid and (B) acetonitrile with a ratio of 4:1 by weight respectively [36]. The analytical column was Aminex HPX 87H ion exclusion column with column size 300 mm × 7.8 mm, and particle size of 9 µm.

4.2.5. Carboxyl content determination using conductometric titration: The carboxyl content of the precipitated lignin from the oxidation reactions was determined using the conductometric titration method [37]. After the oxidation treatment, an aliquot of lignin solution was adjusted to pH below 2 by addition of 1 N HCl in the ratio of 1:3 v/v (lignin solution: 1N HCl). This caused the lignin present in the solution to precipitate out. The precipitated lignin was then recovered by centrifugation and then freeze dried to obtain dry lignin powder with moisture content ≤ 10% by weight. Further, freeze-dried samples of precipitated lignin equivalent to 1.5 g oven dry were added to 300 mL of 0.10 N HCl and stirred for one hour. The lignin was then filtered and washed with de-ionized water until the conductivity of the effluent water was less than 5 μScm^{-1}. The washed lignin was then dispersed in 0.001 N NaCl (250 mL) with further addition of 0.10 N HCl solution (1.5 mL), stirred and titrated with 0.05 N NaOH under continuous bubbling of nitrogen. A Metrohm Autotitrator was used for titration, with an 856 Conductivity module connected to the main module (888 Titrando) coupled with Tiamo^{TM} 2.5 software. The conductivity was plotted against the volume of NaOH resulting in parabolic curve composed of three distinguishable regimes. The first regime shows a decrease in conductivity, which is the neutralization of added HCl. The second regime is a horizontal zone corresponding to the neutralization of weak acid groups, i.e. carboxylic acid groups. Finally, the third regime is associated with the conductivity increase after reaching the equivalence point, due to the introduction of excess NaOH to the suspension. The carboxyl content of the samples was then determined based on the intersection of the three trend lines drawn for each of these regimes.

4.2.6. Comparing results for statistical significance using Tukey test: The yield changes due to optimization of the proposed strategy were analyzed by performing Tukey's honest significance test using Minitab® 19 software.

4.3. Results and discussion

The production of vanillin and vanillic acid from kraft lignin is carried out at highly alkaline conditions (pH ~ 14) and at elevated temperature (between 100 and 200°C). Under such conditions it has been established in the literature that oxidation of lignin to vanillin and vanillic acid is linked to reaction chemistry, temperature, oxygen pressure, pH, reaction time and lignin concentration. The investigation of all these parameters on oxidation of lignin is beyond the scope of this work since the present work is mainly focused on studying the effect of controlling the amount of oxygen charged during the reaction on the yield of vanillin and vanillic acid. In principle, the mechanism of lignin oxidation to vanillin shown in **Figure 4.2** unites the lignin chemistry principles about phenoxyl radicals and quinone methide intermediates with the concept of the retro-aldol reaction as the final process step. It explains the necessity of using strongly alkaline media for the process and the formation of aceto derivatives as by-products.

It is evident from these studies that the retro-aldol reaction plays a key role in the formation of vanillin and vanillic acid. The amount of oxygen charged during this reaction phase may increase the yield of these compounds. This approach has not been examined in optimizing the yield of vanillin and vanillic acid in literature [3, 12, 30]. For the first time, such an attempt to understand this effect has been made and results are discussed in the following sections. The experiments in **Sections 4.3.1, 4.3.2** and **4.3.3** were carried out based on conventional oxidation strategy whereas the **Sections 4.3.4** and **4.3.5** were focused on understanding the effect of controlling the amount of oxygen charged during the reaction.

4.3.1. Effect of temperature on vanillin and vanillic acid yield

In the oxidation of lignin using oxygen, the reaction begins with dehydration (**Figure 4.2**, Step 1) of the C_α-C_β bond followed by electron abstraction from the phenoxyl anion. The oxidation is then

initiated by single electron transfer from activated phenoxyl anion species with the formation of a superoxide anion radical and a phenoxyl radical. The formation of phenoxyl radical in this step happens at elevated temperatures. Also, the dissociation constants of phenolic compounds of the type present in the lignin depend on the temperature of the system. The dissociation constant decreases as the temperature increases due to an increase in the formation of a quinone methide intermediate [38]. The effect of temperature on the yield of vanillin and vanillic acid from oxidation of *SKL* is shown in **Figure 4.4**. Oxidation of *SKL* was carried out by keeping the oxygen pressure at 50 psi, lignin concentration at 60 g/L of solution, pH of 14 and a reaction time of 40 minutes based on the optimized conditions found in literature in which oxygen was introduced throughout the reaction time [3]. The combined yield of vanillin and vanillic acid shows an increasing trend from 120°C to 140°C. The yield increase can be attributed to an equilibrium of depolymerization favoring vanillin under thermodynamic control. The side reaction of phenoxyl radical dimerization is also suppressed with increasing temperature. The maximum yield corresponding to 140°C was 3.10 g/L (5.17% w/w) comprised of 1.75 g/L (2.92% w/w) vanillin and 1.35 g/L (2.25% w/w) vanillic acid. The results also show that increasing the temperature to 160°C increased the degradation of vanillin and vanillic acid. It can be observed that the relative rate of vanillic acid degradation is higher compared to vanillin. Therefore, vanillic acid is more reactive and susceptible to degradation which is in accordance with recent literature [32].

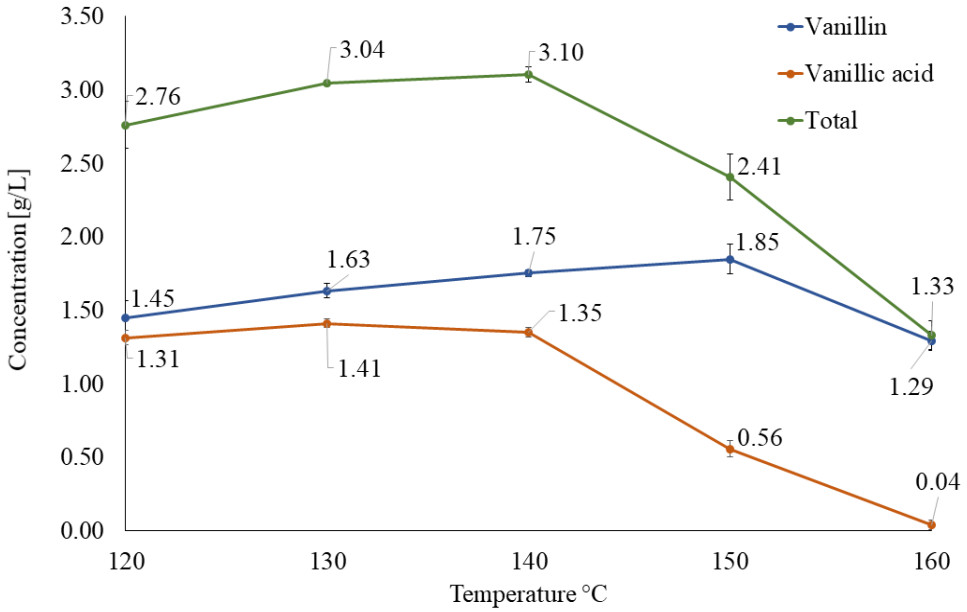

Figure 4.4. Effect of temperature on the yield of vanillin and vanillic acid

4.3.2. Effect of temperature on carboxyl content of lignin

In an effort to provide additional insights on the structural modification of lignin, the oxidized *SKL* sample was isolated and analyzed as a function of temperature. The presence of carboxylic acid groups in lignin is thought to improve lignin solubilization [39-42]. In general, the carboxyl groups can occur in monomeric compounds and in end groups of the lignin macromolecule. The monomeric carboxylic acid derivatives are formed by ring opening reactions of phenolic compounds. Side chain elimination results in the formation of phenolic compounds such as vanillin as described earlier. However, in this study the analysis of carboxyl content was based on the changes in the structure of lignin macromolecule.

The carboxylic acid group formation on the end groups of the lignin macromolecule can arise from electrophilic attack at lignin centers of high electron density causing the formation of a four membered cyclic peroxide intermediate called ‘dioxetane’ [41, 43-45]. This reactive intermediate can further rearrange to induce cleavage of carbon-carbon bonds. The effect of oxidation on

carboxyl content formation in *SKL* is shown in **Figure 4.5**. The carboxyl content of oxygen treated *SKL* increased to 1.41 mmol/g after oxidation at optimum condition. In the temperature range studied, two distinguishing regimes can be observed. The rate of carboxyl content increases up to 130°C. It is likely that temperatures lower than 120°C will result to even lower carboxyl content in lignin. This is because lower temperatures will result only in minor oxidative changes which is also evidenced by lower yields of vanillin and vanillic acid (**Figure 4.4**). The carboxyl content obtained at the peak yield of these compounds was 1.36 mmol/g which is slightly lower compared to the maximum. However, increasing the temperature further to 160°C decreased the carboxyl content to 1.12 mmol/g. It can be observed that in this temperature range, increasing the reaction severity does not increase the carboxyl content correspondingly.

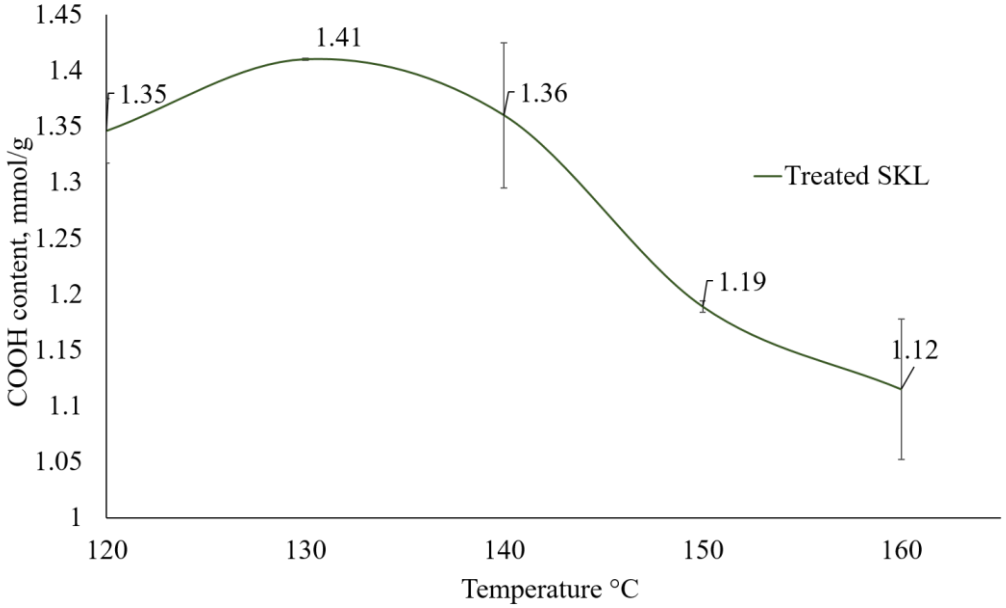

Figure 4.5. Effect of temperature on carboxyl content of SKL

4.3.3. Effect of time

The effect of time on the yield of vanillin and vanillic acid is inter-related to the severity of the other processing parameters. In general, a higher severity of reaction due to higher initial temperatures and oxygen pressures can lead to higher vanillin and vanillic acid yields in a shorter

reaction time; however, the degradation of vanillin and vanillic acid is also higher [3, 6]. The yield profile of these compounds usually follow an increasing trend until the peak yield is obtained at a given time followed by a decreasing trend. Hence, the reaction should be carried out for a certain period of time which optimizes the peak yields. Based on **Figure 4.4 and 4.6**, it is evident that the yield patterns of vanillin and vanillic acid follow increasing and decreasing regimes. The optimum time for which the reaction equilibrium favors the products was obtained at 40 minutes.

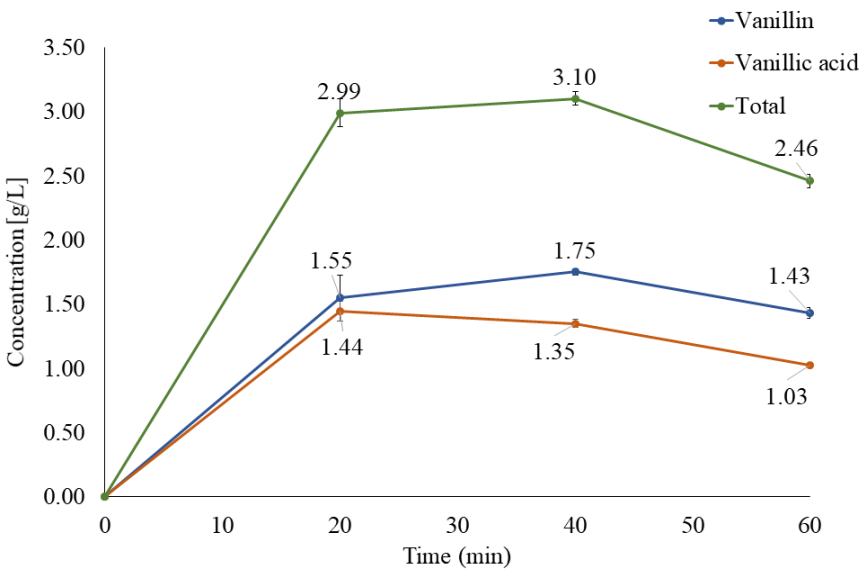

Figure 4.6. Effect of time on the yield of vanillin and vanillic acid

Under the influence of oxygen, the rate of retro-aldol reaction is lower compared to the rate of oxidation of α–unsaturated coniferaldehyde [30]. Therefore, the introduction of oxygen in the reaction media after the peak yield of vanillin and vanillic acid is reached, should negatively affect the yield of these compounds. Based on this understanding, the experiments in **section 4.3.4** were carried out to analyze the effect of controlling the amount of oxygen charged during the reaction on the yield of vanillin and vanillic acid.

4.3.4. Effect of controlling the amount of oxygen charged

In the formation of vanillin and vanillic acid, the rate of the retro-aldol reaction can be improved by controlling the amount of oxygen charged in the reaction. In the conventional oxidation strategy, the oxygen is charged throughout the reaction. In the proposed strategy, the initial t_{max}* represents the amount of oxygen charged to favor oxidation reaction, while during the remaining time $t - t_{max}$* the introduction of oxygen into the reactor is stopped to promote the retro-aldol reaction.

In **Figure 4.7**, the increasing trend corresponds to the reaction phase in which there is a scope to improve yield from oxidation reaction. When oxygen was charged for 5 minutes out of 40 minutes of reaction, the reaction is principally governed by the hydrolysis reaction (**Figure 4.2**, Step 5) and partially proceeds through the oxidation reaction. Therefore, in this phase sufficient time is available for hydrolysis reaction, however due to minor oxidative changes the peak yields are not obtained. Due to this effect, the yields of vanillin and vanillic acid were 1.22 g/L (2.03% w/w) and 1.01 g/L (1.69% w/w) respectively. The peak yields of vanillin and vanillic acid were obtained when oxidation and hydrolysis were each allowed to proceed for 20 minutes out of 40 minutes of reaction. When oxygen was charged for 30 minutes out of 40 minutes, the reaction is mainly governed by the oxidation reaction and the hydrolysis is minimized which explains the decreasing trend. The introduction of oxygen into the reactor for 20 out of 40 minutes of total reaction time resulted in 2.25 g/L (3.75% w/w) vanillin, 1.92 g/L (3.20% w/w) vanillic acid and combined yield of 4.17 g/L (6.95 % w/w). Therefore, the contribution from oxidation and hydrolysis on peak yield is likely to be balanced with this duration of oxygen charge. Hence, the proposed strategy is a viable alternative to the conventional strategy for valorization of lignin. The statistical significance of the yields obtained from this strategy was compared to the conventional strategy (in **section**

4.3.3) using the Tukey test. The *p*-value of 0.008 (p <0.05) was obtained representing significant yield improvement compared to the conventional strategy.

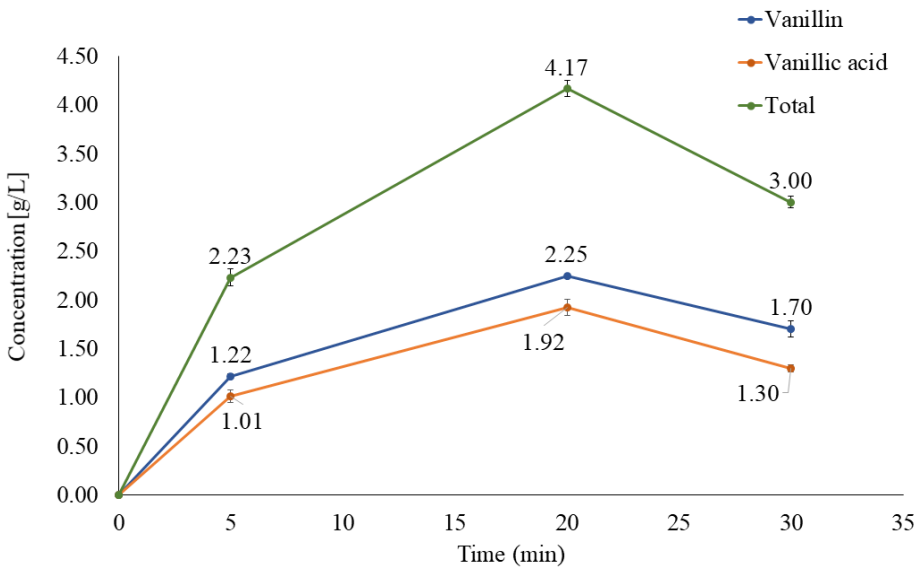

Figure 4.7. Effect of controlling the amount of oxygen charged during the reaction on the yield of vanillin and vanillic acid

It has been hypothesized that vanillic acid is the product of vanillin oxidation [34], however, from **Figure 4.4, 4.6 and 4.7** one can observe that the reduction in vanillin yield after reaching the maximum does not increase the vanillic acid yield correspondingly, which is consistent with the literature [3, 6, 14]. Hence, the formation of vanillic acid in lignin oxidation may be a result of a different pathway not solely linked to vanillin.

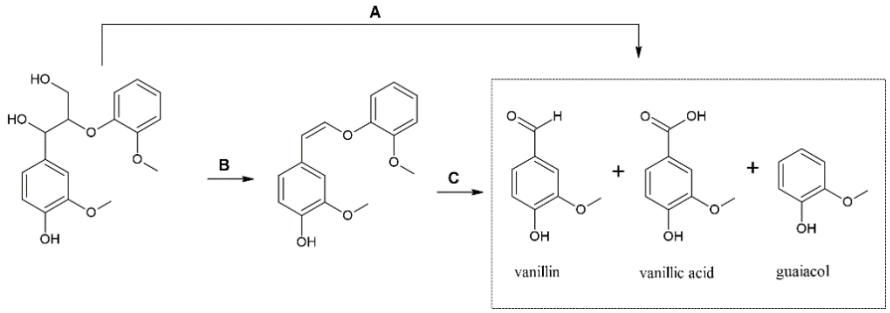

Figure 4.8. Proposed pathway of formation of vanillin, vanillic acid and guaiacol [46] (reproduced from an open access article published by Royal Society of Chemistry)

From the chemistry of the retro-aldol reaction, it is clear that the *γ*-carbon plays an important role in vanillin formation. In a recent study, it has been found that in the absence of a *γ*-carbon, the oxidation of lignin model compounds through **Pathway C** favors vanillic acid formation as shown in **Figure 4.8**. In the presence of a *γ*-carbon, **Pathway A** favored vanillin formation which is in accordance with retro-aldol chemistry. This might explain why the vanillic acid formation is not necessarily linked to vanillin [46].

4.3.5. Effect of controlling the amount of oxygen charged during the reaction on different lignin feedstocks

The structure of lignin is influenced by the wood species, the wood pulping process and the method used for its recovery from pulping liquors [3, 25, 39, 47-52]. In this part of the study, the effect of controlling the amount of oxygen charged during the reaction was analyzed based on different lignin feedstocks. The yields of vanillin and vanillic acid for *SKL* were already optimized based on the parameters discussed in earlier sections. These conditions were then used to analyze other lignin feedstocks. However, it should be noted that the optimized conditions based on different parameters for *SKL* cannot be directly used to represent peak yields from other lignin feedstocks. However, the optimization based on the proposed strategy should be universal to other lignin feedstocks and therefore, this section mainly investigates improvements in yields due to this approach. To compare different feedstocks for analysis, it is also critical to understand the amount of other impurities such as ash, carbohydrate, free sugars and water insolubles.

*carbohydrate content is negligible, **Free sugars and insolubles in water in *H-lignin* account for 18.3% w/w

Lignin	Actual lignin content (% w/w)	Ash (% w/w)	Carbohydrate (% w/w)	Literature source
a. SKL	96.92	0.78	2.30	[3]
b. LInAT	78.20	16.20	5.60	
c. LMarAG	75.04	24.96	*	[33]
d. H-lignin	58.80	**	22.90	

Table 4.2. Ash and carbohydrate content of different lignin feedstocks

SKL and *LInAT* both contain ash and carbohydrates. However, due to the isolation procedure, *SKL* contains lower levels of these impurities compared to *LInAT*. The ash content of *LMarAG* is higher compared to *SKL* and *LInAT*. Usually, the purity of lignosulfonates is lower compared to techincal kraft lignins [53]. *H-lignin* contained the lowest percentage by weight of lignin due to the presence of free sugars, carbohydrates and water insolubles. **Table 4.2** highlights the properties of the technical lignins used in this study.

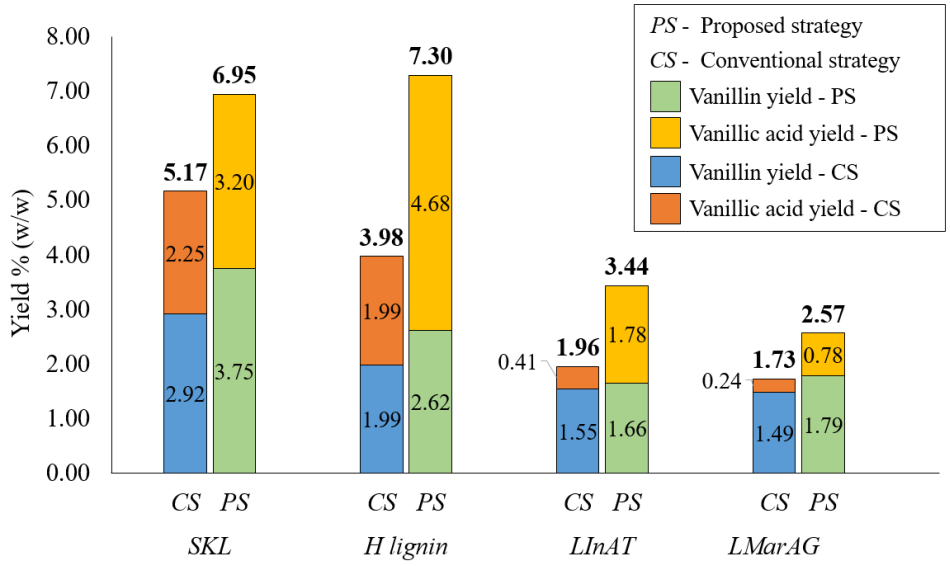

Figure 4.9. Effect of controlling the amount of oxygen charged during the reaction on the yield of vanillin and vanillic acid from different lignin feedstocks

In the kraft process, significant cleavage of β-O-4 and α-O-4 linkages in native lignin takes place. As a result, the kraft lignin that is isolated from this process contains a significant amount of phenolic OH groups. The structural characteristics of lignins obtained from the same kraft process can be different depending upon the chemical charge and extent of cooking. For example, *SKL* and *LInAT* both obtained from the kraft process have significantly different properties. *LInAT* is usually isolated from kraft black liquor from the production of linerboard grade pulp whereas *SKL* is obtained from black liquor from bleachable grade pulp production. Compared to *LInAT*, *SKL* is produced with higher chemical charges and double the cooking time. Therefore, *SKL* contains more phenolic OH groups than *LInAT* [18]. Another major advantage of *SKL* compared to other lignin feedstocks is the lower content of ash, carbohydrates and other impurities which are beneficial for further chemical processing.

From **Figure 4.9**, it can be observed that the yield of vanillin from *SKL* before optimization is higher compared to other lignin feedstocks. However, it should be noted that this yield was previously optimized based on time and temperature. Based on the proposed strategy, considerable improvement in this yield was obtained due to the role played by hydrolysis (**Figure 4.2**, Step 5) in enhancing this yield when oxygen introduction was optimized. The yield improvements observed for *H-lignin*, *LInAT* and *LMarAG* post optimization based on the proposed strategy were also statistically significant as evident by the Tukey test results shown in **Table 4.3**. In comparison, higher increments in yield for all lignin feedstocks were obtained for vanillic acid post optimization as observed in **Figure 4.9**. As discussed earlier, vanillic acid is the compound more susceptible to degradation due to its higher reactivity. Hence, it is likely that the proposed strategy is able to avoid further degradation and promotion of the yield in the absence of oxygen during the hydrolysis phase. The combined yield of vanillin and vanillic acid from *SKL* and *LInAT* was higher

than *LMarAG* likely due to the lower phenolic OH of lignosulfonates compared to kraft lignins [54]. It can also be observed that in the absence of catalysts the yield of vanillin and vanillic acid from lignosulfonates is lower compared to kraft lignin [3, 14].

H-lignin, which is similar to native lignin resulted in a 3.98% yield before optimization which increased 7.30% post optimization with the major contributions coming from an increase in yield from vanillic acid. Similarly, a significant improvement in the yield of vanillic acid was obtained post optimization for *LInAT, LMarAG* and *SKL* with the highest significant improvement obtained from *LInAT*. The *H-lignin* used in this study, contains 93.19% klason lignin content which has not shown to result in significantly higher vanillin yields, in accordance with literature [12, 55]. However, it is evident that the yield of vanillin and vanillic acid can be improved significantly by using the proposed strategy as shown in **Table 4.3**. The statistical significance of the proposed strategy compared to conventional strategy showed *p*-values less than 0.05 for all vanillin and vanillic acid yields obtained from different lignin feedstocks. **Table 4.3** compares the yields of vanillin and vanillic acid obtained before and post-optimization using Tukey's honest significance test.

Compound	Lignin feedstock	Reaction time 40 min (unoptimized)	Standard deviation P (40 min trial)	Reaction time 20 min (optimized)	Standard deviation P (20 min trial)	***p*-value**
Vanillin	*SKL*	2.92	0.04	3.75	0.01	0.002
	H-lignin	1.99	0.05	2.62	0.02	0.007
	LInAT	1.55	0.02	1.66	0.01	0.039

	LMarAG	1.49	0.02	1.79	0.02	0.009
Vanillic	*SKL*	2.25	0.05	3.20	0.14	0.024
acid	H-lignin	1.99	0.07	4.68	0.01	0.001
	LInAT	0.41	0.01	1.78	0.03	0.001
	LMarAG	0.24	0.02	0.78	0.002	0.001
Combined	*SKL*	5.17	0.09	6.95	0.14	0.008
yield	H-lignin	3.98	0.03	7.30	0.01	0.000
	LInAT	1.96	0.03	3.44	0.04	0.001
	LMarAG	1.73	0.04	2.57	0.02	0.003

Table 4.3. Statistical significance of yield improvements using Tukey honest significance test

4.4. Conclusion

The study of the effect of controlling the amount of oxygen charged during the reaction on the yield of vanillin and vanillic acid was the main objective of this work. Based on the results obtained, it was demonstrated for the first time that the efficiency of the retro-aldol reaction can be improved by controlling the amount of oxygen charged, as shown from the yields of vanillin and vanillic acid. This also reduces further degradation of these compounds. The yield improvement using the proposed strategy was validated for different lignin feedstocks, implying a certain level of similarity in the lignin reaction pathways favoring vanillin and vanillic acid. However, in this case, the changes in reaction chemistry due to the presence of reactive sites cannot be eliminated. The results also indicate the degradation of vanillin does not increase the yield of vanillic acid proportionately, supporting the recent reports showing that during oxidation, vanillic acid can be formed from different pathways not solely linked to vanillin. In this regard, the formation of vanillin is linked to the presence of the γ carbon, however in its absence, the preferred

product can be vanillic acid. The higher relative degradation rate obtained for vanillic acid can be linked to the reactivity of this compound. Oxidation of lignin also induced the formation of carboxylic acids in the form of functional groups attached at the end of side of lignin macromolecule. The improvement in the amount carboxylic acid groups allows for new utilization strategies for residual lignin after reaction. In conclusion, oxidation strategy can be a crucial pathway to valorize lignin into high value products.

4.5. References

[1] W. Boerjan, J. Ralph, and M. Baucher, "Lignin biosynthesis," *Annu. Rev. Plant Biol*., vol. 54, no. 1, pp. 519-546, 2003.

[2] G. Cazacu, M.C. Pascu, L. Profire, A. Kowarski, M. Mihaes, and C. Vasile, "Lignin role in a complex polyolefin blend," *Ind. Crops. Prod*., vol. 20 , no. 2, pp. 261-273, 2004.

[3] P. C. Rodrigues Pinto, E. A. Borges da Silva, and A. E. Rodrigues, "Insights into oxidative conversion of lignin to high-added-value phenolic aldehydes," *Ind. Eng. Chem. Res*., vol. 50, no. 2, pp. 741-748, 2011.

[4] F. S. Chakar, and A. J. Ragauskas, "Review of current and future softwood kraft lignin process chemistry," *Ind. Crops. Prod*., vol. 20, no. 2, pp. 131-141, 2004.

[5] M. Culebras, M. Pishnamazi, G.M. Walker, and M.N. Collins, "Facile tailoring of structures for controlled release of paracetamol from sustainable lignin derived platforms," *Molecules*, vol. 26 , no. 6, pp. 1593, 2021.

[6] P.C.R. Pinto, E.A.B. da Silva, and A.E. Rodrigues, "Lignin as source of fine chemicals: vanillin and syringaldehyde," Biomass Conversion, (Eds.) C. Baskar, S. Baskar, R. S. Dhillon, Springer Berlin Heidelberg, pp. 381-420, 2012.

[7] D. Bajwa, G. Pourhashem, A. Ullah, and S. Bajwa, “A concise review of current lignin production, applications, products and their environmental impact,” *Ind. Crops. Prod*., vol. 139, pp. 111526, 2019.

[8] J. Huang, S. Fu, and L. Gan, “Structure and characteristics of lignin,” Lignin Chemistry and Applications. *Elsevier*, Cambridge, MA, USA, 2019.

[9] G. Chatel, and R. D. Rogers, “Oxidation of lignin using ionic liquids: An innovative strategy to produce renewable chemicals,” *ACS Sustain. Chem. Eng*., vol. 2 no. 3, pp. 322-339, 2014.

[10] A. Das, A. Rahimi, A. Ulbrich, M. Alherech, A. H. Motagamwala, A. Bhalla, L. da Costa Sousa, V. Balan, J. A. Dumesic, and E. L. Hegg, “Lignin conversion to low-molecular-weight aromatics via an aerobic oxidation-hydrolysis sequence: comparison of different lignin sources,” *ACS Sustain. Chem. Eng*., vol. 6, no. 3, pp. 3367-3374, 2018.

[11] O.Y. Abdelaziz, K. Ravi, F. Mittermeier, S. Meier, A. Riisager, G. Lidén, and C.P. Hulteberg, “Oxidative Depolymerization of Kraft Lignin for Microbial Conversion,” *ACS Sustain. Chem. Eng*., vol. 7, no. 13, pp. 11640-11652, 2019.

[12] V. E. Tarabanko, and N. Tarabanko, “Catalytic oxidation of lignins into the aromatic aldehydes: general process trends and development prospects,” *Int. J. Mol. Sci*., vol. 18, no. 11, pp. 2421, 2017.

[13] M. Fache, B. Boutevin, and S. Caillol, “Vanillin production from lignin and its use as a renewable chemical,” *ACS Sustain. Chem. Eng*., vol. 4, no. 1, pp. 35-46, 2016.

[14] A. W. Pacek, P. Ding, M. Garrett, G. Sheldrake, and A. W. Nienow, “Catalytic conversion of sodium lignosulfonate to vanillin: engineering aspects. Part 1. Effects of processing conditions on vanillin yield and selectivity,” *Ind. Eng. Chem. Res*., vol. 52, no. 25, pp. 8361-8372, 2013.

[15] M. Culebras, A. Barrett, M. Pishnamazi, G. M. Walker, and M. N. Collins, “Wood-derived hydrogels as a platform for drug-release systems,” *ACS Sustain. Chem. Eng*., vol. 9, no. 6, pp. 2515-2522, 2021.

[16] T. Q. Hu, “Chemical modification, properties, and usage of lignin,” Kluwer Academic/Plenum Publisher, New York, pp. 291, 2002.

[17] D. Schorr, P. N. Diouf, and T. Stevanovic, “Evaluation of industrial lignins for biocomposites production,” *Ind. Crops. Prod*., vol. 52, pp. 65-73, 2014.

[18] Z. Hu, X. Du, J. Liu, H.-m. Chang, and H. Jameel, “Structural characterization of pine kraft lignin: BioChoice lignin vs Indulin AT,” *J. Wood Chem. Technol*., vol. 36, no. 6, pp. 432-446, 2016.

[19] P. Tomani, “The lignoboost process,” *Cell. Chem. Technol*., vol. 44, no. 1, pp. 53, 2010.

[20] D. P. Bezerra, A. K. N. Soares, and D. P. de Sousa, “Overview of the role of vanillin on redox status and cancer development,” *Oxid. Med. Cell. Longev*., vol. 2016, Article ID: 9734816, 2016.

[21] J. Choo, Y. Rukayadi, and J.K. Hwang, “Inhibition of bacterial quorum sensing by vanilla extract,” *Lett. Appl. Microbiol*., vol. 42, no. 6, pp. 637-641, 2006.

[22] S. Buddoo, “Process for the preparation of vanillin from a mixed m-cresol/p-cresol stream,” MSc Thesis, Nelson Mandela Metropolitan University, Port Elizabeth, 2003. [Online accessed 1 April 2021] Retrieved from http://hdl.handle.net/10948/138.

[23] C. S. Calixto-Campos, T. T. Carvalho, M. S. Hohmann, F. A. Pinho-Ribeiro, V. Fattori, M. F. Manchope, A. C. Zarpelon, M. M. Baracat, S. R. Georgetti, and R. Casagrande, “Vanillic acid inhibits inflammatory pain by inhibiting neutrophil recruitment, oxidative stress, cytokine production, and NFκB activation in mice,” *J. Nat. Prod*., vol. 78 no. 8, pp. 1799-1808.

[24] S. G. Yao, J. K. Mobley, J. Ralph, M. Crocker, S. Parkin, J. P. Selegue, and M. S. Meier, "Mechanochemical treatment facilitates two-step oxidative depolymerization of kraft lignin," *ACS Sustain. Chem. Eng*., vol. 6 no. 5 pp. 5990-5998, 2018.

[25] J. Villar, A. Caperos, and F. García-Ochoa, "Oxidation of hardwood kraft-lignin to phenolic derivatives with oxygen as oxidant," *Wood Sci. Technol*., vol. 35 no. 3 pp. 245-255, 2001.

[26] M. B. Hocking, "Vanillin: synthetic flavoring from spent sulfite liquor," *J. Chem. Educ*., vol. 74, no. 9, pp. 1055, 1997.

[27] E. B. da Silva, M. Zabkova, J. Araújo, C. Cateto, M. Barreiro, M. Belgacem, and A. Rodrigues, "An integrated process to produce vanillin and lignin-based polyurethanes from Kraft lignin," *Chem. Eng. Res. Des*., vol. 87, no. 9, pp. 1276-1292, 2009.

[28] J. D. Araújo, C. A. Grande, and A. E. Rodrigues, "Vanillin production from lignin oxidation in a batch reactor," *Chem. Eng. Res. Des*., vol. 88, no. 8, pp. 1024-1032, 2010.

[29] A. Mathias, and A. Rodrigues, "Production of vanillin by oxidation of pine kraft lignins with oxygen," *Holzforschung*, vol. 49, no. 3, pp. 273-278, 1995.

[30] V. E. Tarabanko, and D. V. Petukhov, "Study of mechanism and improvement of the process of oxidative cleavage of lignins into the aromatic aldehydes," *Chem. Sustain. Dev*., vol. 11, pp. 655-667, 2003.

[31] A. More, T. Elder, and Z. Jiang, "A review of lignin hydrogen peroxide oxidation chemistry with emphasis on aromatic aldehydes and acids," *Holzforschung*, vol. 75, no. 9, pp. 806-823, 2021.

[32] F. M. Casimiro, C. A. Costa, C. L. M. Botelho, M. F. Barreiro, and A. E. Rodrigues, "Kinetics of oxidative degradation of lignin-based phenolic compounds in batch reactor," *Ind. Eng. Chem. Res*., vol. 58, no. 36, pp. 16442-16449, 2019.

[33] M. Jablonský, J. Kočiš, A. Ház, and J. Šima, “Characterization and comparison by UV spectroscopy of precipitated lignins and commercial lignosulfonates,” *Cell. Chem. Technol*., vol. 49, no. 3-4, pp. 267-274, 2015.

[34] J.D.P. Araújo, Production of vanillin from lignin present in the Kraft black liquor of the pulp and paper industry, Ph.D. thesis. University of Porto, Porto, Portugal, 2008. [Online accessed 1 April 2021]. Retrieved from https://repositorioaberto.up.pt/bitstream/10216/11944/2/Texto%20integral.pdf.

[35] J. Balej, “Water vapour partial pressures and water activities in potassium and sodium hydroxide solutions over wide concentration and temperature ranges,” *Int. J. Hydrog. Energy*, vol. 10, no. 4, pp. 233-243, 1985.

[36] Guide to Aminex HPLC columns : http://www.hplc.sk/pdf/Biorad/Guide_to_Aminex_HPLC_columns.pdf, in: BIO-RAD (Ed.). [Online accessed 1 April 2021]

[37] S. Katz, and R. P. Beatson, “The determination of strong and weak acidic groups in sulfite pulps,” *Sven. Papperstidn*., vol. 87, no. 6, pp. 48-53, 1984.

[38] J. Kadla, H.m. Chang, and H. Jameel, “The reactions of lignins with hydrogen peroxide at high temperature. Part I. The oxidation of lignin model compounds,” *Holzforschung*, vol. 51, pp. 428-434, 1997.

[39] G. Gellerstedt, K. Gustafsson, and E.L. Lindfors, “Structural changes in lignin during oxygen bleaching,” *Nord. Pulp. Pap. Res. J*., vol. 1 no. 3, pp. 14-17, 1986.

[40] Y. Sun, and D. Argyropoulos, “Fundamentals of high-pressure oxygen and low-pressure oxygen-peroxide (Eop) delignification of softwood and hardwood kraft pulps: a comparison,” J. Pulp Pap. Sci., vol. 21, no. 6, pp. J185-J190, 1995.

[41] F. Asgari, and D.S. Argyropoulos, “Fundamentals of oxygen delignification. Part II. Functional group formation/elimination in residual kraft lignin,” *Can. J. Chem*., vol. 76, no. 11, pp. 1606-1615, 1998.

[42] W. Denissen, J.M. Winne, and F.E. Du Prez, “Vitrimers: permanent organic networks with glass-like fluidity,” *Chem. Sci*., vol. 7, no. 1, pp. 30-38, 2016.

[43] J. Gierer, and F. Imsgard, “The reactions of lignins with oxygen and hydrogen peroxide in alkaline media,” *Sven. Papperstidn*., vol. 80, no. 16, pp. 510-518, 1977.

[44] H. Chang, and J. Gratzl, “Ring cleavage reactions of lignin models with oxygen and alkali,” Chemistry of Delignification with Oxygen, Ozone and Peroxide, pp. 151-163, 1980.

[45] M.R. Fernandes, X. Huang, H.C. Abbenhuis, and E.J. Hensen, “Lignin oxidation with an organic peroxide and subsequent aromatic ring opening,” *Int. J. Biol. Macromol*., vol. 123, pp. 1044-1051, 2019.

[46] T. Hosoya, K. Yamamoto, H. Miyafuji, and T. Yamada, “Selective production of bio-based aromatics by aerobic oxidation of native soft wood lignin in tetrabutylammonium hydroxide,” *RSC Adv*., vol. 10, no. 33, pp. 19199-19210, 2020.

[47] E. Sjostrom, Wood Chemistry, Fundamentals and Applications, New York, Academic Press, 1981.

[48] P.C. Pinto, D.V. Evtuguin, and C.P. Neto, “Effect of structural features of wood biopolymers on hardwood pulping and bleaching performance,” *Ind. Eng. Chem. Res*., vol. 44, no. 26, pp. 9777-9784, 2005.

[49] G. Vázquez, G. Antorrena, J. González, and S. Freire, “The influence of pulping conditions on the structure of acetosolv eucalyptus lignins,” *J. Wood Chem. Technol*., vol. 17, no. 1-2, pp. 147-162, 1997.

[50] D. R. Robert, M. Bardet, G. Gellerstedt, and E.L. Lindfors, “Structural changes in lignin during kraft cooking part 3. On the structure of dissolved lignins,” *J. Wood Chem. Technol*., vol. 4, no. 3, pp. 239-263, 1984.

[51] A. Marques, D. Evtuguin, S. Magina, F. Amado, and A. Prates, “Structure of lignosulphonates from acidic magnesium-based sulphite pulping of Eucalyptus globulus,” *J. Wood Chem. Technol*., vol. 29, no. 4, pp. 337-357, 2009.

[52] J.-Y. Kim, H. Hwang, S. Oh, Y.-S. Kim, U.-J. Kim, and J.W. Choi, “Investigation of structural modification and thermal characteristics of lignin after heat treatment,” *Int. J. Biol. Macromol*., vol. 66, pp. 57-65, 2014.

[53] J. E. Holladay, J.F. White, J.J. Bozell, and D. Johnson, “Top value-added chemicals from biomass-Volume II—Results of screening for potential candidates from biorefinery lignin,” Pacific Northwest National Lab. (PNNL), Richland, WA (United States), 2007.

[54] S. E. Lebo Jr, J.D. Gargulak, and T.J. McNally, “Lignin,” Kirk-Othmer Encyclopedia of Chemical Technology, 2000.

[55] K. Kurshner, “The difficulties in the production of vanillin from sulphite liquors,” Rus. J. Appl. Chem., vol. 28, pp. 957-968, 1955.

Chapter 5 | Effect of oxygen and ozone oxidation on functional group content in softwood kraft lignin

Lignin is one of the most abundant natural polymers, however, it shows incompatibility with other components due to its branched aromatic structure, high molecular weight, and brittle nature. For this reason, understanding the structural changes in lignin during oxidation is crucial for its applications. The softwood kraft lignins after oxygen and ozone oxidations in the LignoForce operating conditions were thoroughly characterized using a variety of conductometric titration and ^{31}P NMR techniques. The progressive reduction in aliphatic and condensed OH units accompanied by the marked increase in carboxylic OH units are the major structural changes occurring in the softwood kraft lignin. Among the oxidizing agents, the amount of carboxylic OH units formed from ozone oxidation was higher compared to the oxygen oxidation under similar conditions. These results indicate the significance of utilizing an ozonation stage at lower temperatures to induce carboxylic OH units in softwood kraft lignin. Further, the utilization of sequential oxidation strategy resulted in kraft lignin with a marked improvement in carboxyl content.

5.1. Introduction

In 1865, F. Schulze coined the term “lignum”, derived from the Latin word for wood, to describe lignin which is the second most abundant biopolymer on earth. Traditionally, it is regarded as a polymer of substituted phenylpropane units [1-3]. It is a complex polymer arising from an enzyme initiated dehydrogenative polymerization of three main precursors: *p*-coumaryl, coniferyl and sinapyl alcohols [4]. Lignin present in raw plant biomass are termed as ‘native lignins’ whereas the byproduct lignin that is obtained from conventional pulping routes – kraft and sulfite are called as ‘technical lignins’ [5-7].

With respect to technical lignins, kraft lignin accounts for 85% of all the lignin produced in the world, which corresponds to approximately 45 million metric tons/year produced worldwide [8]. The highly modified structure of kraft lignin as shown in **Chapter 4**, **Figure 4.1**, is a result of sulfidolytic cleavage of phenolic propane units and alkaline cleavage of non-phenolic propane units by which β-aryl ether bonds are broken in the pulping process. The key reaction intermediate formed during kraft pulping is the quinone methide **3 (Figure 5.1)**. The depolymerization products that are formed in this process are a result of nucleophilic attack by the nucleophiles present in the reaction medium; namely hydrosulfide and hydroxide anions, phenolic OH groups from lignin terminal units and released phenolic fragments, OH groups from carbohydrates and lignin side chains [6, 9-11]. The phenolic OH products **(7-10)** constitute the non-condensed units whereas the products **(11-12)** represent the non-phenolic OH units that are likely to have condensed units.

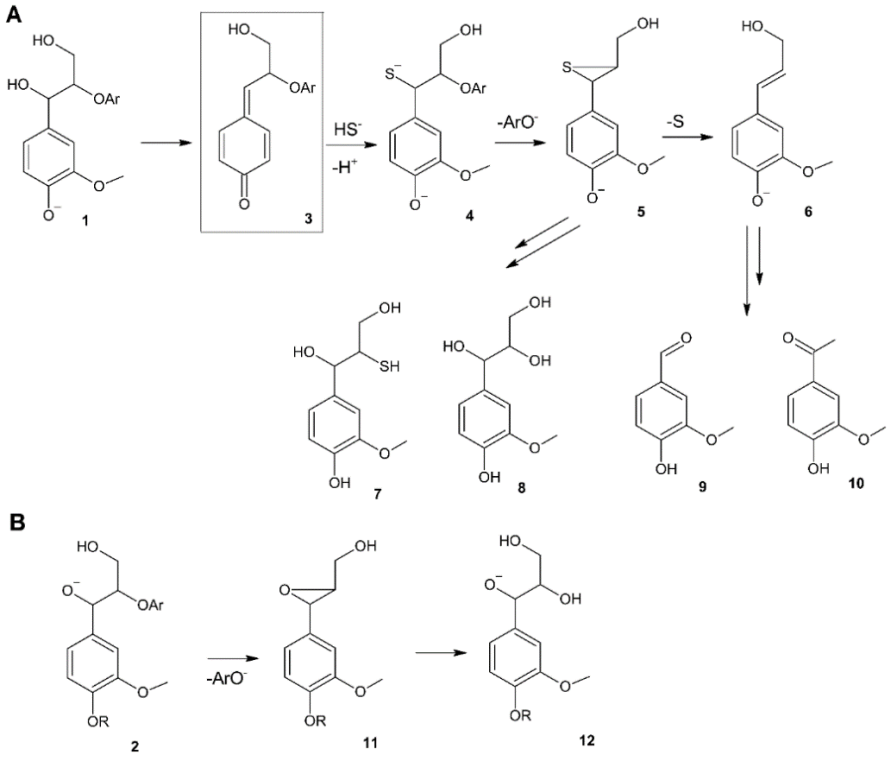

Figure 5.1. (A) Main depolymerization pathways during kraft pulping. Nucleophilic attack of hydrosulfide on quinone methide intermediates **(3)** during kraft pulping leading to fragments

containing thiol groups **(7)** arylglycerols **(8)** vanillin **(9)** and acetovanillone **(10)**; **(B)** protonation followed by an internal nucleophilic substitution of non-phenolic lignin subunits [6]. (Reproduced with permission from Royal Society of Chemistry)

Modern NMR techniques represent the most powerful approach to elucidate structural details of complex lignin subunits [12-17]. The first effort to develop ^{31}P NMR spectroscopy for elucidation of lignin structure was documented by Argyropoulous' group in 1991 [18]. In this aspect, valorization efforts based on kraft lignin have been significantly benefited by the structural characterization using ^{31}P NMR [19-21]. The quantitative analysis allows the identification and quantifications of various phenolic OH, aliphatic OH and carboxylic OH units in softwood kraft lignin in detail. The ^{31}P NMR technique has therefore been applied to measure the overall distribution of various hydroxyl groups present in lignin samples.

The oxidation of softwood kraft lignin using oxygen has attracted increasing interest in recent years [22-25]. The use of oxygen in the pulp and paper industry is preferred due to its low price, high atom economy and environmental friendliness. The phenolic OH units and ring-conjugated structures of lignin are reactive with oxygen [26-29]. In contrast, the progressive formation of carboxylic OH units has been reported in the literature in the temperature range of 80-110°C [30, 31]. However, oxygen is a weak oxidizing agent which limits the overall reactivity towards lignin. Ozone is a relatively strong oxidizing agent which has high reactivity towards both phenolic and non-phenolic nuclei [32]. Ozone has the highest oxidation potential of 2.07 V compared to other bleaching chemicals - hydrogen peroxide (1.77 V), chlorine dioxide (1.57 V), chlorine (1.36 V), oxygen (1.23 V) and hypochlorite (0.94 V) that are used in the pulp and paper industry [33]. In addition to oxygen, ozone has also been widely used in the pulp and paper industries for bleaching [34]. Recent studies have shown that ozone targets lignin subunits through

side chain oxidation and aromatic ring-opening reactions [35-37]. It preferentially attacks the olefin groups present in lignin and then the aromatic ring. In the absence or non-accessibility of these structures, ozone reacts further with carbon-hydrogen bonds of lignin side chains. Under similar operating conditions, higher amounts of carboxylic OH unit formation in ozone oxidation have been reported compared to oxygen oxidation [38].

The need to develop sustainable and integrable technologies is briefly discussed in **Chapter 4, Section 4.1**. In this aspect, the addition of an oxygen stage in the lignin recovery cycle has received recent interest in the LignoForce process [39, 40]. Moreover, the operating temperature of this process is in the range of 80-90°C [41]. In this novel process, an oxygen oxidation step is incorporated into the lignin recovery process for improving the overall efficiency of the recovery process and reducing the emission of volatile sulfur and organic compounds. Therefore, to develop an integrated process for valorization of softwood kraft lignin, it is crucial to understand the structural changes before and after oxidation in the Lignoforce process. In this regard, the present work is focused on elucidating the functional group content in softwood kraft lignin after oxygen and ozone oxidation in the current integrated pulp and paper industrial processes. Further, the optimized conditions for inducing functional groups using oxygen and ozone were then used to sequentially oxidize the softwood kraft lignin.

5.2. Materials and Methods

5.2.1. Oxygen oxidation of SKL. The oxygen oxidation of softwood kraft lignin (SKL) was performed as described in **Section 4.2.3**. In this chapter, in addition, the oxygen oxidation reaction was performed to understand the structural changes in softwood kraft lignin before and after the oxidation treatment. In the present work, the effect of temperature on the oxidation reaction was evaluated at 80°C, 88°C, and 96°C and at a constant reaction time of 40 minutes to understand the

structural changes during the oxidation in the LignoForce process [41]. The precipitated lignin obtained after the reaction was termed as SKL80, SKL88 and SKL96 respectively.

5.2.2. Ozonation of SKL and sequential oxidation of OKL. Ozone is a highly reactive oxidizing agent capable of oxidizing most types of lignin structures. Therefore, oxidation of softwood kraft lignin with ozone will result in a significant increase in the carboxyl content. The ozonation treatment was carried out at ambient pressure in a glass bubbler with a capacity of 1 L. The details of the ozonation procedure are mentioned in the literature [38]. The glass bubbler was heated to 80°C in a water bath with constant stirring. A flow of ozone was supplied by a '5G Lab Benchtop Ozone Generator' from A2Z Ozone providing an ozone dosage of 5000 mg hr^{-1} (100% capacity, oxygen flow rate 2 LPM). The ozone was directly injected into the solution through a long capillary. The off-gas was vented through a wash bottle partially filled with 10% by wt. potassium iodide solution. The ozonation was carried out at different time intervals of 1 hr, 2hr, 3 hr, and 4 hr to optimize the carboxyl content in the softwood kraft lignin. The oxidized kraft liquor (OKL) obtained at optimum conditions from oxygen oxidation **Chapter 4**, **Section 4.2.3** was then further treated with ozone at 80°C for 2 hour treatment to analyze the formation of carboxylic OH units due to their progressive formation during oxidation in different conditions.

5.2.3. ^{31}P NMR characterization: Samples were characterized using N-hydroxy-5-norbornene-2, 3-dicarboxylic acid imide (NHND) as internal standard according to the literature [42]. Before performing the hydroxyl groups determination, samples were dried in a vacuum chamber set at 40°C overnight. Briefly, 30 mg of the accurately weighted sample were mixed with 500 µL of a pyridine/deuterochloroform mixture (1.6/1 v/v), 100 µL of internal standard solution (NHND in pyridine/deuterochloroform + chromium acetylacetonate as relaxation agent) and stirred to dissolve the lignin. In the case of sample 1, 5 drops of N, N'-dimethyl formamide have been added

to favor its dissolution. Then, the sample was derivatized by the addition of 100 μL of 1-choro-4, 4', 5, 5'-tetramethyl-1, 3, 2-dioxaphospholane. The spectra of the phosphorous-labeled lignin preparations were recorded using a 500 MHz Bruker Nuclear Magnetic Resonance Spectrometer. The acquisition parameters used are reported in **Table 5.1** and the spectra have been integrated and processed using MestReNova software.

Parameters	Value
Pulse program	Inverse gated decoupling pulse (zgig)
Nucleus	^{31}P
Spectral width	100 ppm
Acquisition time	0.8 s
Relaxation delay	10 s
Number of scans	128
Centre of spectrum	140 ppm

Table 5.1. Acquisition parameters for ^{31}P NMR

5.2.4. Carboxyl content determination using conductometric titration: The carboxyl content of the ozonated and sequentially oxidized lignin was determined using the conductometric titration method described in **Section 4.2.5**.

5.3. Results and discussion

5.3.1. ^{31}P NMR characterization: The resulting spectra are reported in **Figure 5.2** and the amounts of the various derivatized functional groups are reported in **Table 5.2** and **Figure 5.3**. Among the known reactions that occur in lignin during oxidation is the formation of a significant amount of carboxylic OH units that facilitate subsequent dissolution. This is evidenced by the gradual increase of the carboxylic OH content of the untreated SKL from 0.17 mmol/g to 0.82

mmol/g for sample 3 treated at 88°C. The formation of carboxylic acid groups is accompanied by the elimination of aliphatic hydroxyl groups. The aliphatic OH units in untreated SKL reduced from 1.24 mmol/g to 0.24 mmol/g for sample 2 treated at 80°C. Similar results after oxygen oxidation treatment were also reported in the literature [43, 44].

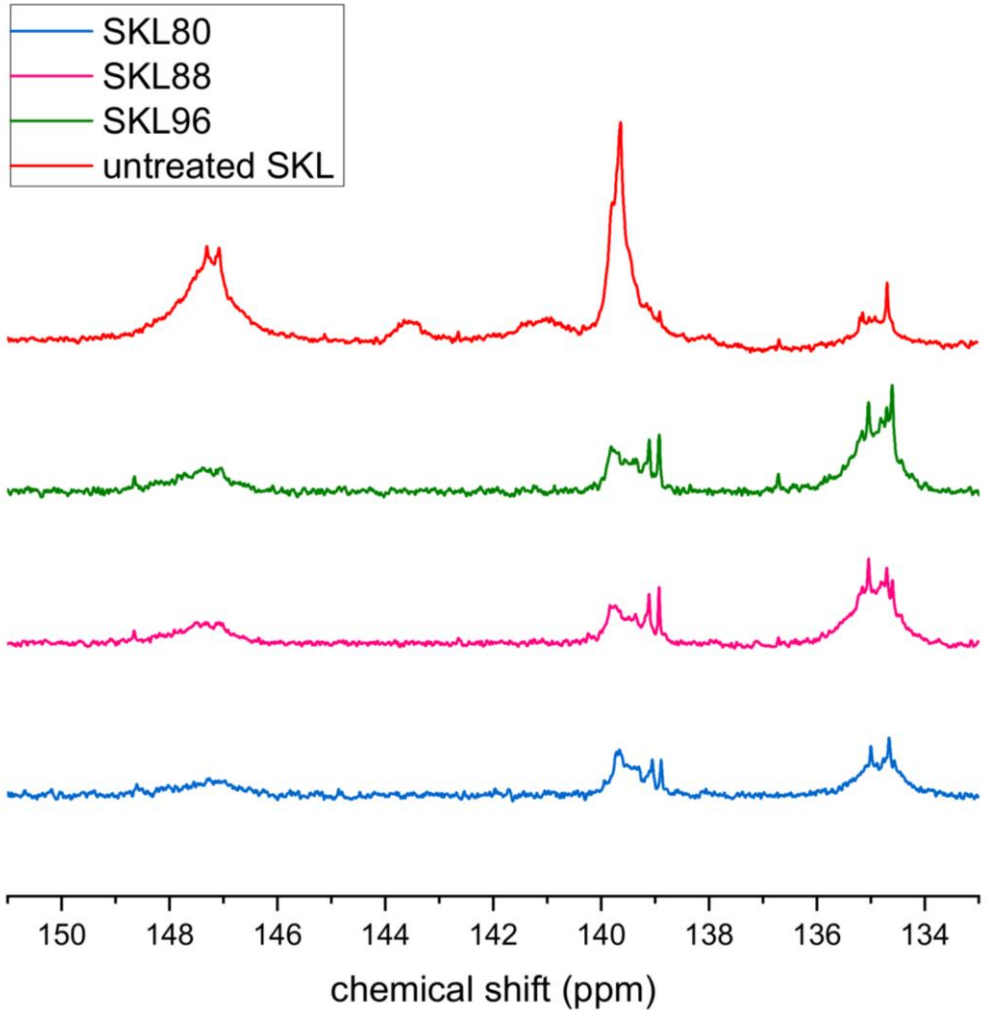

Figure 5.2. ^{31}P NMR spectra of derivatized lignin samples

Lignin Sample	Aliphatic OH	Aromatic OH			Carboxylic OH
		Condensed	Non condensed	Total	
Sample 1 (untreated SKL)	1.24	0.36	1.20	1.56	0.17
Sample 2 (SKL80)	0.24	N.D.	0.37	0.37	0.44*
Sample 3 (SKL88)	0.33	N.D.	0.41	0.41	0.82
Sample 4 (SKL96)	0.25	N.D.	0.33	0.33	0.68

Table 5.2. Functional groups content in SKL before and after oxygen oxidation (mmol/g)

*In case of Sample 2, 5 drops of N, N'-dimethyl formamide have been added to enhance its dissolution

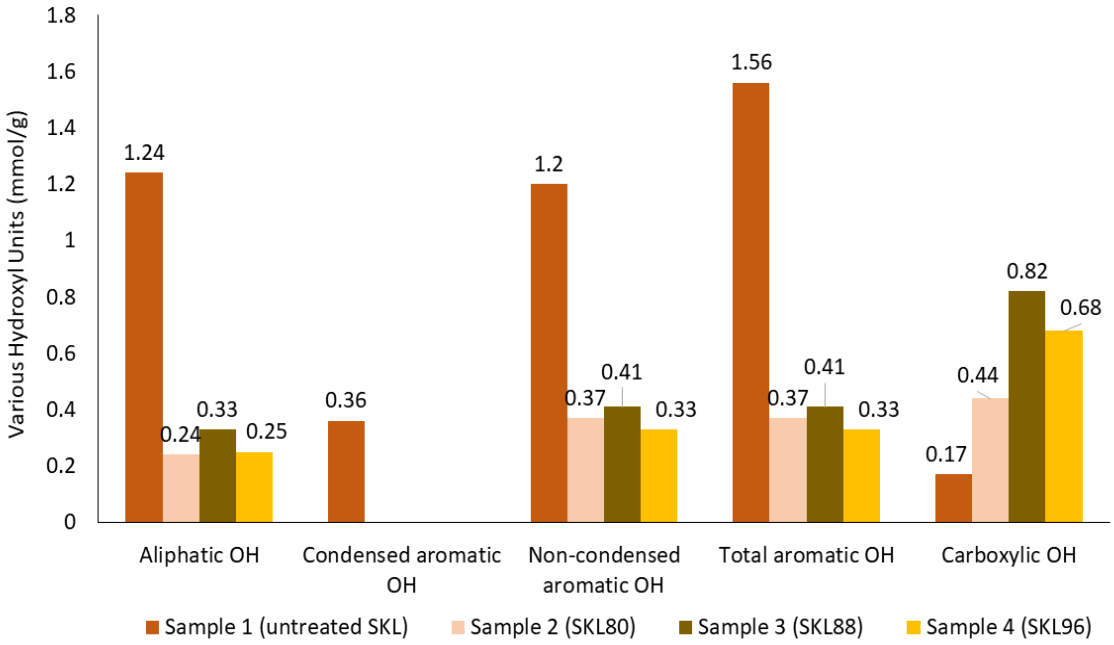

Figure 5.3. The changes in various hydroxyl units present in softwood kraft lignin before and after oxygen oxidation.

Phenolic OH units are known to be reactive sites of attack during oxygen oxidation [45]. This is evidenced by the results shown in **Figure 5.3**, which demonstrates that an oxygen stage decreased the content of all types of phenolic units. It has been hypothesized that different phenolic units have different reactivity towards oxygen and the condensed aromatic OH units are relatively stable compared to the non-condensed units [31]. However, the untreated softwood kraft lignin utilized in this study has much lower condensed aromatic OH units compared to the non-condensed units which in contrast to the lignin feedstock utilized in the literature. The formation of condensed and degradation pathway of non-condensed OH units during oxygen oxidation are highlighted in **Figure 5.4**. A closer inspection of the data reveals that in case of the softwood kraft lignin utilized in this study, the amount of condensed OH units degraded were comparatively higher than the amount of condensed units formed from radical coupling reactions.

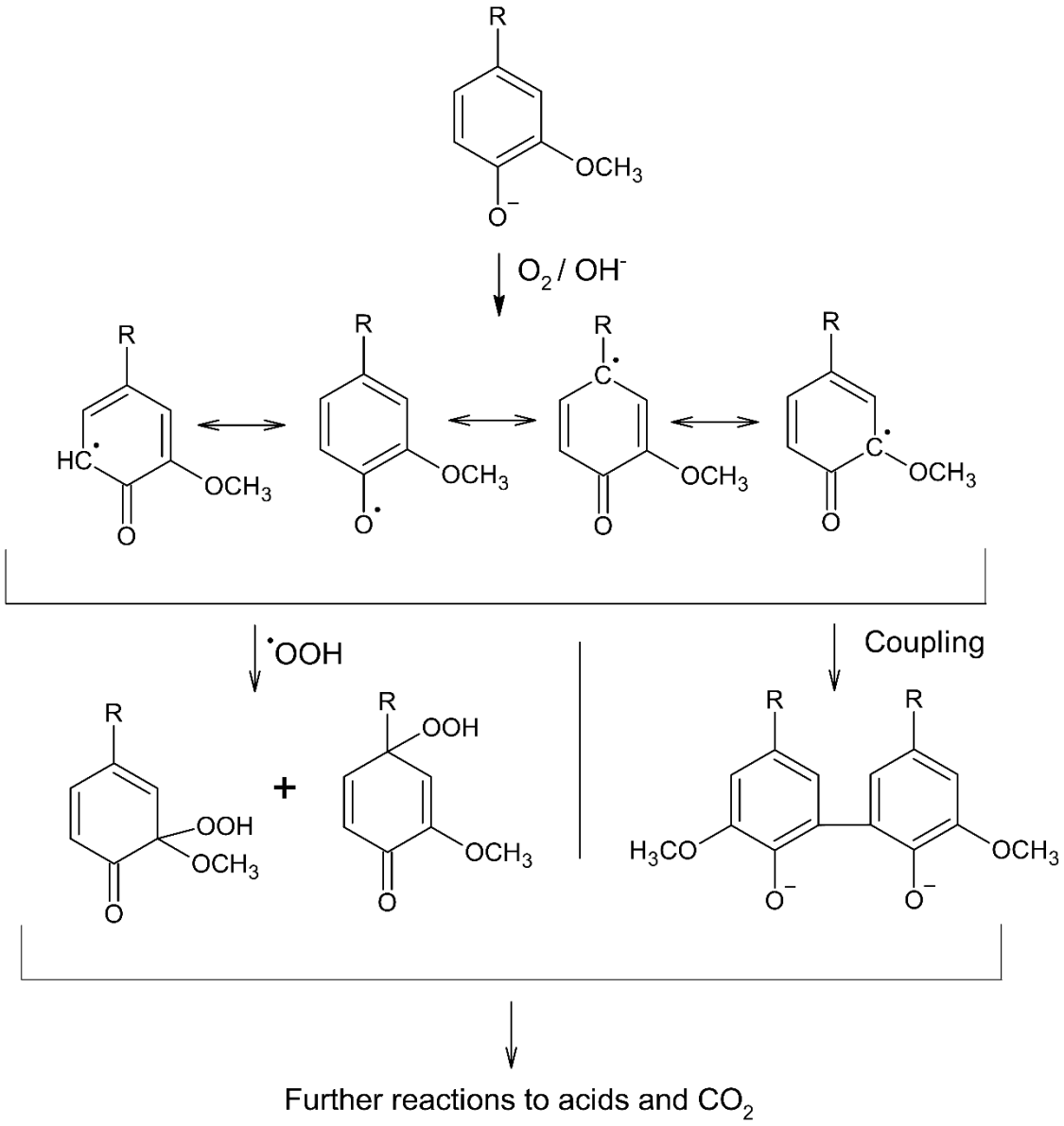

Figure 5.4. A mechanism for the degradation reactions of phenolic units during oxygen delignification of kraft pulps [9], where 'R' represents a lignin interunit.

5.3.2. Carboxyl content in ozonated and sequentially oxidized kraft lignin: Ozone is a highly reactive oxidizing agent capable of reacting all types of lignin structures [32]. The structural changes using oxygen, which is a milder oxidizing agent compared to ozone is evidenced in **Figure 5.3** and **Figure 5.6**. Since, the carboxylic OH units show progressive formation among the various hydroxyl units investigated, the structural changes obtained from ozone are focused on the changes

in carboxylic OH units. Also, complete degradation of the aromatic ring in lignin occurs if ozonation is conducted at high pressures and if ozone is present in excess, therefore, in the present study, the ozone treatment was performed at ambient pressure. **Figure 5.6** graphically represents the changes in the amount of carboxylic OH units versus the time duration of ozonation. As the severity of ozone treatment increases, the amount of carboxylic OH units formed gradually increase reaching a plateau region in the ozonation time duration from 2 hours to 3 hours. Beyond this region, a slight decrease in the carboxyl content is observed with increasing duration of the reaction. It is possible that the consumption of available ozone by radical species limits the lignin degradation in this region.

Lignin Sample	**Treatment duration (hrs)**	**Ozone charged (g/g of lignin)**	**Carboxylic OH (mmol/g)**
Sample A	1	0.21	1.50
Sample B	2	0.42	2.06
Sample C	3	0.62	2.08
Sample D	4	0.83	1.82

Table 5.3. The changes in carboxylic OH groups present in softwood kraft lignin after ozone oxidation.

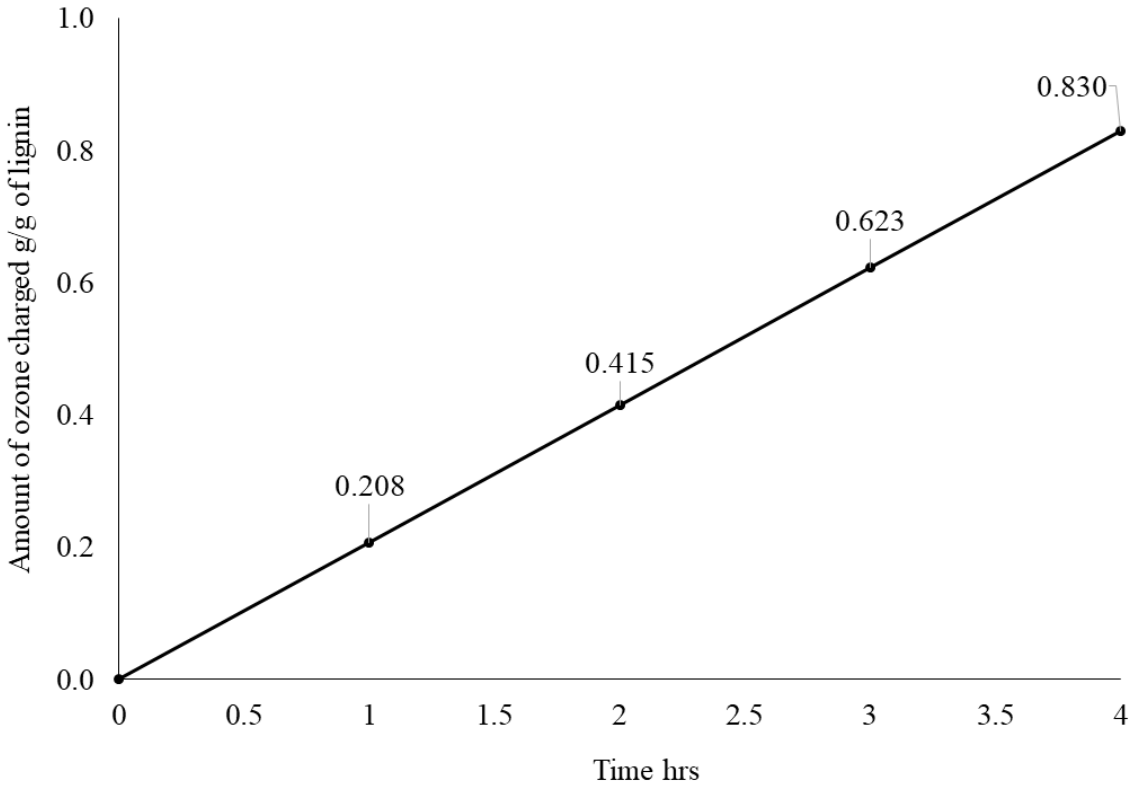

Figure 5.5. The changes in the amount of ozone charged w.r.t to the duration of the reaction

The effect of higher temperatures (120°C to 160°C) on the formation of carboxyl content in softwood kraft lignin after oxygen oxidation is shown in **Chapter 4, Section 4.3.2**. At 130°C, a maximum carboxylic OH unit formation of 1.41 mmol/g was achieved with 5.06% w/w yield of vanillin and vanillic acid. Therefore, for an integrated process, the softwood kraft lignin utilized under these conditions is beneficial as it also allows to form vanillin and vanillic acid which are high value products. The oxidized kraft liquor (OKL) obtained at these conditions from oxygen oxidation was then further treated with ozone at 80°C for 2 hours to analyze the formation of carboxylic OH units due to their progressive formation during oxidation under different conditions. It was observed that the sequentially oxidized softwood kraft lignin (OxL-COOH) had a carboxylic OH unit content of 4.06 mmol/g which is significantly higher than isolated treatment of oxygen and ozone.

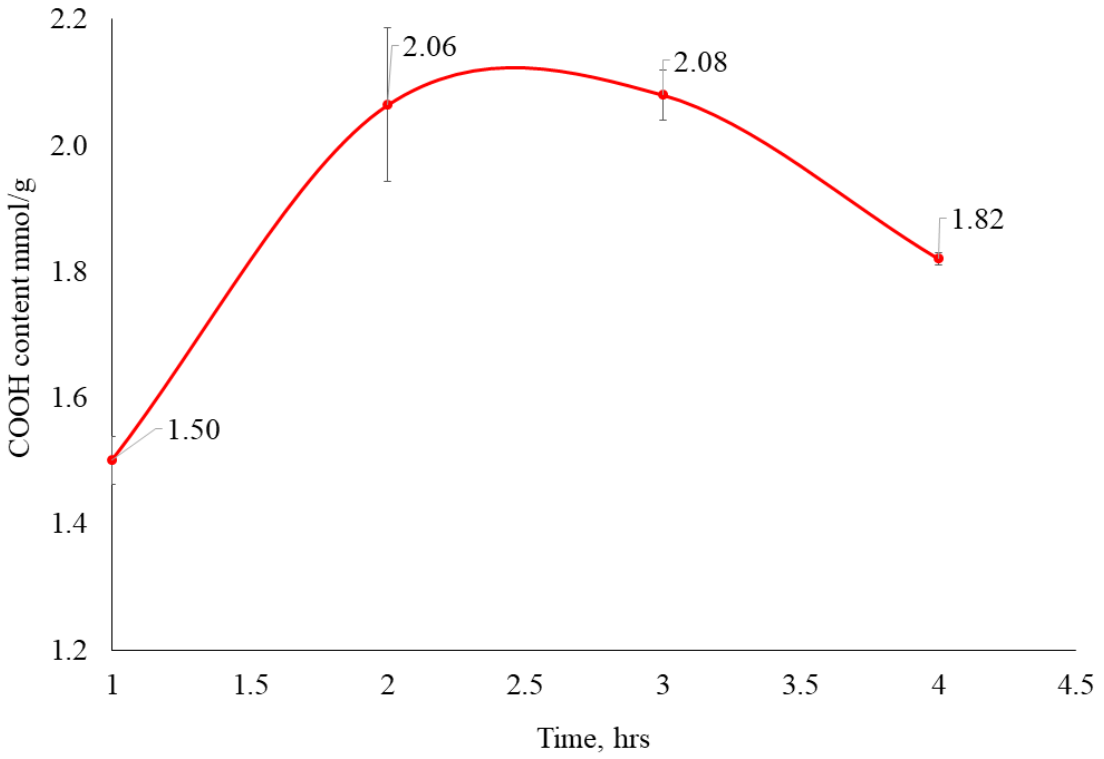

Figure 5.6. The changes in carboxylic OH groups present in SKL after ozone oxidation.

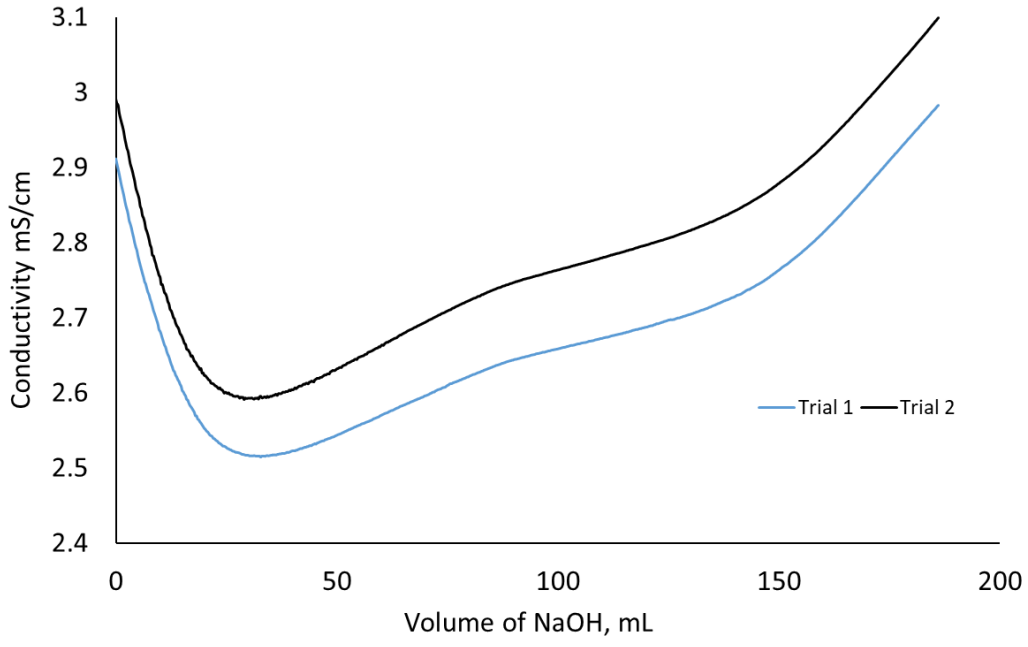

Figure 5.7. Conductometric titration of sequentially oxidized kraft lignin obtained from OKL (oxygen treatment at 130°C for 40 min followed by ozone treatment at 80°C for 2 hours)

5.4. Conclusions: During the course of oxygen oxidation, among the major structural changes in softwood kraft lignin are the progressive formation of carboxylic acids and reduction of aliphatic OH units. In the case of the softwood kraft lignin utilized in this study, the amount of condensed OH units degraded were relatively higher than the amount of condensed units formed from radical coupling reactions. As a result, condensed OH units were not detected after oxygen oxidation treatment in the temperature range of 80-88°C. Overall, the oxygen oxidation treatment led to a decrease of the various phenolic hydroxyl units in the residual lignin. Among the oxidizing agents, the amount of carboxylic OH units formed from ozone oxidation (2.08 mmol/g) was higher compared to the oxygen oxidation (0.82 mmol/g) under similar conditions. These results show the importance of an ozonation stage at lower temperatures to induce carboxylic OH units in softwood kraft lignin. Furthermore, the softwood kraft lignin that is obtained after sequential oxidation treatment from oxygen at 130°C and from ozone at 80°C (OxL-COOH) contained 4.06 mmol/g of carboxylic OH units. The higher amount of carboxylation obtained after sequential oxidation treatment allows for improved compatibility of lignin with other components.

5.5. References

1] I. A. Pearl, “The chemistry of lignin,” Marcel Dekker, New York, 1967.

[2] K. Freudenberg, and A. C. Neish, “Constitution and biosynthesis of lignin,” Springer Verlag, New York, 1968.

[3] K. V. Sarkanen and C. H. Ludwig (eds.), “Lignins”, Wiley-Interscience, New York, 1971.

[4] F.G. Calvo-Flores, J.A. Dobado, J. Isac-García, and F.J. Martín-Martínez, “Lignin and Lignans as Renewable Raw Materials: Chemistry, Technology and Applications,” John Wiley & Sons, 2015.

[5] S. Guadix-Montero, and M. Sankar, “Review on catalytic cleavage of C–C inter-unit linkages in lignin model compounds: towards lignin depolymerization,” *Top. Catal*., vol. 61, pp. 183-198, 2018.

[6] C. Crestini, H. Lange, M. Sette, and D. S. Argyropoulos, “On the structure of softwood kraft lignin,” *Green Chem*., vol. 19, no. 17, pp. 4104-4121, 2017.

[7] A. More, T. Elder, and Z. Jiang, “A review of lignin hydrogen peroxide oxidation chemistry with emphasis on aromatic aldehydes and acids,” *Holzforschung*, vol. 75, no. 9, pp. 806-823, 2021.

[8] H. Lange, S. Decina, and C. Crestini, “Oxidative upgrade of lignin–Recent routes reviewed,” *Eur. Polym. J*., vol. 49, pp. 1151-1173, 2013.

[9] J. Gierer, “Chemical aspects of kraft pulping,” *Wood Sci. Technol*., vol. 14, no. 4, pp. 241-266, 1980.

[10] P. M. Froass, A. J. Ragauskas, and J. E. Jiang, “NMR studies part 3: Analysis of lignins from modern kraft pulping technologies,” *Holzforschung*, vol. 52, no. 4, pp. 385-390, 1998.

[11] G. Gellerstedt, “Softwood kraft lignin: Raw material for the future,” *Ind. Crops. Prod*., vol. 77, pp. 845-854, 2015.

[12] G. Gellerstedt, and D. Robert, “Quantitative 13C NMR analysis of kraft lignins,” *Acta Chem. Scand*., vol. B41, no. 7, pp. 541-546, 1987.

[13] M. Y. Balakshin, and E.A. Capanema, “Comprehensive structural analysis of biorefinery lignins with a quantitative 13 C NMR approach,” *RSC advances*, vol. 5, no. 106, pp. 87187-87199, 2015.

[14] L. Zhang, and G. Gellerstedt, “2D heteronuclear (^{1}H-^{13}C) single quantum correlation (HSQC) NMR analysis of Norway spruce bark components: Characterization of lignocellulosic materials” T. Q. Hu (ed.); Blackwell Publishing Ltd.: Oxford, pp. 3-16, 2008.

[15] H. Kim, and J. Ralph, "Solution-state 2D NMR of ball-milled plant cell wall gels in DMSO-d_6/pyridine-d_5," *Org. Biomol. Chem. Org*., vol. 8, no. 3, pp. 576-591, 2010.

[16] J.C. del Río, P. Prinsen, J. Rencoret, L. Nieto, J.s. Jiménez-Barbero, J. Ralph, A.n.T. Martínez, and A. Gutiérrez, "Structural characterization of the lignin in the cortex and pith of elephant grass (Pennisetum purpureum) stems," *J. Agric. Food Chem*., vol. 60, no. 14, pp. 3619-3634, 2012.

[17] J.C. Del Río, J. Rencoret, P. Prinsen, Á.T. Martínez, J. Ralph, and A. Gutiérrez, "Structural characterization of wheat straw lignin as revealed by analytical pyrolysis, 2D-NMR, and reductive cleavage methods," *J. Agric. Food Chem*., vol. 60, no. 23, pp. 5922-5935, 2012.

[18] Y. Archipov, D. Argyropoulos, H. Bolker, and C. Heitner, "^{31}P NMR spectroscopy in wood chemistry. I. Model compounds," *J. Wood Chem. Technol*., vol. 11, no. 2, pp. 137-157, 1991.

[19] A. Granata, and D.S. Argyropoulos, "2-Chloro-4, 4, 5, 5-tetramethyl-1, 3, 2-dioxaphospholane, a reagent for the accurate determination of the uncondensed and condensed phenolic moieties in lignins," *J. Agric. Food Chem*., vol. 43, no. 6, pp. 1538-1544, 1995.

[20] D. S. Argyropoulos, "Heteronuclear NMR spectroscopy of lignins: Lignin and Lignans: Advances in chemistry," pp. 245-265, 2010.

[21] D. S. Argyropoulos, "^{31}P NMR in wood chemistry: A review of recent progress," *Res. Chem. Intermed*., vol. 21, no. 3, pp. 373-395, 1995.

[22] A. More, T. Elder, and Z. Jiang, "Towards a new understanding of the retro-aldol reaction for oxidative conversion of lignin to aromatic aldehydes and acids," *Int. J. Bio. Macromol*., vol. 183, pp. 1505-1513, 2021.

[23] A.W. Pacek, P. Ding, M. Garrett, G. Sheldrake, and A.W. Nienow, "Catalytic conversion of sodium lignosulfonate to vanillin: engineering aspects. Part 1. Effects of processing conditions on vanillin yield and selectivity," *Ind. Eng. Chem. Res*., vol. 52, pp. 8361-8372, 2013.

[24] P.C. Rodrigues Pinto, E.A. Borges da Silva, and A.E. Rodrigues, “Insights into oxidative conversion of lignin to high-added-value phenolic aldehydes,” *Ind. Eng. Chem. Res*., vol. 50, pp. 741-748, 2011.

[25] P. C. R. Pinto, E.A.B. da Silva, and A.E. Rodrigues, “Lignin as source of fine chemicals: vanillin and syringaldehyde,” Biomass Conversion; C. Baskar, S. Baskar, R.D. Dhillon, Eds; Springer: London, pp. 381-420, 2012.

[26] J. Gierer, “Chemistry of delignification,” *Wood Sci. Technol*., vol. 19, no. 4, pp. 289-312, 1985.

[27] G. Gellerstedt, K. Gustafsson, and E. L. Lindfors, “Structural changes in lignin during oxygen bleaching: Paper dedicated to Prof. Karl Kratzl on the occasion of his 70th birthday,” *Nord. Pulp Pap. Res. J*, vol. 1, no. 3, pp. 14-17, 1986.

[28] G. Gellerstedt, J. Pranda, and E.-L. Lindfors, “Structural and molecular properties of residual birch kraft lignins,” *J. Wood Chem. Technol*., vol. 14, no. 4, pp. 467-482, 1994.

[29] K. Kratzl, P. Claus, W. Lonsky, and J. Gratzl, “Model studies on reactions occurring in oxidations of lignin with molecular oxygen in alkaline media,” *Wood Sci. Technol*., vol. 8, no. 1, pp. 35-49, 1974.

[30] F. Asgari, and D.S. Argyropoulos, “Fundamentals of oxygen delignification. Part II. Functional group formation/elimination in residual kraft lignin,” *Can. J. Chem*., vol. 76, no. 11, pp. 1606-1615, 1998.

[31] Z.-H. Jiang, “Advances and applications of quantitative ^{31}P NMR for the structural elucidation of lignin,” Ph.D. Thesis. McGill University, Canada, 1997. [Online accessed 1 June 2022]. Retrieved from https://escholarship.mcgill.ca/concern/theses/gf06g450n

[32] R. Ma, Y. Xu, and X. Zhang, “Catalytic oxidation of biorefinery lignin to value-added chemicals to support sustainable biofuel production,” *ChemSusChem*, vol. 8, pp. 24-51, 2015.

[33] S. K. Tripathi, N. K. Bhardwaj, and H. Roy Ghatak, “Developments in ozone-based bleaching of pulps,” *Ozone Sci. Eng*., vol. 42, no. 2, pp. 194-210, 2020.

[34] M. Roncero, A. Torres, J. Colom, and T. Vidal, “TCF bleaching of wheat straw pulp using ozone and xylanase. Part A: paper quality assessment,” *Bioresour. Technol*., vol. 87, no. 3, pp. 305-314, 2003.

[35] M. V. Bule, A. H. Gao, B. Hiscox, and S. Chen, “Structural modification of lignin and characterization of pretreated wheat straw by ozonation,” *J. Agric. Food Chem,* vol. 61, no. 16, pp. 3916-3925, 2013.

[36] S.Y. Lin, and C.W. Dence, “Methods in lignin chemistry,” Springer Science & Business Media, 2012.

[37] Y. Kojima, “Oxidative degradation of softwood lignin model compounds with ozone,” *Res. Bull. Coll. Exp. Forests Hokkaido Univ*., vol. 35, no. 1, pp. 165-184, 1978.

[38] O. Musl, M. Holzlechner, S. Winklehner, G. Gübitz, A. Potthast, T. Rosenau, and S. Böhmdorfer, “Changing the Molecular Structure of Kraft Lignins – Ozone Treatment at Alkaline Conditions,” *ACS Sus. Chem. Eng*., vol. 7, no. 18, pp. 15163-15172, 2019.

[39] L. Kouisni, A. Gagné, K. Maki, P. Holt-Hindle, and M. Paleologou, “LignoForce system for the recovery of lignin from black liquor: feedstock options, odor profile, and product characterization,” *ACS Sus. Chem. Eng*., vol. 4, no. 10, pp. 5152-5159, 2016.

[40] L. Kouisni, and M. Paleologou, “Method for separating lignin from black liquor,” United States Patent 8771464, Jul. 2, 2014.

[41] L. Kouisni, P. Holt-Hindle, K. Maki, and M. Paleologou, “The lignoforce system: a new process for the production of high-quality lignin from black liquor,” *J. Sci. Technol. For. Prod. Processes*, vol. 2, no. 4, pp. 6-10, 2012.

[42] X. Meng, C. Crestini, H. Ben, N. Hao, Y. Pu, A.J. Ragauskas, and D.S. Argyropoulos, “Determination of hydroxyl groups in biorefinery resources via quantitative ^{31}P NMR spectroscopy,” *Nat. Protoc.*, vol. 14, no. 9, pp. 2627-2647, 2019.

[43] Z.-H. Jiang, and D. S. Argyropoulos, “The stereoselective degradation of arylglycerol-beta-aryl ethers during kraft pulping,” *J. Pulp Pap. Sci.*, vol. 20, no. 7, pp. J183-J188, 1994.

[44] G. Gellerstedt, and E.-L. Lindfors, “Structural changes in lignin during kraft pulping,” *Holzforschung*, vol. 38, no. 3, pp. 151-158, 1984.

[45] L. Hu, H. Pan, Y. Zhou, and M. Zhang, “Methods to improve lignin’s reactivity as a phenol substitute and as replacement for other phenolic compounds: A brief review,” *BioResources*, vol. 6, no. 3, pp. 3515-3525, 2011.

Chapter 6 | A novel and integrated process for the valorization of kraft lignin to produce lignin-based vitrimers

The valorization of lignin into value-added products by oxidative conversion is one of the most widely studied strategies. However, the majority of these approaches have a limited scope for integration into industrial processes. The objective of our work is to maximize overall lignin utilization to produce diverse value-added products with a focus on integration in the existing industrial pulp and paper processes. In our previous work, we have optimized the yields of vanillin and vanillic acid by oxidation of softwood kraft lignin using oxygen. In this work, the oxidized kraft liquor (OKL) after the oxidation reaction was further treated with ozone to form a significant amount of carboxyl groups. The oxidized lignin (OxL-COOH) was then cured with polyethylene glycol diglycidyl ether (PEG-epoxy) to form high lignin content (>48 wt.%) vitrimers with high thermal stability, fast relaxation, and self-healing due to the presence of bond exchangeable cross-linked networks. The lignin-based vitrimers were not soluble in aqueous alkaline solutions, but exhibited notable swelling properties which is a key indicator of dynamic transesterification in the cured network. Overall, this study provides a novel approach for the multi-dimensional valorization of lignin and demonstrates an integrated approach for kraft lignin valorization in the pulp and paper industry.

6.1. Introduction

Currently, the disposal of thermoset waste in our environment is one of the most challenging problems that needs to be addressed. Due to the lack of suitable methods for recycling or repairing, most of the thermoset waste is disposed of by incineration and landfill [1]. The concept of circular economy which was introduced by the Ellen MacArthur Foundation allows for a sustainable future for generations to come [2]. Two key aspects of this concept involve that the

vast majority of thermoset waste should be re-usable and that the materials used in the chain should be bio-based. Conventional epoxy-based thermosets possess excellent hardness, adhesion, and chemical resistance, however, once damaged, they cannot be repaired by heating due to the presence of a permanently cross-linked network. To address this issue, researchers have considered the modification of thermosetting polymers using vitrimer chemistry [3-6]. This allows for the introduction of dynamic covalent linkages in the cross-linked network which imparts repairability and recyclability to the thermosetting polymers. However, the recently developed vitrimer materials are based on petrochemical feedstocks. Therefore, the utilization of bio-based renewable feedstocks in the vitrimer matrix is crucial to fit into the concept of a circular economy [7-9].

Lignin is one such bio-based renewable feedstock that is abundantly available and accounts for about 30% of non-fossil carbon on earth [10-12]. The lignin obtained from technical processes has different structural properties and characteristics based on how the delignification is accomplished, the recovery process, and wood species [13, 14]. Kraft lignin accounts for about 85% of all lignin produced worldwide which corresponds to approximately 45 million metric tons $year^{-1}$. It is mainly utilized as a source of low-grade fuel in the pulping operation and only about 100,000 tons of it is valorized every year [15, 16]. Oxidative conversion of lignin to produce vanillin (4-hydroxy-3-methoxy benzaldehyde, $C_8H_8O_3$) and vanillic acid (4-hydroxy-3-methoxy benzoic acid, $C_8H_8O_4$) is widely proposed [17-20]. Vanillin is one of the most widely produced aromatic aldehydes worldwide. It has useful applications in the food, cosmetic, chemical and pharmaceutical industries [21, 22]. Recently, vanillic acid has also been gaining interest due to its antibacterial, antimicrobial, and chemo-preventive properties [23]. Oxidative conversion of kraft lignin using oxygen is preferred due to its environmental friendliness, high atom economy, and low price. Current approaches of oxidative conversion of lignin using oxygen apply the oxygen

oxidation treatment as an additional and standalone step to kraft lignin after its isolation from black liquor.

Recently, the addition of an oxygen stage in the lignin recovery cycle from black liquor has been gaining interest [24-26]. **Figure 6.1 (a)** shows the LignoForce process jointly developed by FPInnovations and NORAM [27]. In this novel process, an oxygen oxidation step is incorporated into the lignin recovery process for improving the overall efficiency of the lignin recovery process and reducing the emission of volatile sulfur and organic compounds. Building on the LignoForce process, we proposed a novel and integrated process for the valorization of kraft lignin **Figure 6.1 (b)**. In this proposed process, the oxygen oxidation step was optimized for producing vanillin and vanillic acid. The optimization of oxygen oxidation to form vanillin and vanillic acid was reported in our previous paper [28]. In this work, we report the ozone treatment of oxidized kraft liquor (OKL) after the optimized oxygen oxidation reaction to produce lignin-based vitrimers. The OKL stream after the permeation step is subjected to ozonation to induce a significant amount of carboxyl groups. After the ozone treatment, the modified lignin (OxL-COOH) is then precipitated by acidification. Further, the OxL-COOH which is a rich source of carboxyl groups is cured with polyethylene glycol diglycidyl ether (PEG-epoxy) to form lignin-based vitrimers.

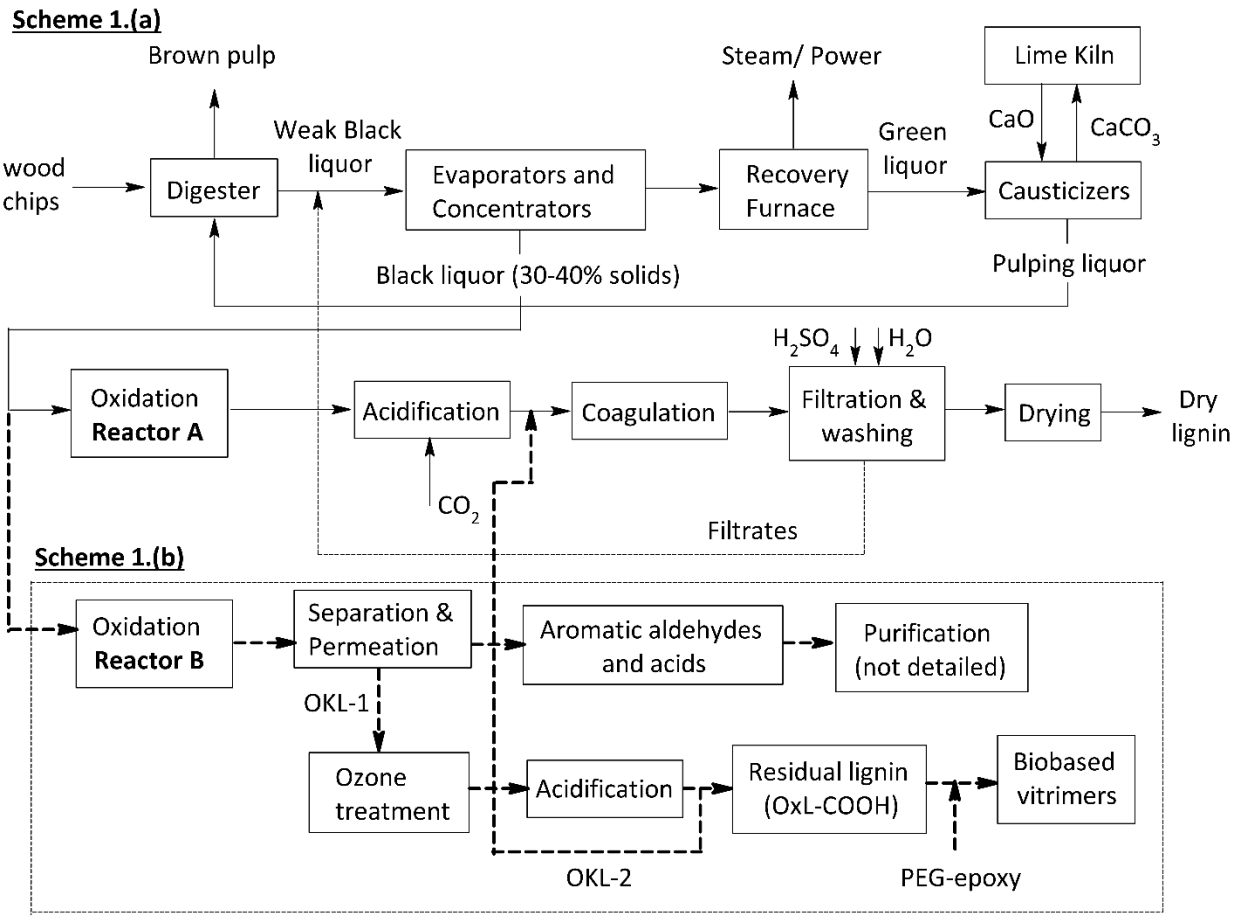

Figure 6.1 (a). LignoForce process and **(b).** Modified LignoForce process for the development of high-value products [27] (reproduced in part with permission from American Chemical Society)

Among the various vitrimer formation chemistries reported in the literature, transesterification is most suitable for oxidized kraft lignin conversion into vitrimers [5, 29, 30]. As shown in **Figure 6.2 (a)**, the modified lignin is a result of sequential oxidation using oxygen and ozone (OxL-COOH). During oxidation, electrophilic attack at lignin centers of high electron density can cause the formation of a four-membered cyclic peroxide intermediate which tends to rearrange and induce cleavage of carbon-carbon bonds [31-34].

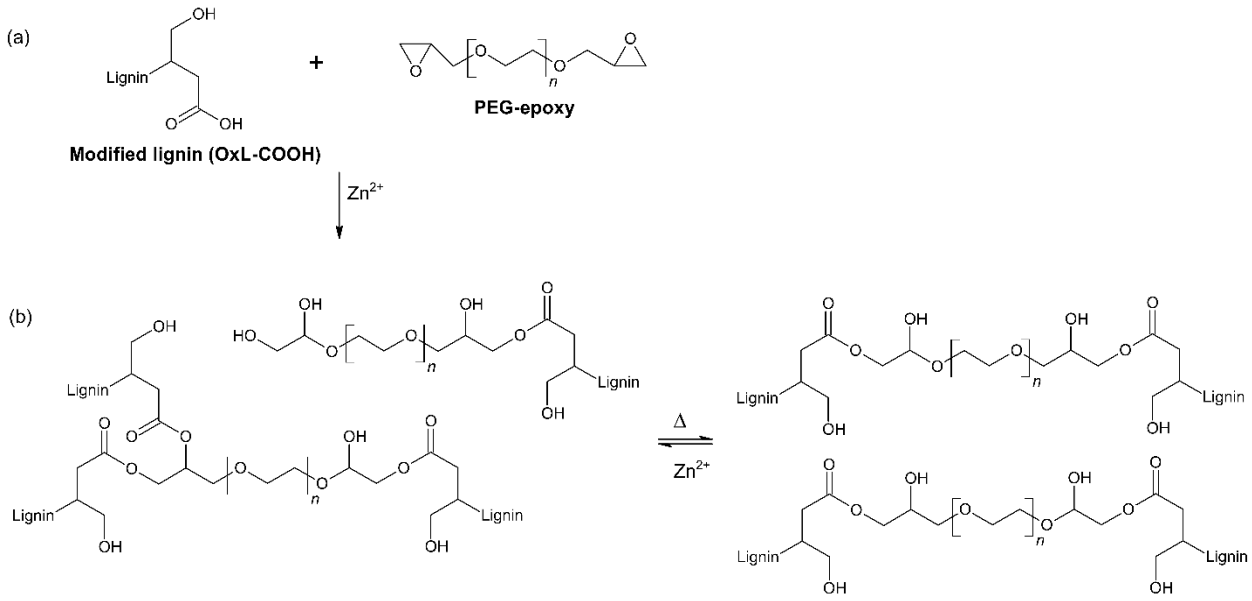

Figure 6.2. Proposed reaction pathway for vitrimer formation **(a).** Curing reaction of OxL-COOH and PEG-epoxy and **(b)**. Transesterification exchange reaction (TER) within the cross-linked network

In the first step, the modified lignin (OxL-COOH) reacts with the PEG-epoxy to cause ring-opening to produce an ester bond and a secondary hydroxyl group. This secondary hydroxyl group can further react with the –COOH group to form an ester. In **Figure 6.2 (b)**, bond rearrangement takes place without a disruption in connectivity due to reversible exchange reactions [35]. The stoichiometric ratio 'R' which relates to the ratio of epoxy to carboxyl groups can be varied to form different curing systems. In principle, the 'R' value is correlated to the amount of lignin present in the vitrimers. The objective of this work is to maximize the overall lignin utilization to produce diverse value-added products with a focus on integration in the existing pulp and paper industrial processes.

6.2. Materials and methods

6.2.1. Chemicals: Oxygen and nitrogen of ultra-high purity were supplied by Airgas USA (purity ≥ 97%), sulfuric acid (1.0 N laboratory reagent grade) and ethanol (200 proof) were purchased

from VWR chemicals, poly (ethylene glycol) diglycidyl ether (PEG-epoxy, Sigma Aldrich M_n = 500 g mol^{-1}), $Zn(acac)_2$ (Sigma Aldrich, 99.995%) and sodium chloride (assay ≥ 99%) were supplied by Fischer Chemical™, USA.

6.2.2. Carboxyl content determination using conductometric titration: The carboxyl content of the oxygen treated lignin, ozone treated lignin and sequentially oxidized lignin was determined using the conductometric titration method described in the literature [36]. After the oxidation treatment, a sample of lignin solution was adjusted to pH below 2 by the addition of HCl. As a result, the lignin is precipitated from the solution and recovered by centrifugation followed by freeze drying. In general, 1.5 g of freeze-dried lignin sample (with moisture content ≤ 10% by weight) was added to 300 mL of 0.10 N HCl and stirred for 1 hour. The lignin was then filtered and washed with de-ionized water to ensure that the conductivity of effluent water was less than 5 μScm^{-1}. Further, the washed lignin was dispersed in 0.001 N NaCl (250 mL) followed by the addition of 0.10 N HCl solution (1.5 mL). The resultant dispersion was stirred and titrated with 0.05 N NaOH under continuous bubbling of nitrogen. The conductometric titration was performed using a Metrohm Autotitrator equipped with an 856 Conductivity module connected to the main module (888 Titrando) coupled with Tiamo^{TM} 2.5 software. The output plot of conductivity against the volume of NaOH results in a parabolic curve with three distinguishable regimes. The first regime is the decrease in conductivity associated with the neutralization of added HCl. The second regime is usually a horizontal zone that corresponds to the neutralization of weak acid groups, i.e, carboxylic acid groups. Finally, the third regime is linked to the increase in conductivity after reaching the equivalence point due to the introduction of excess NaOH to the suspension.

6.2.3. Ozonation of SKL and sequential oxidation of OKL. Ozone is a highly reactive oxidizing agent capable of oxidizing most types of lignin structures. Therefore, oxidation of oxygen pre-

treated lignin with ozone will result in a further increase in the carboxyl content. The ozonation treatment was carried out at ambient pressure in a glass bubbler with a capacity of 1 L. The details on the ozonation procedure are mentioned in the literature [37]. The glass bubbler was heated to 80°C in a water bath with constant stirring. A flow of ozone was supplied by a '5G Lab Benchtop Ozone Generator' from A2Z Ozone providing an ozone dosage of 5000 mg hr^{-1} (100% capacity, oxygen flow rate 2 LPM). The ozone was directly injected into the solution through a long capillary. The off-gas was vented through a wash bottle partially filled with 10% by wt. potassium iodide solution. The ozonation was carried out at different time intervals of 1 hr, 2hr, 3 hr, and 4 hr to optimize the carboxyl content in the softwood kraft lignin. The optimized conditions for oxygen and ozone oxidations were then used to the sequentially oxidized OKL.

6.2.4. Preparation of OxL-COOH/PEG-epoxy vitrimers. The formulation of OxL-COOH/PEG-epoxy systems was varied based on stoichiometric ratio 'R' which represents the ratio of epoxy groups to carboxyl groups. OxL-COOH was allowed to dissolve in 200 proof - ethanol (1:3 w/v) completely. The use of ethanol as a solvent allows the mixing of all the components before curing the reaction. Softwood kraft lignin is hydrophobic and apolar solvents are unable to dissolve the lignin. Also, the introduction of -COOH groups in OxL-COOH results in added affinity towards polar solvents. Aliphatic alcohols have varying abilities to dissolve lignin due to the different number of carbon atoms present in them. A higher number of carbon atoms in the aliphatic alcohol are prone to have less mobility and more steric hindrance to surround the lignin moieties. Therefore, ethanol which has a limited number of carbon atoms and reasonable polarity represents a suitable solvent to homogenize all the components in the solution. After dissolution, $Zn(acac)_2$ was added at 5 mol% based on the content of carboxylic acid groups. Further, PEG-epoxy was added based on the desired stoichiometric ratios 'R' of 1.0, 1.3 and 1.5. All the

components were homogeneous in the solvent system, which is a key parameter for uniform vitrimer film formation. The optimized solvent evaporation conditions are discussed briefly in the **Section 6.3.2** about film formation. After solvent evaporation, the homogeneous solution in a PTFE mold was cured at 150°C for 1 hr and post-cured at 190°C for 2 hr.

6.2.5. Characterizations of the lignin-based vitrimers. FTIR measurements were performed using a ThermoScientific Nicolet 6700 FTIR instrument equipped with attenuated total reflection (ATR). Each spectrum was collected with 64 scans in the wavenumber range of 4000-400 cm^{-1} at a resolution of 4 cm^{-1}. Background spectra were recorded before every sample. The spectra were analyzed using OMNIC 7.3 software. The storage modulus of all films was characterized with a dynamic mechanical analysis (DMA, Dynamic Mechanical Analyzer TA Instruments RSA III) in a tensile mode at 1% min^{-1} strain rate. The dimensions of the test specimen were approximately 30 mm × 10 mm × 0.4 mm. Samples were scanned from -40°C to 150°C at a heating rate of 5°C min^{-1}. The frequency and the amplitude were set at 1 Hz and 15 μm, respectively. Isothermal stress relaxation tests were performed with an 8 mm parallel plate geometry. The thickness of the sample was approximately 0.4 mm. An axial force of 2 N was applied to attain a good contact of the sample with the parallel plate. During the test, 1% strain was applied and the trend of modulus as a function of time was recorded. The thermal stability of the samples was examined using a TA-Instruments Q-50 thermogravimetric analysis (TGA) system. The sample was loaded into a platinum pan and scanned from 25 to 800°C at a heating rate of 10°C min^{-1} under a nitrogen atmosphere. Thermal repair of the films was studied by monitoring the recovery of scratches by using an OLYMPUS 52 × 7 optical microscope. A crack was made on the surface of the film using a razor blade and the width of the crack was determined using the microscope (d_1). The cracked film was placed in between two tin plates and clamped using clips to fix the tin plates. This system

was then placed in a convection oven at 200°C for heating durations from 0 min to 30 min and the sample was observed every 15 min. The width change of the crack was measured using the microscope (d_2) and the rate of repair was calculated using the equation (1):

Equation (1) $$R = \frac{d_2 - d_1}{d_1} \times 100\%$$

The swelling of the OxL-COOH/PEG-epoxy system was determined in aqueous NaOH solutions at room temperature. In general the swelling ratio can be based on weight or volume changes in the sample. In this work, the swelling ratio was defined based on the weight changes in the sample. The sample with dimensions 0.5 cm × 0.5 cm × 0.1 cm was weighed (W_1) and added to a 20 mL glass vial containing aqueous NaOH solutions ranging in concentration from 0.01 M, 0.05 M, 0.1 M, and 0.2 M (10 mL). The glass vial was capped and kept still at room temperature. At time intervals of 5 min, 10 min, 15 min, 20 min, 30 min, and 60 min the sample was taken out, the free water was wiped off with filter paper and the sample weight was measured (W_2). The percentage swelling (S_r) at a given time was calculated according to the equation (2):

Equation (2) $$S_r = \frac{W_2 - W_1}{W_1} \times 100\%$$

6.3. Results and discussion

6.3.1. Sequential oxidation of softwood kraft lignin. Oxidation of kraft lignin results in the formation of carboxylic acid groups in the form of monomeric compounds and as end groups of the lignin macromolecule. The formation of carboxyl groups on the chain end can arise from electrophilic attack at lignin centers of high electron density. The presence of carboxyl groups in lignin is known to improve solubilization in polar solvents [31, 38-40]. In our previous work, we demonstrated the effect of oxygen oxidation on carboxyl content in softwood kraft lignin (SKL) [28]. The amount of carboxyl groups in the lignin plays a key role in vitrimer formation. Theoretically, the stoichiometric ratio between epoxy and carboxyl groups should be 1:2 for

complete consumption of reactive groups and to achieve a high crosslink density. In this study, the PEG-epoxy with Epoxide Equivalent Weight (EEW) of 250 g $equiv^{-1}$ which corresponds to 4 mmol g^{-1} of epoxy groups was used. Therefore, to achieve the theoretical stoichiometric ratio of 1:2 with a higher lignin percentage by weight, the carboxyl content should be proximate to or higher than the epoxy group content. The optimum carboxyl content of 1.41 mmol g^{-1} was obtained in the modified lignin (L-COOH) using oxygen at 130°C for 40 min of reaction time. The amount of carboxyl groups formed in L-COOH is lower than the theoretical requirement for vitrimer formation. Therefore, further modification of SKL to increase carboxyl groups is necessary to achieve the desired tensile properties in vitrimers with high lignin content. The sequential oxidation of softwood kraft lignin using oxygen and ozone results in 4.06 mmol/g of carboxylic OH units.

6.3.2. Film formation. Vitrimers exhibit superior strength and repairability properties due to the dynamic transesterification reaction in a cross-linked network. However, one of the key phenomena that also allows vitrimers to possess these properties is the ‘film formation’ during the curing process. For the first time, in our work, we discuss the main factors that govern the uniform and non-porous film formation in vitrimers which is only briefly discussed in the recent literature [41-44]. During the curing process, the carboxylic acid groups from OxL-COOH react with the epoxy groups from PEG-epoxy, in the presence of $Zn(acac)_2$.

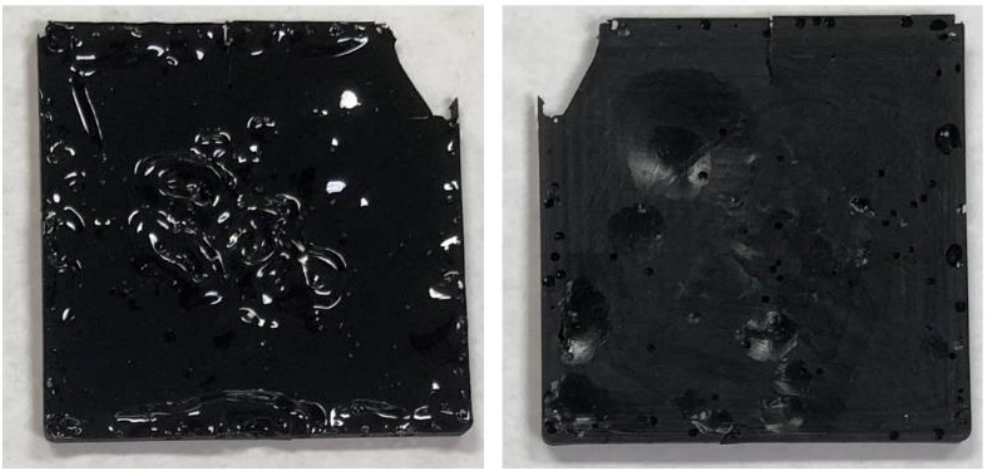

Figure 6.3. Bubble formation in vitrimers before troubleshooting

During vitrimer formation, bubble formation was one of the main challenges encountered as shown in **Figure 6.3**. Bubble formation in the film is linked to the non-homogeneous mixing of OxL-COOH in ethanol and the leftover traces of solvent in the film before curing at the reaction temperatures. To address this, traces of insoluble impurities from OxL-COOH/ethanol solution were initially separated from the ethanol. In the soluble fraction, OxL-COOH was completely dissolved in the solvent which is crucial for uniform film formation. Furthermore, the addition of $Zn(acac)_2$ and PEG-epoxy to this fraction allows for a completely homogeneous solution. Typically, the ethanol is allowed to evaporate at 25°C for 1 hr and followed by 80°C for 1 hr [1, 30]. However, the OxL-COOH/PEG-epoxy systems possessed traces of ethanol before its transfer to the PTFE mold. As a result, non-uniform and brittle films were formed limiting the overall tensile properties of the polymer. To address this, experiments were conducted by heating at 25°C for 1 hr followed by heating for 1 hr, 2 hr, 3 hr, and 4 hr at 80°C, 90°C, 100°C, and 110°C. The optimum conditions for uniform film formation were observed at 110°C with a heating duration of 4 hrs. At the optimized conditions, a homogeneous and uniform film was formed without any bubble formation as shown in **Figure 6.4**.

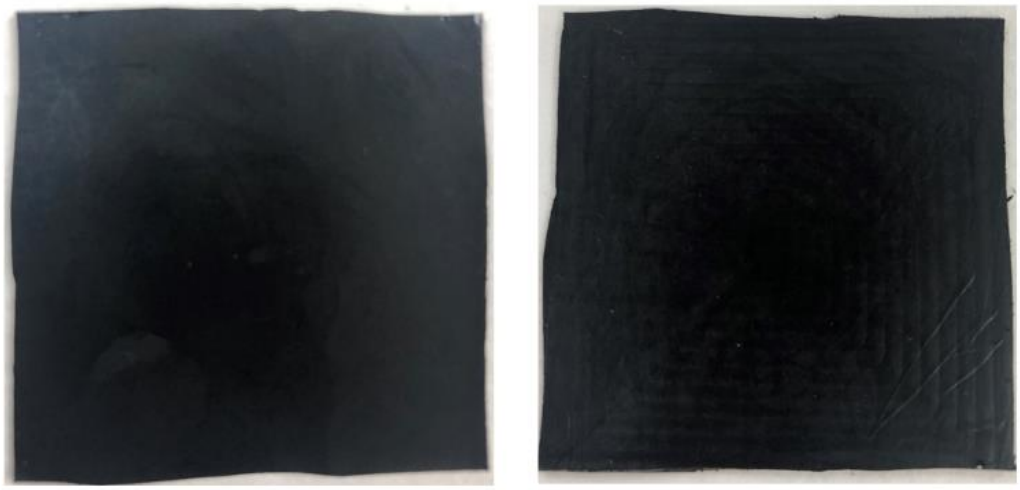

Figure 6.4. Front and back view of vitrimers after post troubleshooting

6.3.3 Structural characterization

6.3.3.1. FTIR Analysis: FTIR analysis was performed for untreated SKL, oxygen treated (stage 1) L-COOH, and ozone-treated OxL-COOH (stage 2) lignin samples. **Figure 6.5** shows the broadening of peaks for -C=O and -OH groups at 1708 cm^{-1} and 2500-3500 cm^{-1}, respectively, as the severity of oxidation increased from oxygen to ozone. The -OH group belongs to the -COOH group. Therefore, from the qualitative analysis, it was confirmed that sequential oxidation enhances the carboxyl group formation in lignin. In our previous work, we studied the effect of oxygen and ozone oxidation on carboxyl group formation in SKL. **Chapter 5** briefly highlights the carboxyl group formation in softwood kraft lignin after oxidation under different conditions. Among the oxidizing agents, the amount of carboxylic OH units formed from ozone oxidation (2.08 mmol/g) was higher compared to the oxygen oxidation (0.82 mmol/g) under similar conditions. Further modification using ozone under optimized conditions resulted in a carboxyl content of 4.06 mmol g^{-1}. Thus, the improvement in carboxyl content was confirmed qualitatively and quantitatively using FTIR and conductometric titrations.

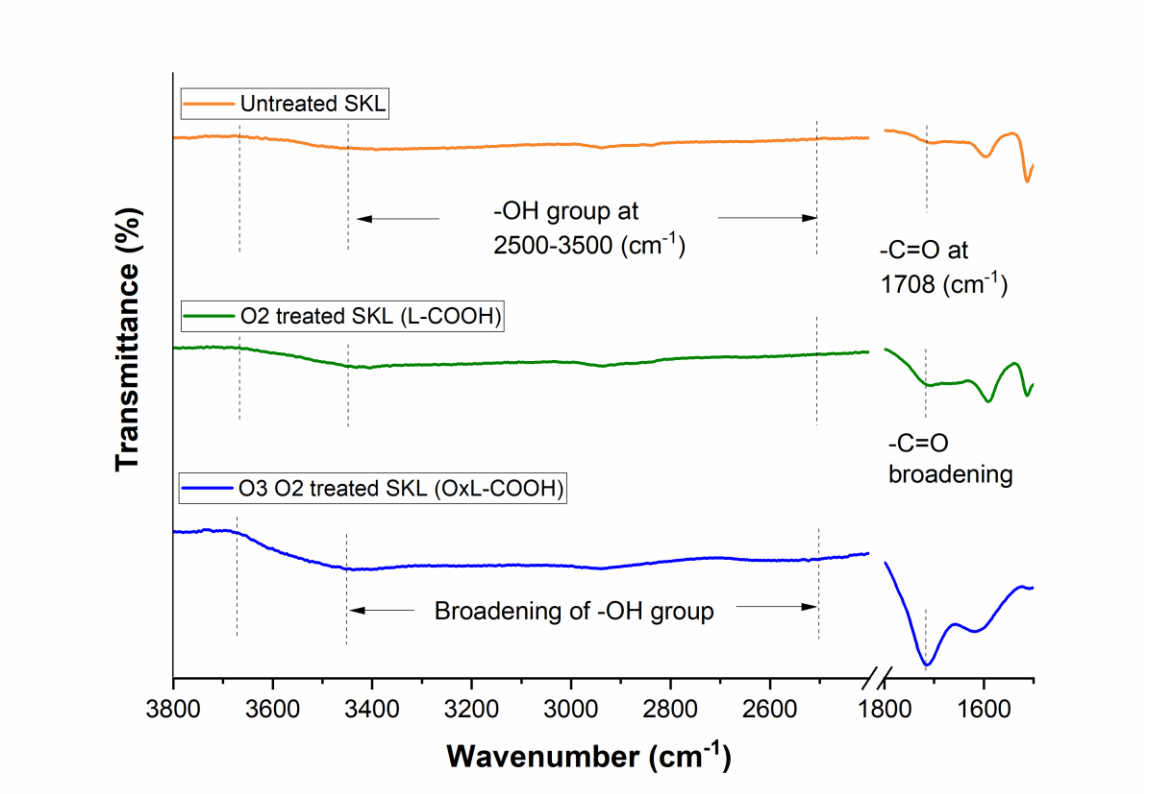

Figure 6.5. Comparative FTIR spectra of untreated SKL, oxygen oxidized SKL (L-COOH), and ozone & oxygen treated SKL (OxL-COOH)

Table 6.1 shows the different stoichiometric formulations of the OxL-COOH/ PEG-epoxy systems. All systems had high lignin content (≤ 50 wt. %) with varying 'R' values implying a high biomass content in the polymer films. **Figure 6.6** shows the FTIR spectra of the cured PEG-epoxy/OxL-COOH samples with different 'R' values. The peak intensity of epoxy groups from -C–O stretching (1090 cm^{-1}), -OH groups (3000 to 3700 cm^{-1}), and -C–H groups (2860 cm^{-1}) changed consistently with varying stoichiometric ratios. The increase in the 'R' value from 1 to 1.5 increased the peak intensity of hydroxyl groups. As the 'R' value approaches the stoichiometric value of R_t: 0.5, more complete curing is obtained, as a result, the peak intensity at 910 cm^{-1} and 3400 cm^{-1} is reduced. However, as the 'R' value increases, a high content of hydroxyl groups due

to the ring-opening of epoxy groups in the PEG-epoxy occurs, which increases the peak intensity of the hydroxyl groups.

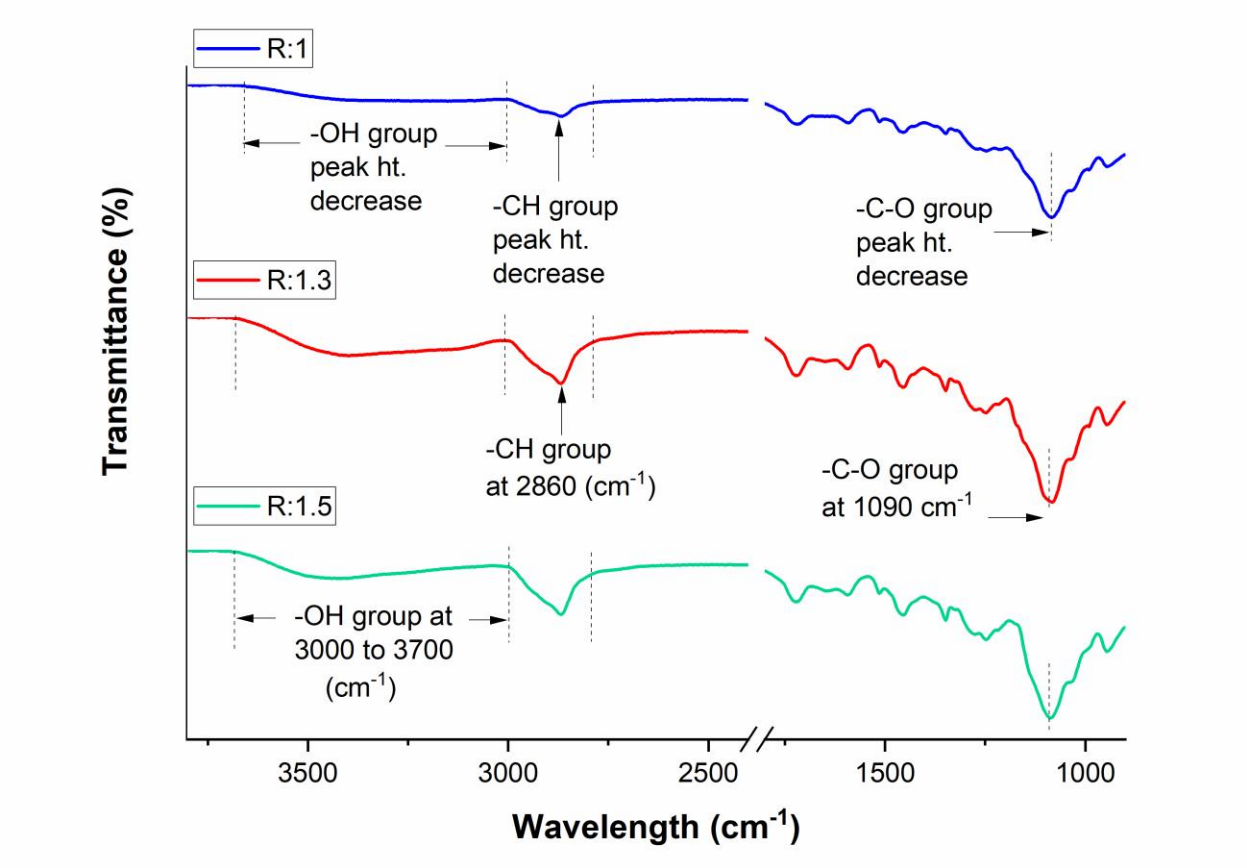

Figure 6.6. FTIR spectral changes of the cured OxL-COOH/PEG-epoxy system at different stoichiometric '*R*' values

Lignin content (% by wt.)	**Stoichiometric ratio 'R' (epoxy/carboxyl)**	**Mass ratio 'R' (epoxy/carboxyl)**	**FWHM of tan δ (°C)**	**T_{d5} (°C)**
39.6	1.5	1: 0.65	-15	270
43.1	1.3	1: 0.76	-10	276
49.5	1.0	1: 0.98	-8	260

Table 6.1. Different stoichiometric formulations of OxL-COOH/PEG-epoxy systems.

6.3.3.2. Dynamic mechanical properties: Dynamic mechanical analysis (DMA) was performed for all OxL-COOH/PEG-epoxy systems. **Figure 6.7** shows the tensile modulus versus temperature of the cured OxL-COOH/PEG-epoxy systems. All curves exhibit a high storage modulus which defines the stiffness of the backbone structure and crosslink density. The storage modulus of the OxL-COOH/PEG-epoxy increases as the lignin content increases as lignin is much stiffer and possesses multiple reactive groups compared to the PEG-epoxy. The full width at half minimum (FWHM) which relates to the uniformity of the network was also determined using DMA (**Figure 6.8**). The increase in lignin content also resulted in an increase in the full width at a half minimum due to the poly-disperse nature of lignin. All OxL-COOH/PEG-epoxy systems showed a single glass transition based on the peak temperature of tan δ. The maximum storage modulus value of 2.08×10^8 Pa was obtained at the stoichiometric value of R:1. However, as the 'R' value increased the initial storage modulus values dropped to 8.7×10^7 Pa and 7.06×10^7 Pa for R:1.30 and R:1.50, respectively.

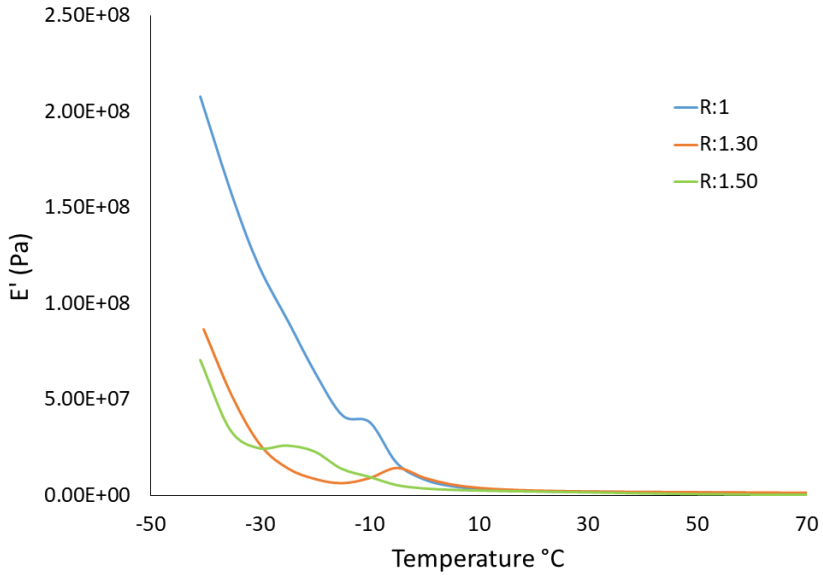

Figure 6.7. The storage modulus of OxL-COOH/PEG-epoxy films with different R values

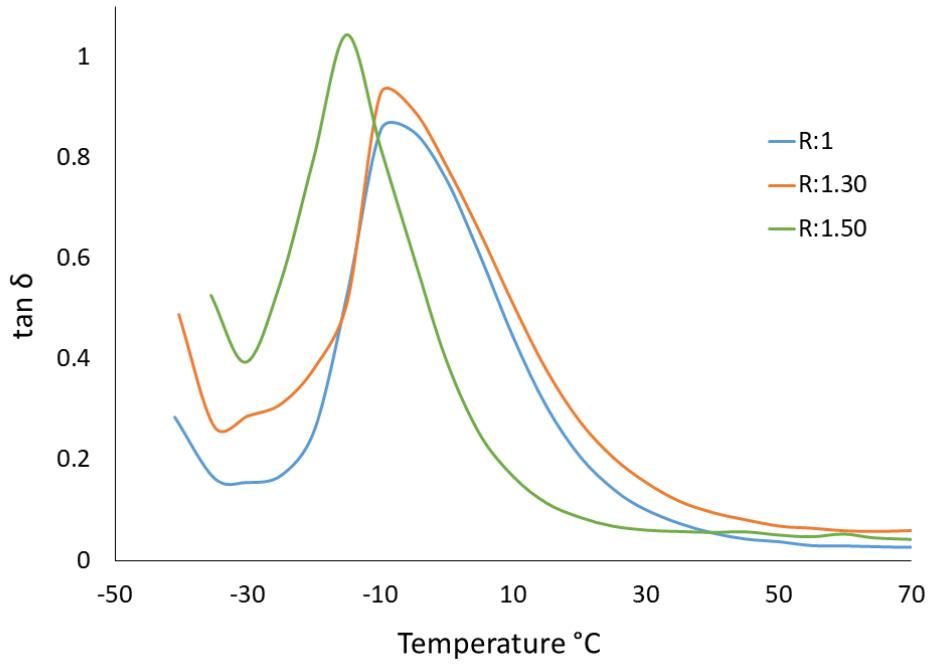

Figure 6.8. tan δ of OxL-COOH/PEG-epoxy films with different R values

6.3.3.3. Thermal stress relaxation and repairability: The thermogravimetric analysis and derivative thermogravimetric analysis study of polyethylene glycol diglycidyl ether (PEGDE) with molecular weight M_w: 500 g mol^{-1} has been reported in the literature [45]. **Figure 6.9** shows that the 5% weight loss temperature (T_{d5}) of PEG-epoxy is below 200°C. It was found that the PEG-epoxy thermal decomposition started at about 125°C and was completely combusted at about 500°C. From the DTG curve, the temperature at which the maximum weight loss rate occurred (T_{max}) was approximately 300°C.

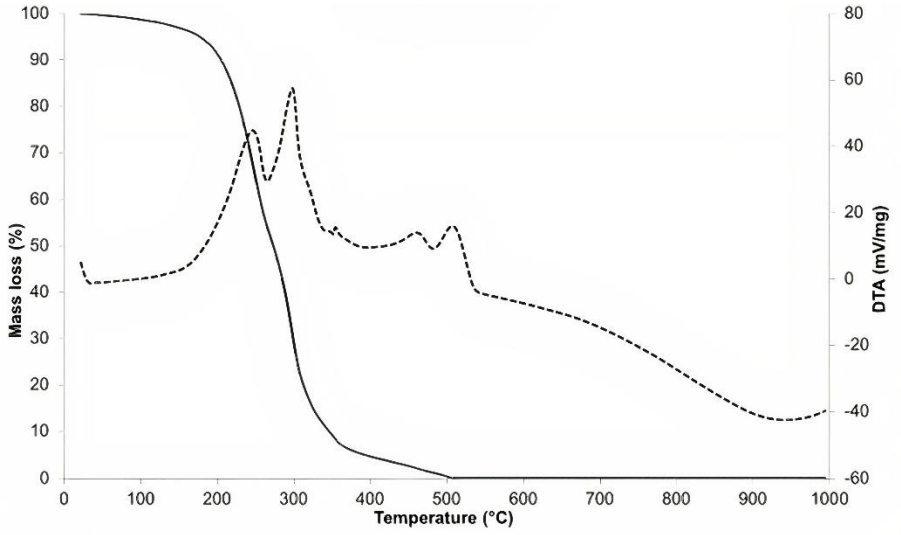

Figure 6.9. Thermogravimetric analysis (TGA) and derivative thermogravimetric analysis (DTG) study of PEG-epoxy (DTA* in the graph corresponds to DTG analysis) [45]

Thermogravimetric analysis (TGA) was performed on untreated SKL and all PEG-epoxy/OxL-COOH systems. The data obtained from TGA is crucial for understanding the thermal processing and stability of the vitrimers. The untreated SKL sample showed a 5% weight loss temperature at 112°C. The weight loss at this temperature is the result of the expulsion of water molecules from the surface of SKL. In contrast, all PEG-epoxy/OxL-COOH systems showed similar 5% weight loss temperatures of approximately 270°C which was markedly higher than the untreated SKL as shown in **Figure 6.10**. A higher residue content was obtained as the lignin content increased due to the higher thermal stability of the sample and higher aromatic ring content. The temperature at which maximum weight loss rate occurred for the OxL-COOH/PEG-epoxy systems was around 397°C (**Figure 6.11**). These results indicate an adequate thermo-stability of the samples for relaxation tests at elevated temperatures.

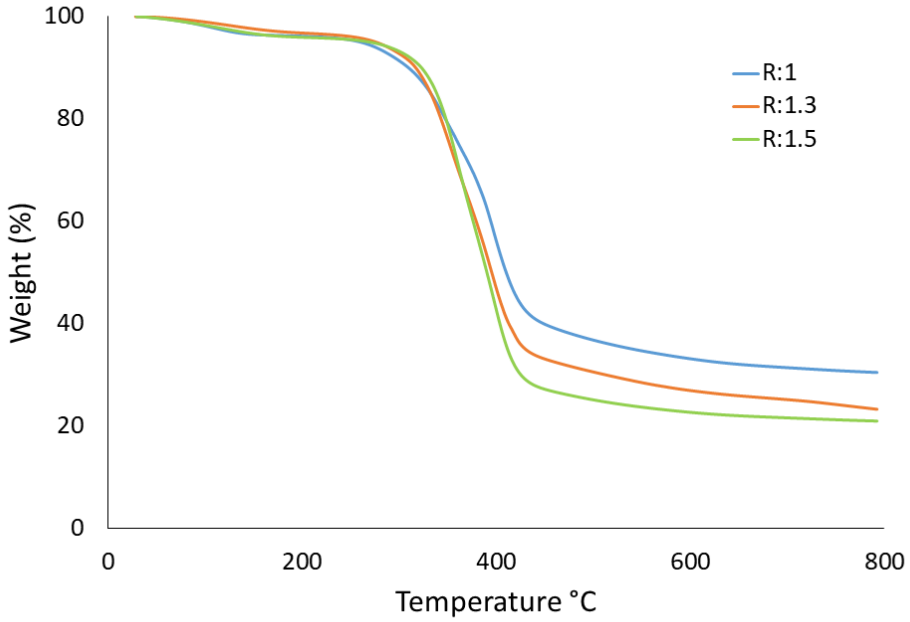

Figure 6.10. Thermogravimetric analysis (TGA) of OxL-COOH/PEG-epoxy films with different R values

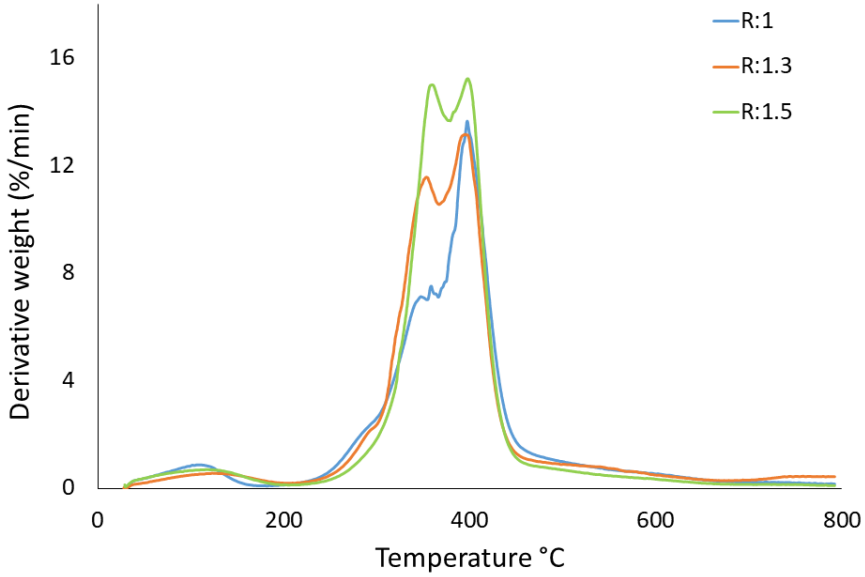

Figure 6.11. Derivative thermogravimetric analysis (DTG) of OxL-COOH/PEG-epoxy films with different R values

Conventional thermosets are difficult to stress relax due to the permanent covalent bonds in the cross-linked structure. **Figure 6.12** shows the stress relaxation behavior of a conventional epoxy thermoset at different temperatures ranging from 80°C to 200°C reported in the literature [46]. This epoxy thermoset was prepared by diglycidyl ether of Bisphenol A (DGEBA), glutaric anhydride and zinc acetylacetonate $Zn(acac)_2$. From the graph, it is evident that conventional epoxy based thermosets are difficult to stress relax at lower temperatures. However, due to the nature of associative bond exchange chemistry, vitrimers can undergo stress relaxation.

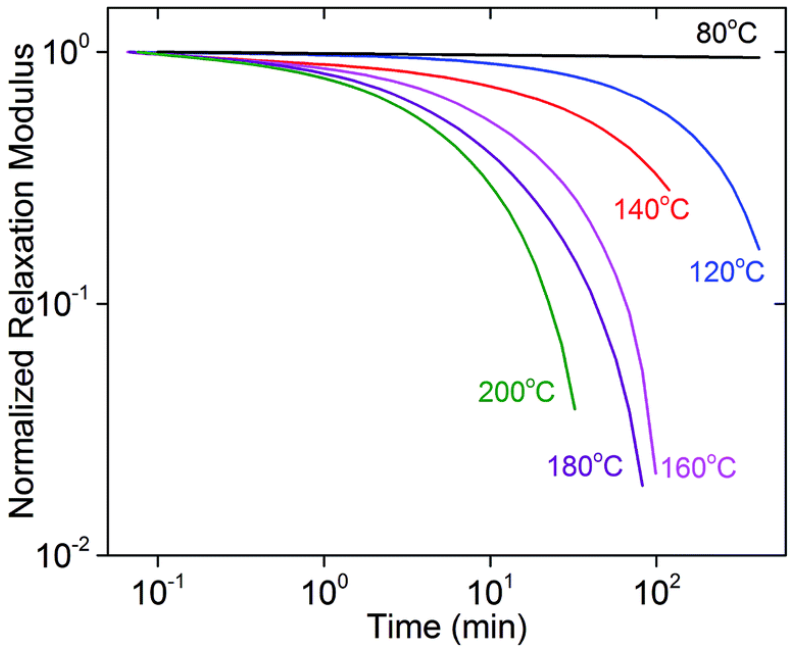

Figure 6.12. The stress relaxation behavior of epoxy thermoset prepared from DGEBA, glutaric anhydride and $Zn(acac)_2$ at different temperatures ranging from 80°C to 200°C [46]

In this type of covalent adaptable network, bonds are only broken when a new covalent bond is formed resulting in a fixed cross-link density and making the network permanent as well as dynamic. Therefore, a stress relaxation test can provide direct evidence of transesterification

exchange reactions (TER). **Figure 6.13** shows the stress relaxation modulus of OxL-COOH/PEG-epoxy films as a function of time at room temperature. All samples exhibited clear stress relaxation. The sample with R:1 demonstrated the fastest relaxation rate due to efficient TERs with ester bonds. However, the increase in the stoichiometric value led to a slower relaxation rate due to the presence of unreacted hydroxyl groups from the ring-opening of epoxy groups.

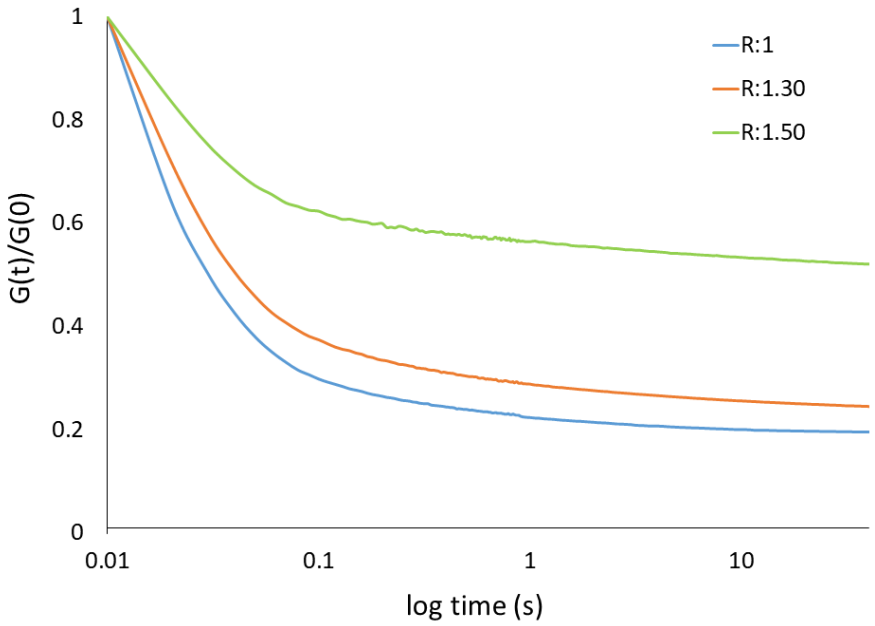

Figure 6.13. Stress relaxation curves of OxL-COOH/PEG-epoxy films with different R values

6.3.3.4 Swelling study: In response to temperature and solvents, thermoplastic polymers completely dissolve and behave like a viscoelastic liquid when heated above a certain temperature whereas, thermosetting polymers can only swell, and even at higher temperatures become softer but do not flow and only a fraction of the polymer material dissolves. Vitrimer polymers represent a third category of organic polymers that behave like a viscoelastic liquid when heated and resist dissolution in good solvents [47]. OxL-COOH shows excellent solubility in aqueous NaOH solutions due to the nature of the lignin macromolecule. The protonation of lignin molecules is

more favorable with a higher pK_a value, thereby contributing to its solubility in aq. NaOH solutions 24, 48]. In contrast, at lower pH values, there is less dissociation of the charged phenolic OH groups in lignin. Also, the phenol and carboxyl groups from lignin can transform into sodium phenolate and sodium carboxylate ions in aqueous NaOH solutions, thereby contributing to the solubility. Therefore, aq. NaOH solutions represents an excellent medium to test the swelling nature of OxL-COOH/PEG-epoxy system. **Figure 6.14** shows the swelling OxL-COOH/PEG-epoxy with R=1 in NaOH solution with concentrations 0.01 M, 0.05 M, 0.1 M, and 0.2 M with swelling time fixed at 10 min. The swelling trend showed a slow increase from 0.01 M to 0.05 M followed by a rapid increase to 0.2 M. As the concentration changed from 0.01 M to 0.2 M, the swelling increased from 13.5% to 44.9% which shows significant improvement in swelling of the vitrimer. To understand the effect of time on the swelling of OxL-COOH/PEG-epoxy systems, the sample was monitored at continuous time intervals starting from 0 min up to 60 min (**Figure 6.15**) in 0.1 M NaOH solution. The swelling increased rapidly to 40.1% in the first 15 mins. The swelling continuously increased further but at a slower rate. The noteworthy swelling of the vitrimer in alkaline solution signifies the occurrence of transesterification exchange reactions of the OxL-COOH/PEG-epoxy systems.

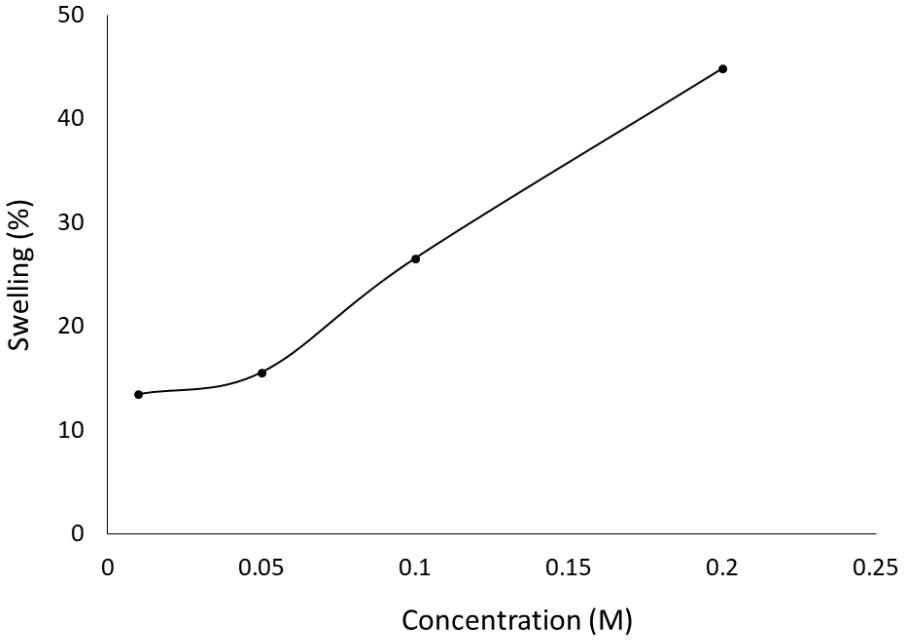

Figure 6.14. Swelling of OxL-COOH/PEG-epoxy with R: 1 in NaOH solution with different concentrations (0.01 M, 0.05 M, 0.1 M, and 0.2 M)

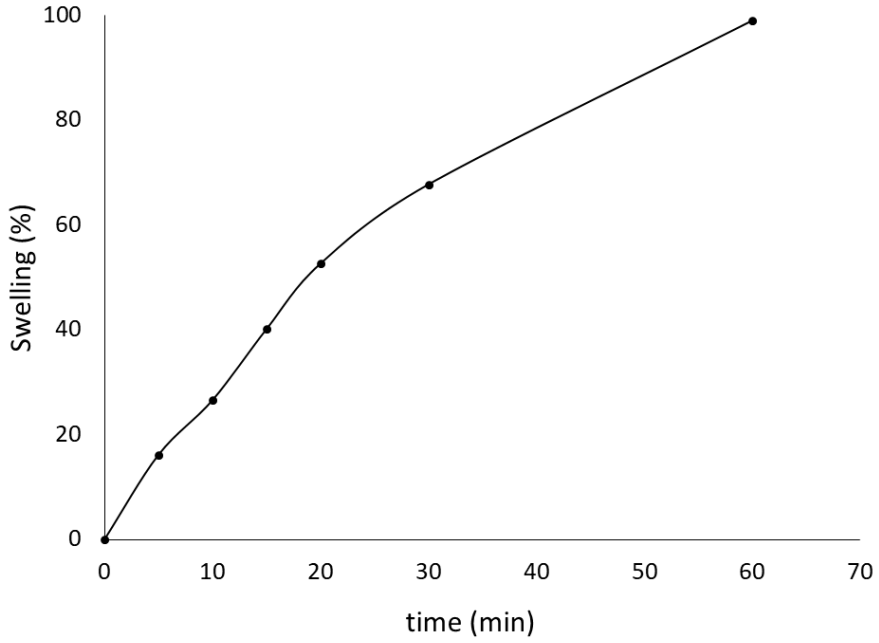

Figure 6.15. Swelling of OxL-COOH/PEG-epoxy with R: 1 in 0.1 M NaOH solution at different time intervals (0, 5, 10, 15, 20, 30, and 60 min)

6.3.3.5. Self-healing. In addition to swelling, self-healing constitutes an important feature of vitrimers due to the dynamic transesterification exchange reactions. The detailed image description of self-healing for R:1 is shown in **Figure 6.16**. For the sample with R:1, the average crack width of 17.5 μm changed to 11.87 μm in the first 15 min and to 8.03 μm in the next 15 min. Overall, the crack width of this sample healed to about 54.1% in the first 30 min. In contrast, in the sample with R: 1.3, the average crack width of 10.33 μm changed rapidly to 6.15 μm in the first 15 min and slowly to 5.01 μm in the next 15 min. At R: 1.5, the initial crack width of 8.37 μm changed slightly to 7.6 μm in the first 15 min and to 6.09 μm. Overall, this sample represented the slowest repairability compared with R: 1.3 and R: 1. As confirmed with other studies, the sample with R: 1 represented efficient transesterification exchange reactions due to the nature of self-healing observed in this sample.

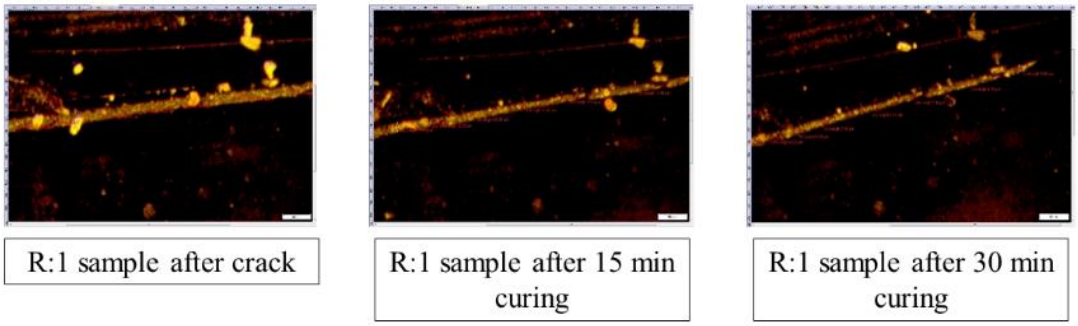

Figure 6.16. Self-healing for R:1 sample after crack, after 15 min curing and after 30 min curing

6.4. Conclusions: The objective of this work was to maximize lignin utilization to produce diverse value-added products with a focus on integration in existing pulp and paper industrial processes. Based on the results obtained, sequential oxidation of SKL represents a new approach for simultaneous production of vanillin, vanillic acid, and lignin-based vitrimers which diversify the value-added product profile from lignin. The modification of SKL using ozone represents a lignin source with high carboxyl content which is crucial for vitrimer formation with PEG-epoxy. All

OxL-COOH/PEG-epoxy systems possessed a high lignin content (>48 wt%). All systems showed thermal stability, fast relaxation, and self-healing due to the presence of bond exchangeable cross-linked networks. In aqueous NaOH solutions, the lignin-based vitrimer did not dissolve and exhibited noteworthy swelling properties which is a key indicator of the dynamic transesterification in the cured network. Overall, this study represents a novel and integrated process for the valorization of kraft lignin into value-added products.

6.5. References

[1] S. Zhang, T. Liu, C. Hao, L. Wang, J. Han, H. Liu, and J. Zhang, "Preparation of a lignin-based vitrimer material and its potential use for recoverable adhesives," *Green Chem.*, vol. 20, no. 13, pp. 2995-3000, 2018.

[2] W. Post, A. Susa, R. Blaauw, K. Molenveld, and R. J. Knoop, "A review on the potential and limitations of recyclable thermosets for structural applications," *Polym. Rev.*, vol. 60, no. 2, pp. 359-388, 2020.

[3] D. Montarnal, M. Capelot, F. Tournilhac, and L. Leibler, "Silica-like malleable materials from permanent organic networks," *Science*, vol. 334, no. 6058, pp. 965-968, 2011.

[4] C. J. Kloxin, T. F. Scott, B. J. Adzima, and C.N. Bowman, "Covalent adaptable networks (CANs): a unique paradigm in cross-linked polymers," *Macromolecules*, vol. 43, no. 6, pp. 2643-2653, 2010.

[5] W. Denissen, J. M. Winne, and F. E. Du Prez, "Vitrimers: permanent organic networks with glass-like fluidity," *Chem. Sci.*, vol. 7, no. 1, pp. 30-38, 2016.

[6] T. Liu, X. Guo, W. Liu, C. Hao, L. Wang, W.C. Hiscox, C. Liu, C. Jin, J. Xin, and J. Zhang, "Selective cleavage of ester linkages of anhydride-cured epoxy using a benign method and reuse

of the decomposed polymer in new epoxy preparation," *Green Chem*., vol. 19, no. 18, pp. 4364-4372, 2017.

[7] T. Liu, C. Hao, L. Wang, Y. Li, W. Liu, J. Xin, and J. Zhang, "Eugenol-derived biobased epoxy: shape memory, repairing, and recyclability," *Macromolecules*, vol. 50, no. 21, pp. 8588-8597, 2017.

[8] F. I. Altuna, V. Pettarin, and R. J. Williams, "Self-healable polymer networks based on the cross-linking of epoxidized soybean oil by an aqueous citric acid solution," *Green Chem*., vol. 15, no. 12, pp. 3360-3366, 2013.

[9] Z. Ma, Y. Wang, J. Zhu, J. Yu, and Z. Hu, "Bio-based epoxy vitrimers: Reprocessibility, controllable shape memory, and degradability," *Polym. Chem*., vol. 55, no. 10, pp. 1790-1799, 2017.

[10] W. Boerjan, J. Ralph, and M. Baucher, "Lignin biosynthesis," *Annu. Rev. Plant Biol*., vol. 54, no. 1, pp. 519-546, 2003.

[11] G. Cazacu, M. C. Pascu, L. Profire, A. Kowarski, M. Mihaes, and C. Vasile, "Lignin role in a complex polyolefin blend," *Ind. Crops. Prod*., vol. 20, no. 2, pp. 261-273, 2004.

[12] A. More, T. Elder, and Z. Jiang, "A review of lignin hydrogen peroxide oxidation chemistry with emphasis on aromatic aldehydes and acids," *Holzforschung*, vol. 75, no. 9, pp. 806-823, 2021.

[13] P.C.R. Pinto, E.A.B. da Silva, and A.E. Rodrigues, "Lignin as source of fine chemicals: vanillin and syringaldehyde," Biomass Conversion; C. Baskar, S. Baskar, R.D. Dhillon, Eds; Springer: London, pp. 381-420, 2012.

[14] D. Bajwa, G. Pourhashem, A. Ullah, and S. Bajwa, "A concise review of current lignin production, applications, products and their environmental impact," *Ind. Crops. Prod*., vol. 139, pp. 111526, 2019.

[15] T. Q. Hu, "Chemical modification, properties, and usage of lignin," Kluwer Academic/Plenum Publisher, New York, pp. 291, 2002.

[16] D. Schorr, P. N. Diouf, and T. Stevanovic, "Evaluation of industrial lignins for biocomposites production," *Ind. Crops. Prod*., vol. 52, pp. 65-73, 2014.

[17] G. Chatel, and R. D. Rogers, "Oxidation of lignin using ionic liquids: An innovative strategy to produce renewable chemicals," *ACS Sustain. Chem. Eng*., vol. 2 no. 3, pp. 322-339, 2014.

[18] A. Das, A. Rahimi, A. Ulbrich, M. Alherech, A. H. Motagamwala, A. Bhalla, L. da Costa Sousa, V. Balan, J. A. Dumesic, and E. L. Hegg, "Lignin conversion to low-molecular-weight aromatics via an aerobic oxidation-hydrolysis sequence: comparison of different lignin sources," *ACS Sustain. Chem. Eng*., vol. 6, no. 3, pp. 3367-3374, 2018.

[19] O.Y. Abdelaziz, K. Ravi, F. Mittermeier, S. Meier, A. Riisager, G. Lidén, and C.P. Hulteberg, "Oxidative Depolymerization of Kraft Lignin for Microbial Conversion," *ACS Sustain. Chem. Eng*., vol. 7, no. 13, pp. 11640-11652, 2019.

[20] V. E. Tarabanko, and N. Tarabanko, "Catalytic oxidation of lignins into the aromatic aldehydes: general process trends and development prospects," *Int. J. Mol. Sci*., vol. 18, no. 11, pp. 2421, 2017.

[21] D. P. Bezerra, A. K. N. Soares, and D. P. de Sousa, "Overview of the role of vanillin on redox status and cancer development," *Oxid. Med. Cell. Longev*., vol. 2016, Article ID: 9734816, 2016.

[22] J. Choo, Y. Rukayadi, and J.K. Hwang, "Inhibition of bacterial quorum sensing by vanilla extract," *Lett. Appl. Microbiol*., vol. 42, no. 6, pp. 637-641, 2006.

[23] C. S. Calixto-Campos, T. T. Carvalho, M. S. Hohmann, F. A. Pinho-Ribeiro, V. Fattori, M. F. Manchope, A. C. Zarpelon, M. M. Baracat, S. R. Georgetti, and R. Casagrande, "Vanillic acid

inhibits inflammatory pain by inhibiting neutrophil recruitment, oxidative stress, cytokine production, and NFκB activation in mice," *J. Nat. Prod*., vol. 78 no. 8, pp. 1799-1808.

[24] L. Kouisni, and M. Paleologou, "Method for separating lignin from black liquor," United States Patent 8771464, Jul. 2, 2014.

[25] L. Kouisni, P. Holt-Hindle, K. Maki, and M. Paleologou, "The lignoforce system: a new process for the production of high-quality lignin from black liquor," *J. Sci. Technol. For. Prod. Processes*, vol. 2, no. 4, pp. 6-10, 2012.

[26] K. Wells, D. Pors, J. Foan, K. Maki, L. Kouisni, and M. Paleologou, "CO_2 Impacts of Commercial Scale Lignin Extraction at Hinton Pulp Using the LignoForce Process & Lignin Substitution into Petroleum-Based Products," *PACWEST Conference*, pp. 10-13, 2015.

[27] L. Kouisni, A. Gagné, K. Maki, P. Holt-Hindle, and M. Paleologou, "LignoForce system for the recovery of lignin from black liquor: feedstock options, odor profile, and product characterization," *ACS Sus. Chem. Eng*., vol. 4, no. 10, pp. 5152-5159, 2016.

[28] A. More, T. Elder, and Z. Jiang, "Towards a new understanding of the retro-aldol reaction for oxidative conversion of lignin to aromatic aldehydes and acids," *Int. J. Bio. Macromol*., vol. 183, pp. 1505-1513, 2021.

[29] J. Han, T. Liu, C. Hao, S. Zhang, B. Guo, and J. Zhang, "A catalyst-free epoxy vitrimer system based on multifunctional hyper branched polymer," *Macromolecules*, vol. 51, no. 17, pp. 6789-6799, 2018.

[30] C. Hao, T. Liu, S. Zhang, L. Brown, R. Li, J. Xin, T. Zhong, L. Jiang, and J. Zhang, "A High-Lignin-Content, Removable, and Glycol-Assisted Repairable Coating Based on Dynamic Covalent Bonds," *ChemSusChem*, vol. 12, no. 5, pp. 1049-1058, 2019.

[31] F. Asgari, and D.S. Argyropoulos, “Fundamentals of oxygen delignification. Part II. Functional group formation/elimination in residual kraft lignin,” *Can. J. Chem*., vol. 76, no. 11, pp. 1606-1615, 1998.

[32] J. Gierer, and F. Imsgard, “The reactions of lignins with oxygen and hydrogen peroxide in alkaline media,” *Sven. Papperstidn.*, vol. 80, no. 16, pp. 510-518, 1977.

[33] H. Chang, and J. Gratzl, “Ring cleavage reactions of lignin models with oxygen and alkali: Chemistry of Delignification with Oxygen, Ozone and Peroxide,” *Uni Pub. Co. Ltd*., pp. 151-163, 1980.

[34] M. R. Fernandes, X. Huang, H. C. Abbenhuis, and E. J. Hensen, “Lignin oxidation with an organic peroxide and subsequent aromatic ring opening,” *Int. J. Biol. Macromol*., vol. 123, pp. 1044-1051, 2019.

[35] T. Liu, B. Zhao, and J. Zhang, “Recent development of repairable, malleable and recyclable thermosetting polymers through dynamic transesterification,” *Polymer*, vol. 194, pp. 122392, 2020.

[36] S. Katz, and R. P. Beatson, “The determination of strong and weak acidic groups in sulfite pulps,” *Sven. Papperstidn*., vol. 87, no. 6, pp. 48-53, 1984.

[37] O. Musl, M. Holzlechner, S. Winklehner, G. Gübitz, A. Potthast, T. Rosenau, and S. Böhmdorfer, “Changing the Molecular Structure of Kraft Lignins – Ozone Treatment at Alkaline Conditions,” *ACS Sus. Chem. Eng*., vol. 7, no. 18, pp. 15163-15172, 2019.

[38] G. Gellerstedt, K. Gustafsson, and E. L. Lindfors, “Structural changes in lignin during oxygen bleaching,” *Nord. Pulp. Pap. Res. J.*, vol. 1, no. 3, pp. 14-17, 1986.

[39] Y. Sun, D. Argyropoulos, “Fundamentals of high-pressure oxygen and low-pressure oxygen-peroxide (EOP) delignification of softwood and hardwood kraft pulps: a comparison,” *J. Pulp Pap. Sci*., vol. 21, no. 6, pp. J185-J190, 1995.

[40] D. Zhang, “Characterization and enhancement of carboxyl groups in softwood kraft pulps during oxygen delignification,” Ph.D. thesis. Georgia Institute of Technology, Georgia, USA, 2006. [Online accessed 8 June 2022] Retrieved from: https://smartech.gatech.edu/bitstream/handle/1853/13941/dongcheng_zhang-200612_phd.pdf.pdf

[41] A. Moreno, M. Morsali, and M. H. Sipponen, “Catalyst-Free Synthesis of Lignin Vitrimers with Tunable Mechanical Properties: Circular Polymers and Recoverable Adhesives,” *ACS Appl. Mater. Interfaces,* vol. 13, no. 48, pp. 57952-57961, 2021.

[42] H. Geng, Y. Wang, Q. Yu, S. Gu, Y. Zhou, W. Xu, X. Zhang, and D. Ye, “Vanillin-based polyschiff vitrimers: reprocessability and chemical recyclability,” *ACS Sus. Chem. Eng*., vol. 6, no. 11, pp. 15463-15470.

[43] B. Xue, R. Tang, D. Xue, Y. Guan, Y. Sun, W. Zhao, J. Tan, and X. Li, “Sustainable alternative for bisphenol A epoxy resin high-performance and recyclable lignin-based epoxy vitrimers,” *Ind. Crops. Prod*., vo. 168, pp. 113583, 2021.

[44] G. F. Bass, and T. Epps III, “Recent developments towards performance-enhancing lignin-based polymers,” *Polym. Chem*., vol. 12, pp. 4130-4158, 2021.

[45] I. Mallard, D. Landy, and S. Fourmentin, “Evaluation of polyethylene glycol crosslinked β-CD polymers for the removal of methylene blue,” *Appl. Sci.*, vol. 10, pp. 4679, 2020.

[46] K. Yu, P. Taynton, W. Zhang, M. L. Dunn, and H. J. Qi, “Influence of stoichiometry on the glass transition and bond exchange reactions in epoxy thermoset polymers†,” *RSC Adv*., vol. 4, pp. 48682-48690, 2014.

[47] J. M. Winne, L. Leibler, and F. E. Du Prez, “Dynamic covalent chemistry in polymer networks: A mechanistic perspective,” *Polym. Chem*., vol. 10, no. 45, pp. 6091-6108, 2019.

[48] W. Zhu, and H. Theliander, “Precipitation of lignin from softwood black liquor: an investigation of the equilibrium and molecular properties of lignin,” *BioResources*, vol. 10, no.1, pp.1696-1714,2015.

Chapter 7 | Conclusions and future work

This dissertation demonstrated the integrated processes for the valorization of kraft lignin to synthesize high-value products. The major contribution areas include comprehensive reviews of lignin oxidation chemistry using oxygen and hydrogen peroxide and the strategies to produce bio-based vitrimer polymers using kraft lignin; new insights of the retro-aldol reaction to enhance the yields of vanillin and vanillic acid; effect of oxygen and ozone oxidation on functional group content in softwood kraft lignin; a novel and integrated approach to produce transesterification based vitrimer polymers using kraft lignin.

7.1. Summary

In this work, the author aims to explore the utilization of a novel and integrated approach to diversify the product portfolio obtained from the oxidation of kraft lignin in the pulp and paper industrial processes. The retro-aldol reaction is one of the key pathways explaining the formation of aromatic aldehydes and acids from the oxidation of kraft lignin. The author demonstrates that the efficiency of the retro-aldol reaction can be improved by controlling the amount of oxygen charged. The author provides a brief understanding of the functional group content in the precipitated lignin after oxidation treatments to highlight the potential scope for valorization. A major challenge in the valorization of kraft lignin using oxidative treatment is the large amount of lignin precipitated after the reaction which remains unutilized. The author addresses this challenge by utilizing the modified lignin to produce novel lignin-based vitrimer polymers with an integrated approach in the pulp and paper industry.

7.1.1. Towards a new understanding of the retro-aldol reaction for oxidative conversion of lignin to aromatic aldehydes and acids

The production of vanillin and vanillic acid from kraft lignin proceeds at highly alkaline conditions and at elevated temperatures. Under these conditions, the oxidation of lignin is linked to the reaction temperature, oxygen pressure, pH, reaction time, lignin concentration, type of lignin feedstock and the reaction chemistry. The investigation of all these operating parameters on the yield profile is beyond the scope of this work. In conventional approach of oxidation of kraft lignin, the oxygen is charged throughout the duration of reaction at the specified operating conditions. Using this approach, at 140°C, the oxidation of kraft lignin results in combined maximum yield of 5.17% (by wt.) of vanillin and vanillic acid. In principle from the chemistry of the reaction, the retro-aldol reaction which is the final step in the oxidation of lignin, proceeds in the absence of oxygen. Also, the degradation of vanillin and vanillic acid occurs at severe oxidation conditions if the oxygen is charged beyond the final phase of product formation. The author investigates this phenomena by controlling the amount of oxygen charged during the reaction. Using this new approach in which oxygen was charged for only 20 min during the 40 min reaction improved this yield considerably to 6.95% (by wt.). The author also validated yield improvements by comparing the yields from the proposed approach against conventional approach on different lignin feedstocks. Oxidation also improved the carboxyl content in lignin from to 1.41 mmol/g at optimum conditions of 130°C and 40 min duration. In summary, oxidation strategy represents a crucial pathway to valorize kraft lignin.

7.1.2. Effect of oxygen and ozone oxidation on functional group content in softwood kraft lignin

The use of modern ^{31}P NMR technique for quantitative analysis enabled to identify and quantify the abundances of various phenolic OH, aliphatic OH and carboxylic OH units in softwood kraft lignin before and after oxidation in detail. The softwood kraft lignin utilized in this study showed a considerable reduction in the aliphatic and aromatic OH units after oxygen oxidation. The reduction in non-condensed aromatic OH units is possibly due to the higher reactivity of the phenolic OH groups. It was also observed that the amount of condensed OH units degraded were higher compared to the amount of condensed units formed from radical coupling units. The formation of carboxylic OH units is linked to the side-chain elimination and ring-opening reactions. The amount of carboxylic OH units from ozone oxidation (2.08 mmol/g) was significantly higher compared to oxygen oxidation (0.82 mmol/g) due to the higher reactivity of ozone. This allows for potential scope for integration under the operating conditions of LignoForce process. Further, the utilization of sequential oxidation strategy resulted in kraft lignin with a marked improvement in carboxyl content to 4.06 mmol/g. Therefore, the carboxylated kraft lignin can be further utilized as a source for transesterification exchange reaction to form bio-based vitrimer polymers.

7.1.3. A novel and integrated process for the valorization of kraft lignin to produce lignin-based vitrimers

The conventional oxidation strategies of lignin have limitations in regard to the amount of lignin utilized to form high value products. The author addresses this challenge encountered by simultaneous production of lignin-based vitrimer polymers, vanillin and vanillic acid. The modification of kraft lignin using sequential oxidation treatments results in a lignin source with

high carboxyl content which crucial for vitrimer formation with PEG-epoxy. All OxL-COOH/PEG-epoxy systems possessed a high lignin content (>48 wt%). The stoichiometric ratios 'R' which represent the ratio of epoxy groups and carboxyl groups was varied from 1, 1.3 & 1.5. All systems showed fast relaxation, thermal stability and self-healing due to the presence of bond exchangeable cross-linked networks. In aqueous NaOH solutions, the lignin-based vitrimer did not dissolve and exhibited noteworthy swelling properties which is a key indicator of the dynamic transesterification in the cured network. Overall, this study represents a novel and integrated process for the valorization of kraft lignin into value-added products.

7.2. Potential directions for future work

In this section, the author sheds some light on potential future directions in the areas of this research and thus enhance these proposed approaches further.

7.2.1. Towards a new understanding of the retro-aldol reaction for oxidative conversion of lignin to aromatic aldehydes and acids

Vanillin and vanillic acid are high value-added products from oxidation of lignin that have applications in diverse areas. In our study we investigated the role of retro-aldol reaction in the oxidation of lignin. The retro-aldol reaction which predominantly proceeds via hydrolysis reaction can be utilized to study the effect of hydrogen peroxide at lower temperatures. The optimum combination of both these oxidizing agents for degradation of lignin is still under investigation. Another factor that impact the vanillin yield is the characteristics of lignin feedstock utilized for oxidation treatment. The understanding of lignin molecule should not be limited to mean molecular weight or ratio of lignin precursors but also details at the level of chemical structure which includes types and amounts of functional groups that deviate the purpose of oxidation of lignin molecule. Pretreatment of kraft lignin with phenolation is a useful strategy to improve the reactivity and

decrease the molecular weight of lignin, thereby making it more useful for various applications. The phenolic-OH substitution allows for improved reactivity towards thermosets application and the development of transacetalized vitrimers. Lignosulfonates can produce higher yields of phenolic aldehydes and acids due to the elimination of C-α position under alkaline oxidative conditions. Also, treatment of lignosulfonates with hydrogen peroxide has not been reported in various literatures and there is a scope for investigation. Under optimized conditions, there is a scope to develop value-added products using different oxidizing agents.

7.2.2. Effect of oxygen and ozone oxidation on functional group content in softwood kraft lignin

In this work, the characterization of softwood kraft lignin by modern NMR techniques and conductometric titration allows for a greater understanding of the structural changes in softwood kraft lignin before and after oxidation treatment. This study highlights that significant carboxylic OH group formation allows for further research to utilize carboxylated kraft lignin to produce bio-based vitrimer polymers via transesterification exchange reaction. However, considering the overall scope for lignin valorization, there is also potential to understand the factors leading to the improvement in non-condensed aromatic OH units. The structural characteristics of lignin molecule that is used as a feedstock for oxidation treatment can have significant impact in the distribution of condensed and non-condensed aromatic OH units. Compared to native lignins, technical lignins have more condensed structures resulting in higher C-C linkages than C-O linkages. The undesired condensation of phenolic OH units occurs during delignification processes and can be minimized by (1) in-situ trapping of the reactive intermediates to convert them into stable molecules and (2) direct stabilization of the β-O-4 ether linkages (either physically or chemically). In regards to oxidation, there is a scope to investigate the use of hydrogen peroxide

in alkaline conditions in the presence of stabilizing agents to form non-condensed phenolic OH units.

7.2.3. A novel and integrated process for the valorization of kraft lignin to produce lignin-based vitrimers

In this work, the utilization of carboxylated lignin allows for diversification of the product portfolio obtained by sequential oxidation treatment. The use of sequential oxidation strategy to improve the carboxyl content results in an additional stage in the current integrated process of valorization of lignin. Therefore, this results in incremental costs of operation due to the use of an additional stage in the pulp and paper industrial processes. In order to eliminate the additional ozonation stage, two approaches can be utilized for the oxygen oxidized lignin: (1) The oxidized lignin with structural modifications in aliphatic and aromatic OH content can be utilized to make bio-based vitrimers. In this case, new type of vitrimer chemistries can be utilized to form bio-based vitrimers from structurally modified lignin. (2) The oxidized lignin with improved carboxyl group content can be reacted with epoxy thermosets having epoxy equivalent weight (EEW) in the range of –COOH value. As a result, the ozonation stage can be eliminated and the new process can be directly integrated in the modified LignoForce process improving the overall economic and environmental viability of this process.